P-7825

PERFORMANCE ANALYSIS OF COMPOSITE PROPULSION SYSTEMS

PHASE II FINAL REPORT

(25 March 1968 through 24 March 1969)

By

J. A. Wrubel

Prepared For

National Aeronautics and Space Administration

April 1969

Contract NAS7-521

Rocketdyne
A Division of North American Rockwell Corporation
6633 Canoga Avenue, Canoga Park, California 91304

R-7825

PERFORMANCE ANALYSIS OF COMPOSITE PROPULSION SYSTEMS

Phase I Final Report
(25 March 1968 through 24 March 1969)

By
J. A. Wrubel

Prepared For
National Aeronautics and Space Administration

April 1969

Contract NAS7-521

ROCKETDYNE
A Division of North American Rockwell Corporation
6633 Canoga Avenue, Canoga Park, California 91304

APPROVAL

The draft of this report, dated 25 April 1969, was approved for formal printing on 20 May 1969 by letter S&E-AERO-AT, dated 16 May 1969 signed by David C. Seymour, NASA Technical Manager.

FOREWORD

The effort described in this report was performed under G.O. 08912 from 25 March 1968 through 24 March 1969, and was technically managed by the Marshall Space Flight Center for the National Aeronautics and Space Administration under Contract No. NAS7-521.

The contributions of Dr. G. A. Hosack, Mr. R. L. Proffit, Dr. W. F. Herget, Mr. G. L. Cline, Mr. W. S. Bose, Mr. E. J. Ostrowski, Mr. R. J. Guthrie, Mr. C. A. Labertew, Mr. J. P. Daugherty, Mr. B. T. McDunn, Mr. J. T. Sabol, and Mr. S. Zeldin to the technical effort are gratefully acknowledged.

ABSTRACT

The improved understanding of gas-stream turbulent mixing is contingent upon obtaining a more comprehensive description of the resultant flow field and a more precise evaluation of the turbulent transport properties. The second phase of a continuing program to accomplish these goals is described herein. The flow field being experimentally studied is the two-dimensional mixing of fuel-rich supersonic hydrogen-oxygen combustion products and a subsonic heated airstream. The mixing is accomplished in a chamber accessible to both optical- and probe-type instrumentation systems. The second phase of the program included flow facility check-out, instrumentation installation, probe instrumentation survey, and preliminary testing.

CONTENTS

ILLUSTRATIONS

TABLES

INTRODUCTION

Technological developments are required for advanced vehicle propulsion systems. One of the required technology development efforts, which is the subject of this study, is the improved understanding of high-speed gas mixing. Both fundamental and applied knowledge of turbulent mixing are required by engine designers to optimize the design of composite propulsion systems such as ramjets, scramjets, and air-augmented rockets. In addition, this information is applicable to the study of rocket engine exhaust plume afterburning. Here it can be utilized in such diverse fields as missile base heating and radio-frequency communication interference.

An extensive body of phenomenological theory on turbulent mixing exists. However, the proof of the validity of these theories, which are usually formulated in terms of an eddy transport coefficient or eddy viscosity, is greatly impeded by the limited knowledge of turbulent transport properties. This is particularly true in the case of mixing involving chemical reactions, as in flames. Therefore, the goal of this investigation is to experimentally determine in detail the developing free shear layer in a particular turbulent mixing process with combustion. The data thus obtained will be used to generate a comprehensive description of the flow field and to determine the turbulent transport properties of the mixing process.

In the past, probe-type instrumentation systems have been the primary source of data collection. These systems have the common disadvantage of disrupting the flow field in the vicinity of the measurement station which in turn introduces an inherent uncertainity into these data. This fundamental problem is overcome through utilization of optical instrumentation devices which can gather the same data, except velocity, without disturbing the flow field. These devices have been successfully used at Rocketdyne for a number of years.

The three optical instruments (spectroradiometer, large aperture spectrometer/spectrograph (LASS), and photographic pyrometer) utilized on this program were designed and constructed by the Rocketdyne Physics organization to conduct spectroscopic studies of rocket plume radiation. Measurements are taken through appropriate internal optics from a line of sight through the region of interest. If this region is confined, care must be taken in the selection of the window materials to ensure that they allow transmission of the particular specie radiation. Quartz is usually selected because of its excellent mechanical and optical properties. It is transparent to radiation from 2000 angstroms to 3 microns. Other more costly materials are required for transmission beyond this range.

The spectroradiometer is a versatile instrument, capable of both spatial and spectral scanning for quantitative emission and absorption measurements from the ultraviolet to the infrared spectral regions. It consists of a grating monochromator, detectors, entrance optics, radiation calibration sources, a tuning fork radiation chopper capable of rapid startup or stop, and a zone ranging device, which enables the instrument to spatially scan across the exhaust plume. It can be used in a conventional manner to obtain spectral radiance and spectral absorption coefficients of a body of gas as a function of wavelength. Also, it can be used at a fixed wavelength to obtain spectral radiance, absorption coefficients, temperatures, and partial pressures of species as a function of spatial position.

The LASS consists of a McPherson Model 216 combination spectrometer and spectrograph having a relative aperture of f/8.7 and a resolution of 0.1A. It is trailer mounted with entrance optics, calibration source, and fiducial camera integrated into the assembly. When utilized as a spectrometer the LASS provides, by means of photoelectric detection, an immediate record of spectral wavelength and intensity. If photographic records are desired, it can be converted, within seconds, to a spectograph. The determination of temperatures and combustion specie concentration,

e.g., OH, can be accomplished when the LASS is used in conjunction with a water discharge absorption source. The resolution capabilities of the LASS are two orders of magnitude superior to the telespectrograph, originally planned for use on this program. The instrument was designed for observations in the spectral region from 2500 to 8000 angstroms.

The ultraviolet photographic pyrometer produces a photographic record of the spatial distribution of the apparent spectral radiance of the mixing region, or its equivalent brightness temperature, at low spectral resolution. Included in its field of view are both the hot gases to be measured and a radiation standard. The radiation standard consists of a calibrated tungsten filament lamp and a set of neutral density filters. The optical components of the pyrometer all transmit or reflect ultraviolet light.

The application of these Rocketdyne-developed optical instruments to the study of mixing of the practical composite propulsion system propellant combination of LOX/GH_2 and hot air* will provide, for the first time, high precision measurements of the parameters that affect mixing. It is anticipated that the approach taken will establish a concrete experimental basis for the evaluation of the available theories in addition to providing the designer with empirical information.

The 12-month Phase II portion of the program entitled, "Performance Analysis of Composite Propulsion Systems," was initiated by the Rocketdyne Research Division under Contract NAS7-521 on 25 March 1968. The objective of the program is to perform an exploratory experimental investigation of two-dimensional mixing of supersonic hydrogen-oxygen combustion products and a subsonic heated air stream. Utilization of the flow system fabricated during Phase I and the existing optical and

* This propellant combination is optically clean, i.e., it does not contain solid particles. Although flows containing solid particles can be handled by appropriate techniques developed by the optics personnel, the complexities introduced do not warrant the study of propellant systems containing solid particles at this time.

selected probe instrumentation systems for measurement of the spatial distributions of the various parameters will allow delineation of the developing free shear layer. The experimentally measured parameters include: concentration of both stable and transient species, temperature, pressure, and velocity.

The Phase II effort discussed in this final report was divided into six tasks consisting of:

1. Facility Checkout - Repair of the combustor components and minor rework of the injector, preparation of the experiment operating manual, and facility activation (cold flow and full-scale hot flow checkout tests).
2. Instrumentation Installation - Installation of the spectroradiometer, LASS, photographic pyrometer, test-section static pressure taps, and manometer bank.
3. Probe Instrumentation - The evaluation and procurement of special probe-type instrumentation devices for the determination of velocity and total pressure.
4. Testing - The experimental determination of the two-dimensionality of the flow, determination of the effect of test-section film coolant on the mixing process, characterization of a reference configuration, study of the effect of air stream temperature on the mixing process, and evaluation of the effect of relative turbulence level on the two-dimensional developing free shear layer.
5. Analysis - Support for the previously mentioned tasks and the data analysis required for adequate presentation of the test results.
6. Reports - Writing and processing of all contractually required reports.

A detailed description of the accomplishment of these tasks is presented in subsequent sections of this report.

SUMMARY

This report discusses the Phase II program which is a logical extension of the Phase I effort described in Ref. 1. The tasks completed under Phase I consisted of:

1. The design and procurement of an integral, combustor-exhaust nozzle and test section.
2. The establishment of test stand subsystems requirements.
3. The installation of test stand propellant and coolant subsystems.

Figure 1 shows the apparatus prior to final assembly and installation of the optical instrumentation. A schematic of the mixing chamber is given in Fig. 2.

Major accomplishments made in this second phase of the program consisted of:

1. Optical instrumentation systems including the zone radiometer and greybody source, the LASS, and the photographic pyrometer were readied for data collection. These instruments are used for a non-interference determination of partial pressure, temperature, and specie concentration in the flow field.
2. Both cold flow and hot flow check-out tests of the individual sub-system were successfully completed.
3. A probe instrumentation survey was accomplished. A commercial probe fulfilling the program requirements was procured, and the traversing mechanism designed.
4. A hot fire data reduction computer program was written and checked out.
5. Full integrated hot-fire testing was initiated, however, as a result of previous and subsequent problems, the planned test matrix was not completed.

Although the quantity of data did not meet expectations, this phase demonstrated that successful data collection is imminent.

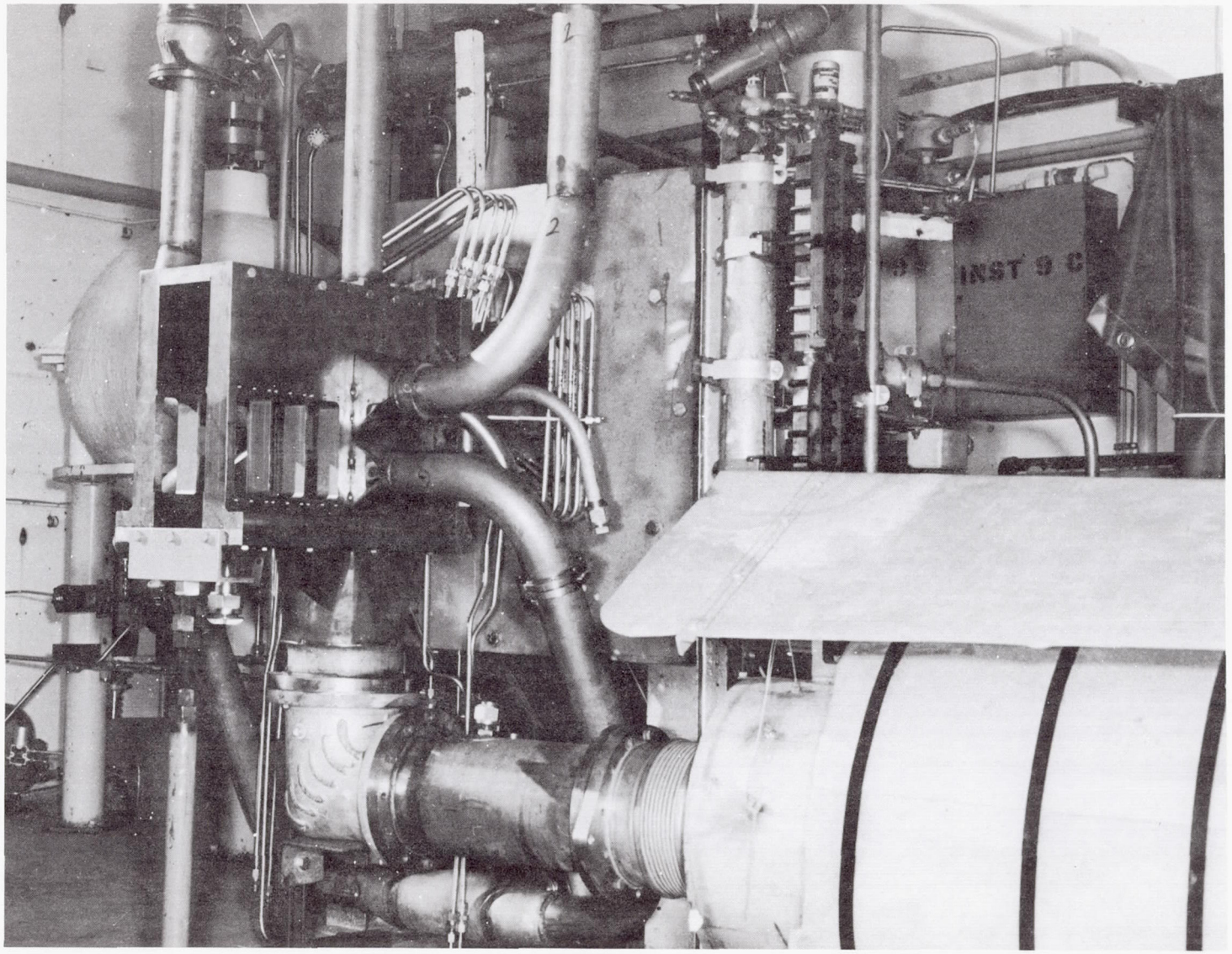

Figure 1. Mixing Apparatus Prior to Final Assembly

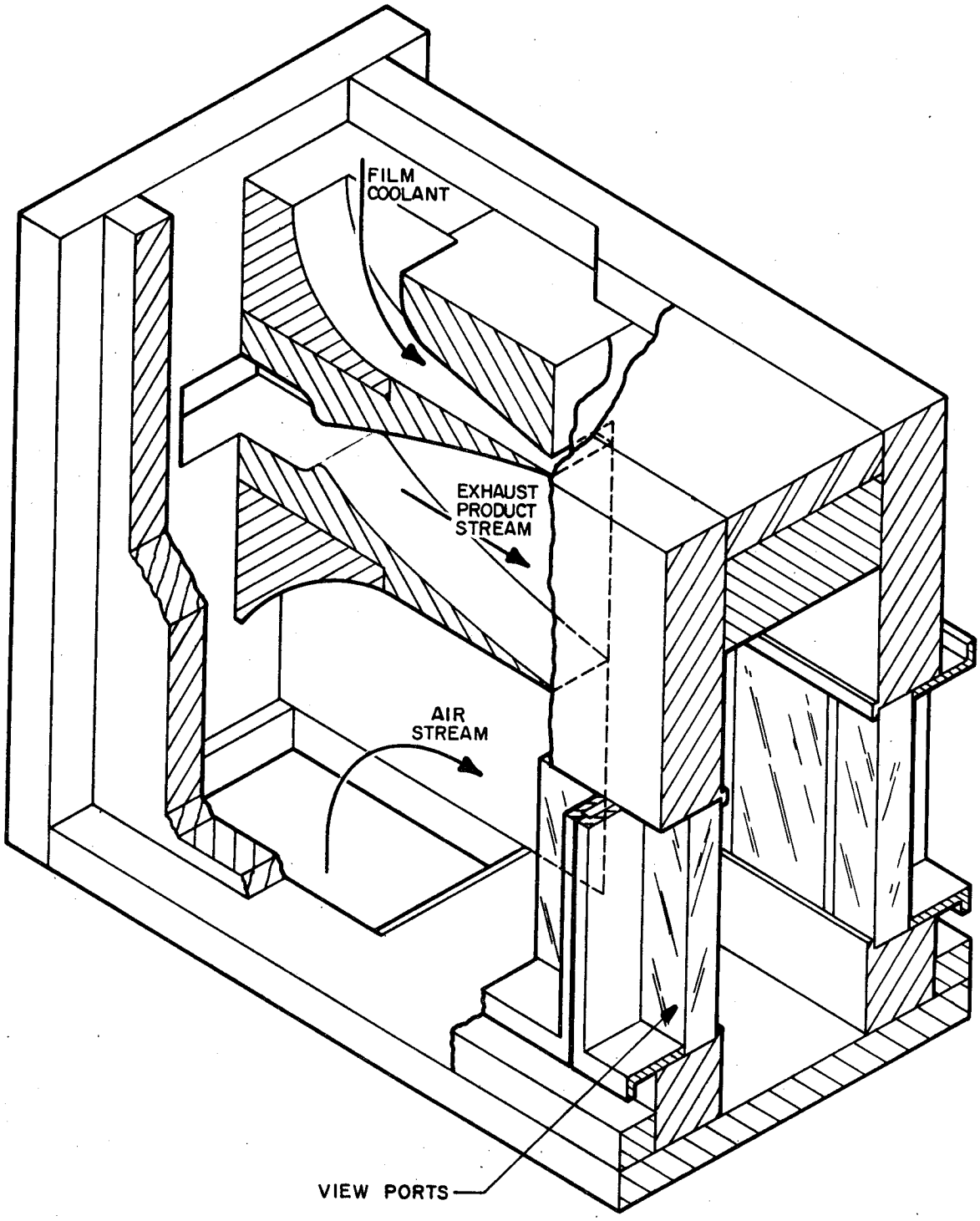

Figure 2. Combustor Exhaust Nozzle and Test Section Schematic

This program was plagued with a wide variety of difficulties. The most incessant problem was coolant water leakage. Its elimination required four modifications to the assembled hardware. This precluded the gathering of a wide range of experimental data.

DISCUSSION

A number of systems analyses have theoretically proven that airbreathing rocket vehicles can outperform any existing rocket engine in the arsenal of weapons and space boosters of the United States. Although these analyses are extremely optimistic about the improvements that can be made within the constraints of existing propulsion systems, e.g., a tripling of range or a doubling of payload, practical problems do exist. These problems, both fundamental and developmental in nature, include:

(1) mixing between the combustor exhaust and the air stream
(2) ignition delay vis-a-vis mixing chamber residence time
(3) cooling of the vehicle and combustion chamber with fuels rather than oxidizers which have higher specific heats
(4) a practical determination of the optimum method of air ingestion.

Discussed below is the second phase of a program to provide precise experimental data for the elucidation and delineation of the mixing problem.

FACILITY CHECKOUT

The small amount of test-stand plumbing remaining from the Phase I effort was completed. This included welding of the film coolant ducting, attachment of the cooling water drain lines to the test section, extension of the LOX bleed line, insertion of an LN_2 line to simplify injector chill-down, and installation of the engine afterburner and facility torches. The apparatus was subsequently removed from the thrust mount to facilitate combustor refurbishment. A handling fixture for ease of removing and replacing the apparatus was fabricated.

Combustor refurbishment included enlargement of the GH_2 orifices in the injector to accomodate the 1 lb/sec hydrogen flow required for

the mixing experiments. In addition, a number of water coolant passage leaks on the combustor body were repaired with silver braze and all sealing surfaces between combustor body sections were cleaned. Proof tests of the water coolant passages at full water coolant flow rates were successful.

Prior to final assembly of the apparatus a water coolant leak was noted (Appendix 1). After repairs were completed, the apparatus was mounted in the test stand and all utility, engine, and test section instrumentation was attached. Following this, all sub-system checkouts were successfully completed. These included flows of the water coolant, film coolant, injector chilldown system, engine and pad Firex, hot air system, liquid oxygen, hypergol, facility torches, and gaseous hydrogen. The response and operating characteristics of these sub-systems were deemed satisfactory to proceed with fully integrated checkout firings.

Full-scale system checkout tests, utilizing cold air, were conducted. Two ignition sequence tests and a 150-millisecond mainstage test were successful; however, significant errosion of the upper combustion chamber was experienced during a 2-second mainstage test (Appendix 1). No damage to the 2-D contoured exhaust nozzle or injector occurred.

A new combustor was assembled utilizing additional upper combustion chambers from the storage yard, and the propellant feed lines and coolant water lines were attached. An available nozzle was utilized in place of the 2-D contoured exhaust nozzle that is integrally attached to the mixing chamber. Coolant water blow-downs were made, and the combustor was successfully hot fired. Firing durations were 1, 2, and 5 seconds, respectively. Steady-state heat transfer rates to the coolant were extablished in approximately one second. Therefore, the ability of the combustor to meet the planned 22-second test duration was proven.

This completed the Facility Checkout task.

INSTRUMENTATION INSTALLATION

A 50-tube manometer bank for mapping the test-section static pressure was procured and installed adjacent to the test pit (Fig. 3). A total of 30 static pressure taps were located on the four test-section walls and were plumbed to the bank. The manometer bank is also used to monitor the pressure in the air heater transfer ducting.

Buildup for the optical instrumentation was completed. The required control wiring for the instruments was installed in instrumentation boxes at two locations: in the pit adjacent to the location of the spectroradiometer and on the exterior of the blockhouse wall near the location of the LASS and photographic pyrometer.

A mounting fixture for the zone radiometer was fabricated and installed, and an optical tunnel/mirror system that attaches to the spectroradiometer and provides an optical access to the mixing region that is free of atmospheric water vapor was fabricated.

Figure 4 shows schematically the arrangement of the major system components. The folded optical path allows the spectroradiometer to be protected by a blast wall and also provides the proper path length for forming an image of the mixing region on the monochromator entrance slit. Prevention of excessive vibrations in the tunnel was provided by structural supports that mount to the blast plate and test stand floor.

The zone radiometer was inactive for more than a year and required a modest effort to return it to operational status. Several electronic components were relocated to provide increased protection from the elements. The instrument was then placed in the test pit, and wired to its instrumentation box. Dust was observed in the zone radiometer after some particularly windy weather and it was necessary to clean the instrument prior to connection to the optical tunnel and attachment of the GN_2 environmental purge.

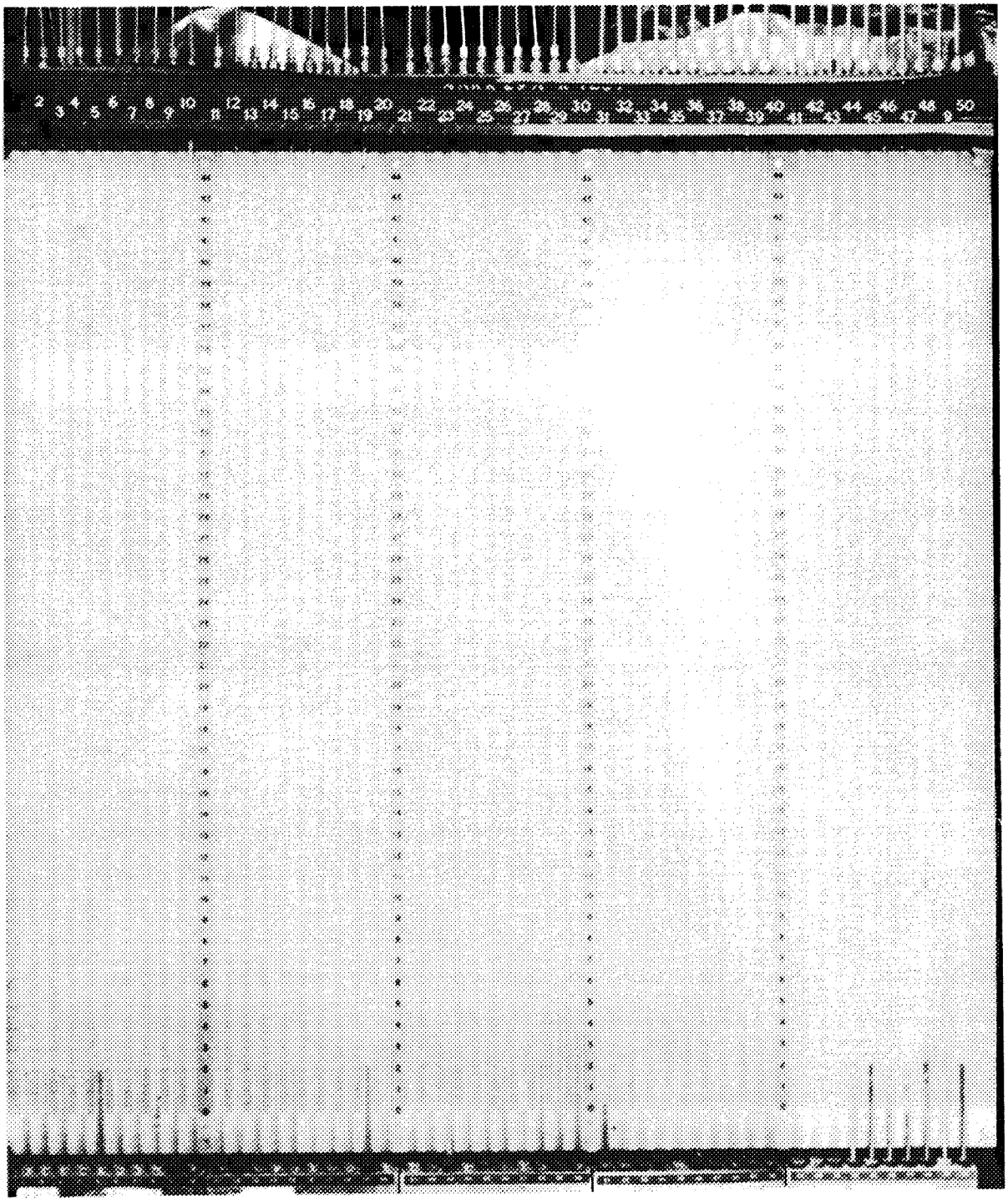

Figure 3. 50-Tube Manometer Bank

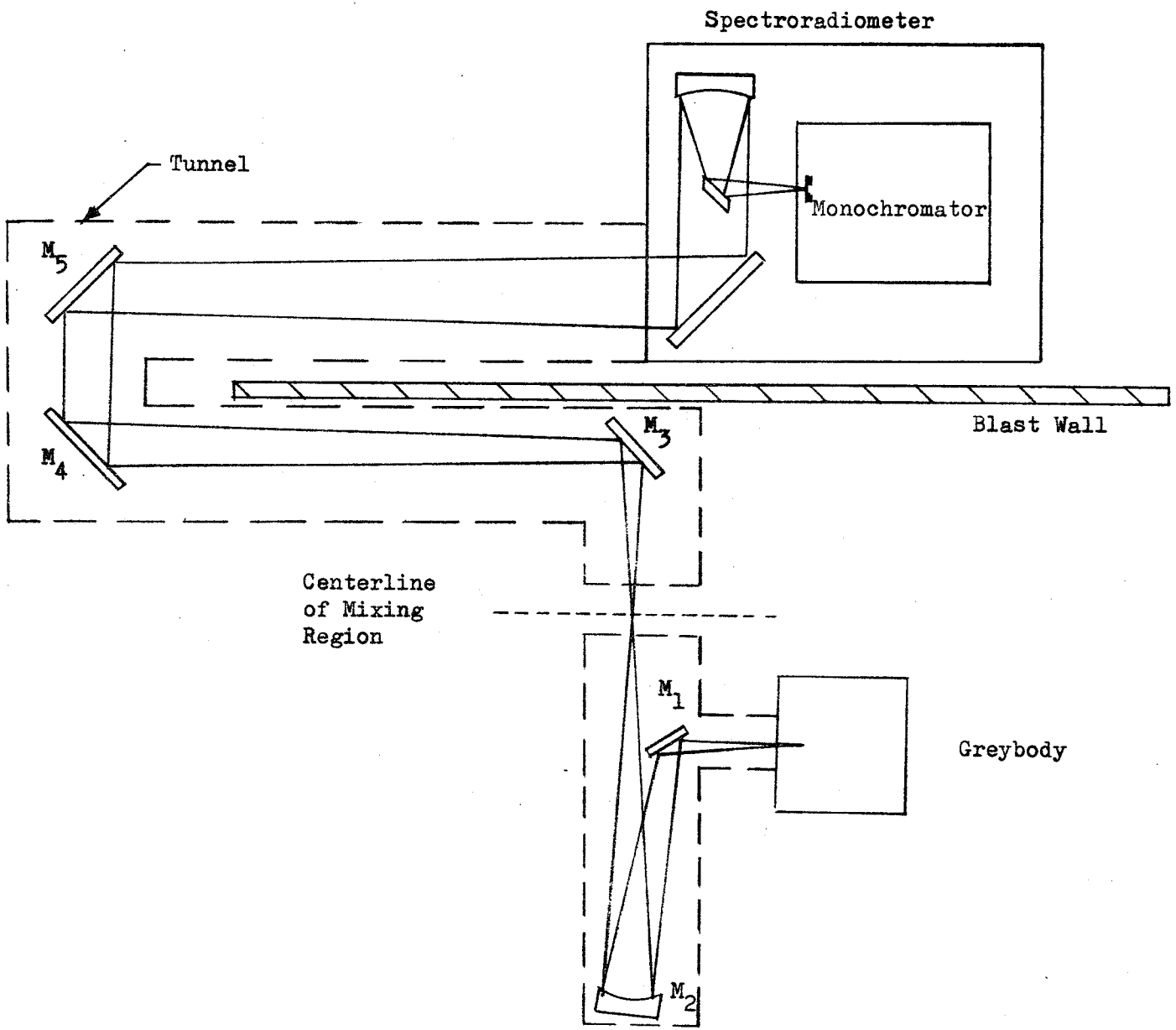

Figure 4. Zone Radiometry Schematic

The extra dry GN_2 purge prevents contamination of the instrument by dust and water vapor. The purge exhausts at the junction of the optical tunnel and the mixing chamber and serves the additional purpose of keeping the optical line of sight free of atmospheric water vapor during a test firing.

The greybody source is mounted above the mixing chamber on the opposite side of the zone radiometer line-of-sight. The structural supports for the source and its optical tunnel were located so that they would not block the view into the mixing region for the LASS, photopyrometer, and motion picture cameras.

The two-dimensional flow experiments require the zone radiometer to view the mixing region in the vertical direction. Special mirror mounts with their attendant optical tunnel were fabricated and modifications to the existing tunnel were made to accommodate this fixture. A comprehensive description of zone radiometry is given in Appendix 2.

The assembly of the LASS was completed under a Rocketdyne capital job order (Fig. 5). All subsystem components were mounted in the LASS trailer and the instrument successfully passed checkout. Mounting the instrument in a trailer makes it easily portable and enables installation at any facility in a matter of a few hours. The LASS is used for the spectroscopic determination of OH rotational temperature in the excited and ground state, identification of reaction zones and distinguishment of these zones from zones of thermal emission, and measurement of OH concentration. A detailed description of the instrument, the measurement technique, and the methods of data reduction are given in Appendix 3.

The location and types of photographic coverage for the mixing experiments was formulated and the requirements for the experiments were delivered to photographic personnel. This information included the film, filters, lenses, camera placement, and cameras to be utilized for high-speed photography, photopyrometry, schlieren photography,

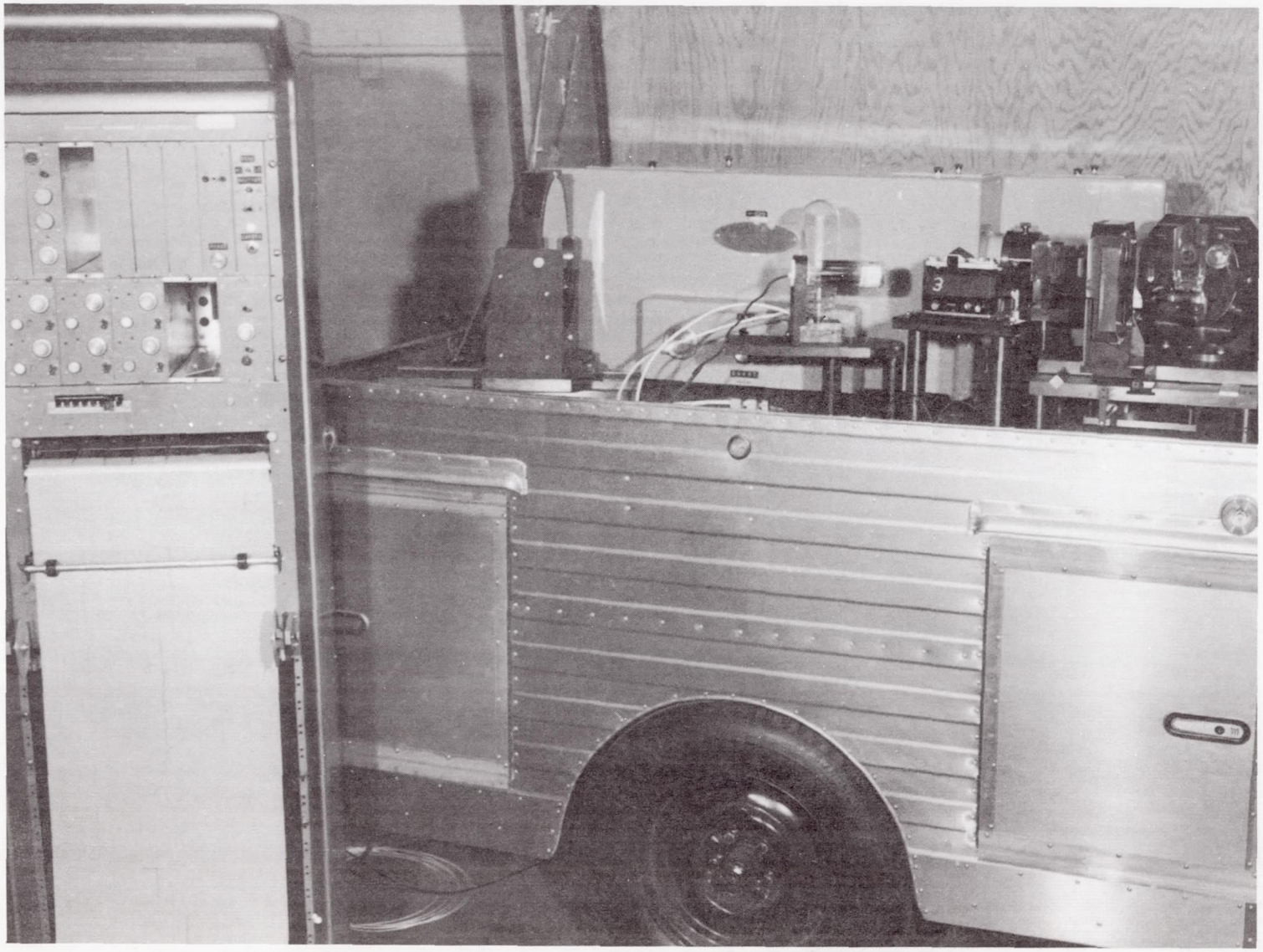

Figure 5. Large Aperture Spectrometer/Spectrograph

and overall photography. Low framing rate cameras are utilized to monitor the manometer bank, the back side of the injector, and the entire facility. Various camera speed ranges are required for coverage of the mixing region in the visible, ultraviolet, and infrared spectral regions. All cameras have been located in the test pit.

For the initial runs, a full gamut of photographic coverage was employed. After a critical evaluation of the initial photographic information, infrared photography was eliminated and only those camera settings that yielded specifically useful information were used.

A more compressive discussion of the photographic techniques employed is given in Appendix 4.

PROBE INSTRUMENTATION

For the probe instrumentation survey, available literature was gathered and reviewed. Emphasis was placed on methods that did not interfere with optical data acquisition while allowing the determination of velocity and total pressure; however, consideration was given for future use of these systems for collection of data identical to that gathered by the optical devices. Articles evaluated are included in Ref. 2 through 21. This evaluation concluded that probes satisfying the program requirements were commercially available.

Upon concurrence of the technical monitor, a Greyrad (Model G-13D-3) 3/8-inch, high sensitivity probe with static pressure taps was purchased, Figure 6. The probe can withstand the extreme thermal environment of a rocket exhaust while being capable of the determination of velocity, static pressure, total pressure, static temperature, stagnation temperature, enthalply, and specie concentration.

Design of the probe traversing mechanism was completed. Fabrication of the mechanism will be accomplished during the anticipated follow-on program.

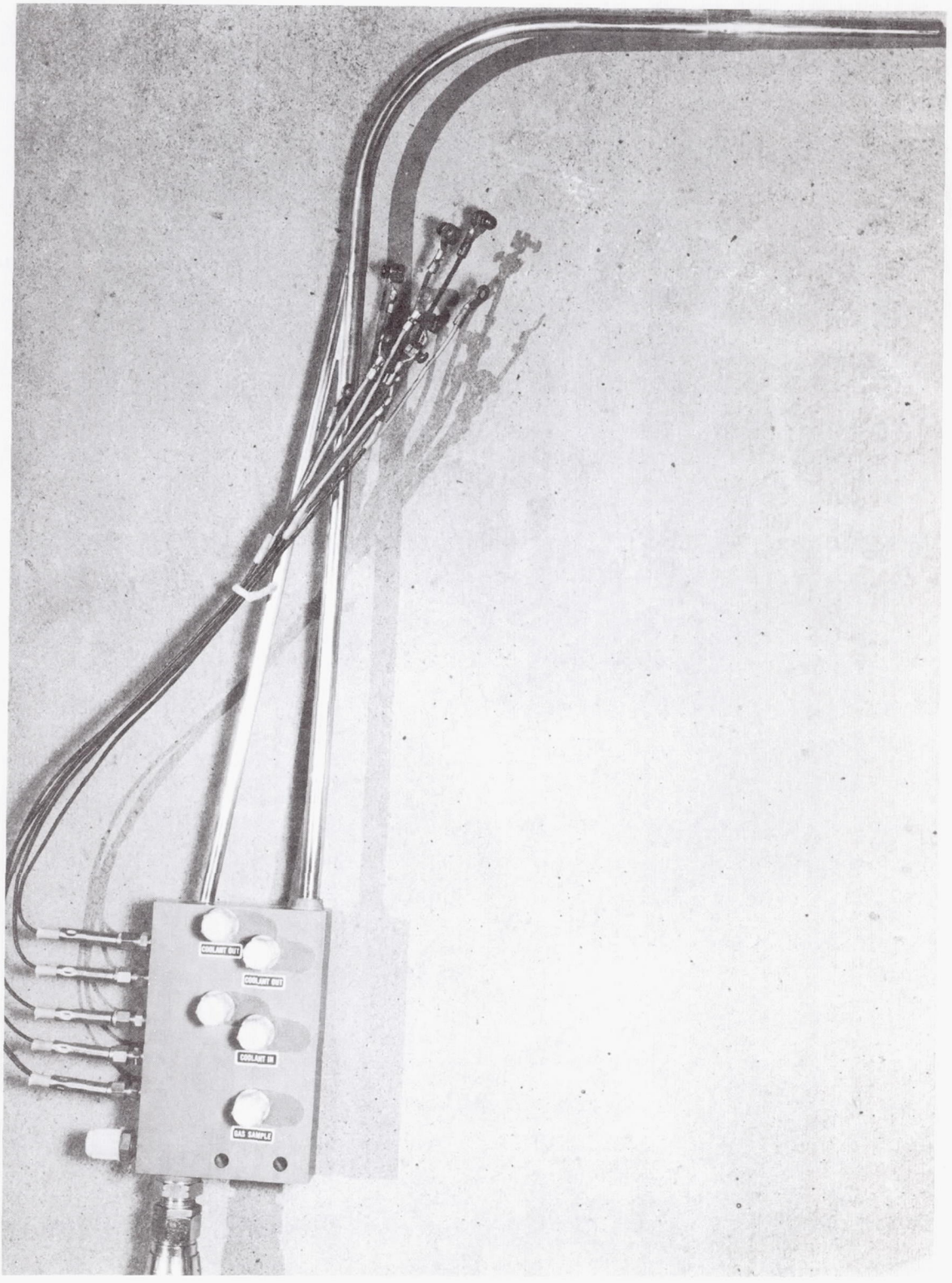

Figure 6. Greyrad Probe

TESTING

Following successful demonstration of the integrity of the new combustor, it was mated with the two-dimensional nozzle which is integrally attached to the mixing chamber. Leak tests of the assembled apparatus indicated water leaks at some of the brazed joints on the 2-D contoured exhaust nozzle. The apparatus was disassembled and the faulty braze joints were repaired, i.e., TIG welded. The mixing chamber was then reassembled and mounted in the test stand.

Preliminary to full-scale hot firing tests a determination of the two-dimensional properties of the film coolant and air stream was made. Measurements of the film coolant and air stream velocity profiles were taken at the entrance to the mixing chamber with pitot probe rakes (0.060 diameter). The total pressure was measured by a mercury-filled manometer bank.

The velocity profile data for the air and film coolant streams are presented in Fig. 7 and 8. It should be noted that the air stream is reasonably two-dimensional except near the bottom wall where a separate flow region exists. The separated flow region at the bottom of the air stream is a consequence of the sharp turning angle of the flow upstream of its entrance to the mixing chamber. Since this region is relatively far from the theoretically calculated mixing region, it should have a negligible influence on the mixing. Further, it should be noted that the film coolants are reasonably two-dimensional at the interfaces of the primary streams, i.e., air and combustor exhaust products. Again, a separated flow region is evident near the side wall. This, also, should have a minimal influence on the mixing region. The tabs depicted on the figures are used to retain the quartz windows.

The present configuration of the mixing apparatus in total is approximately 3-inches shorter than the original engine-mixing chamber

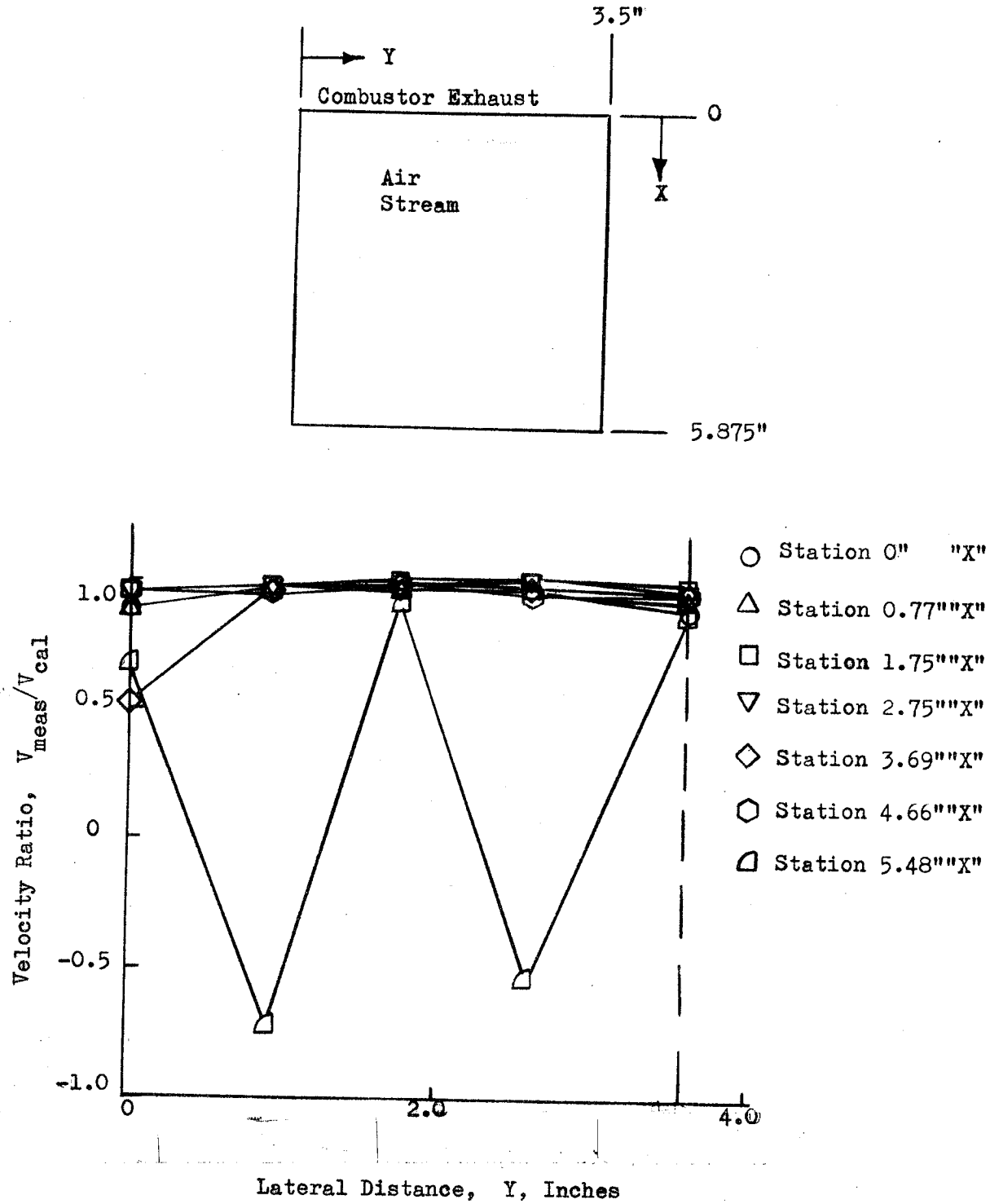

Figure 7. Air Stream Velocity Profiles

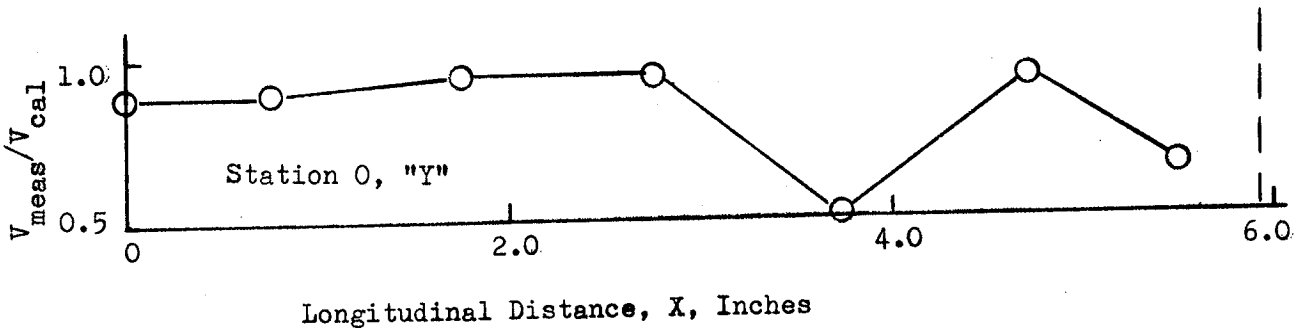

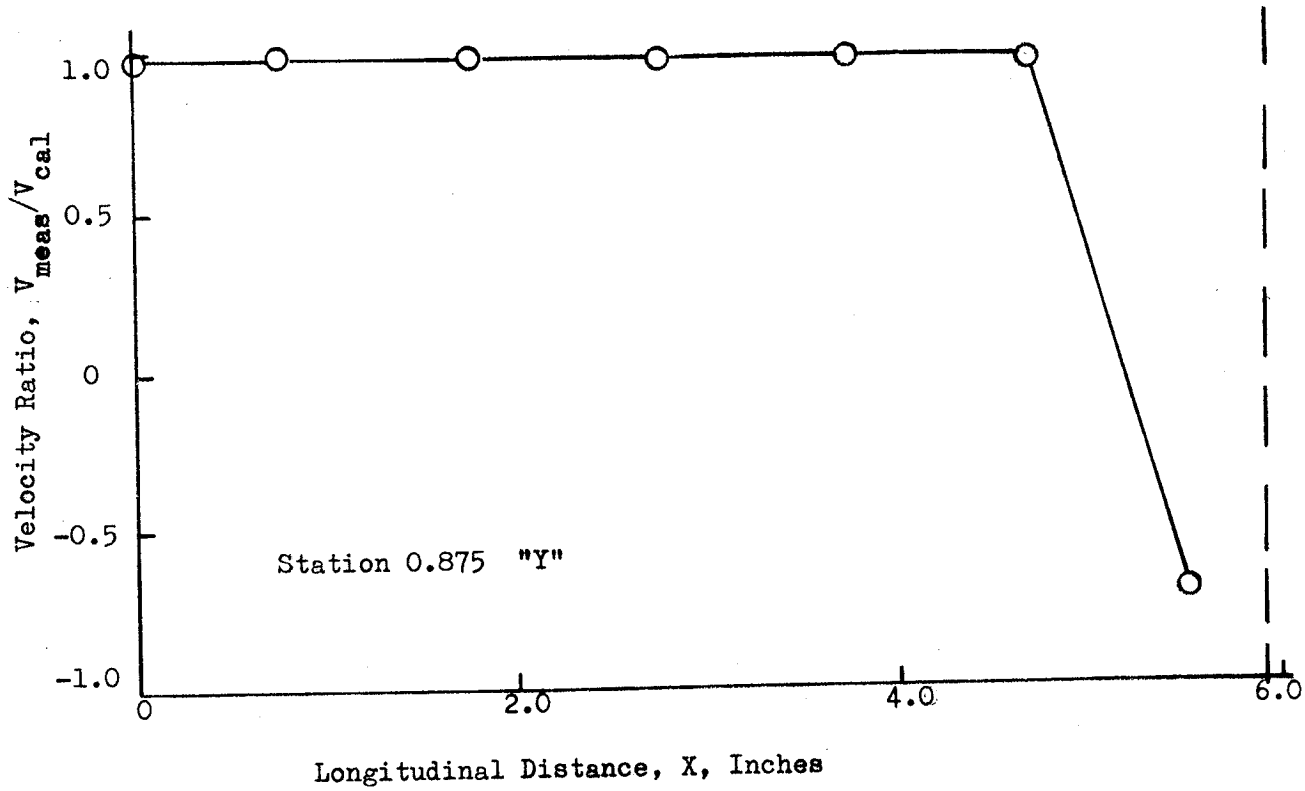

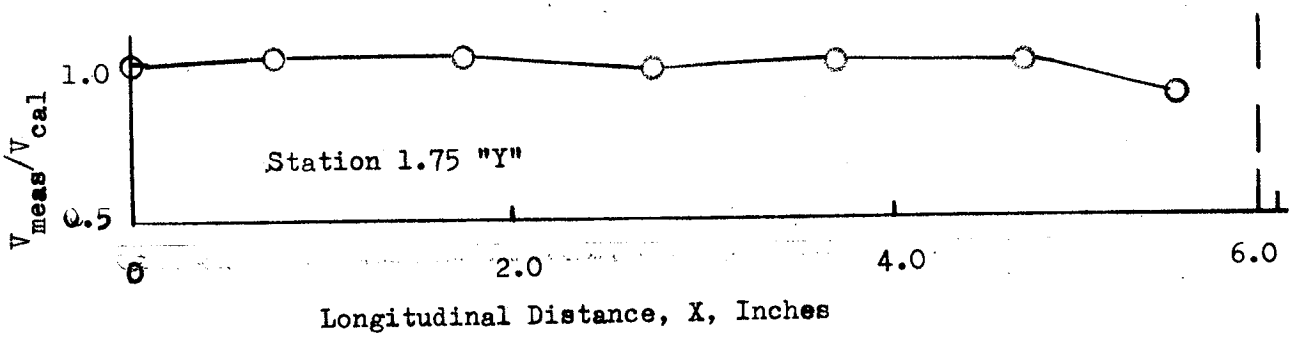

Figure 7 (Cont). Air Stream Velocity Profiles

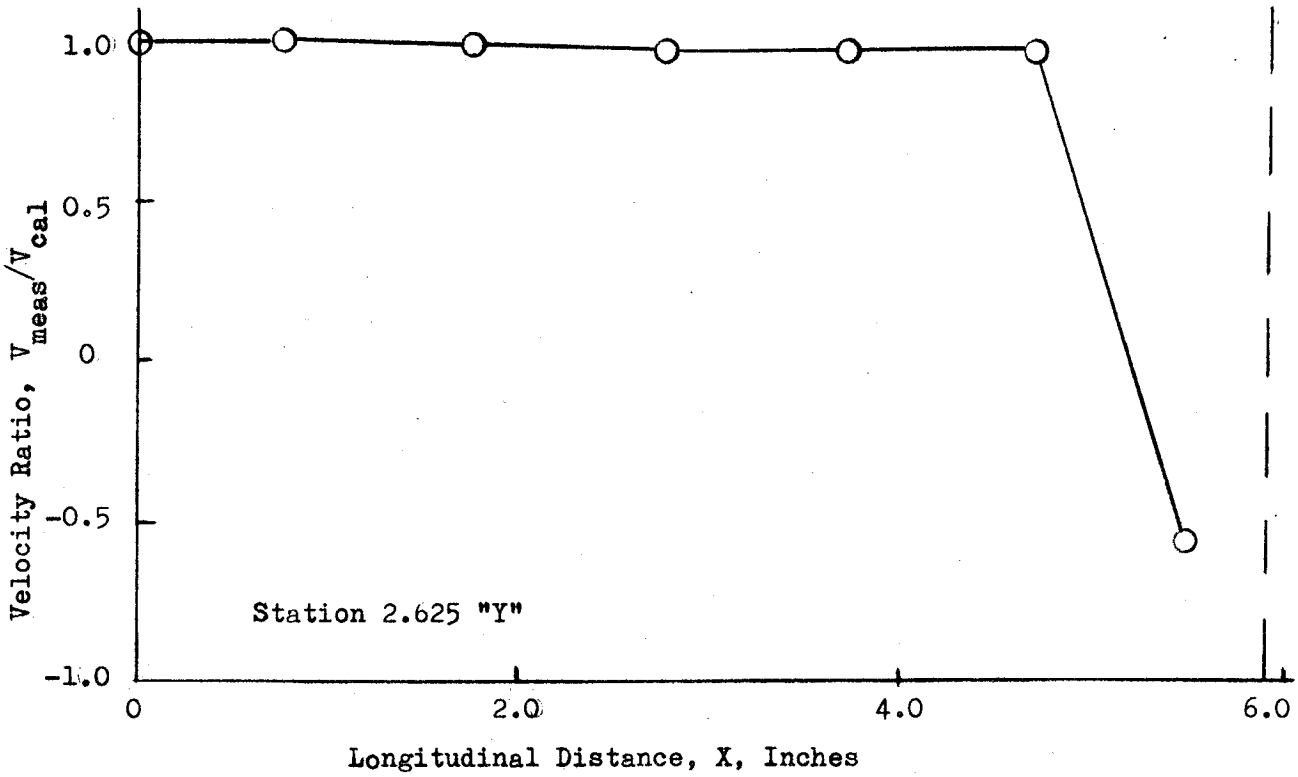

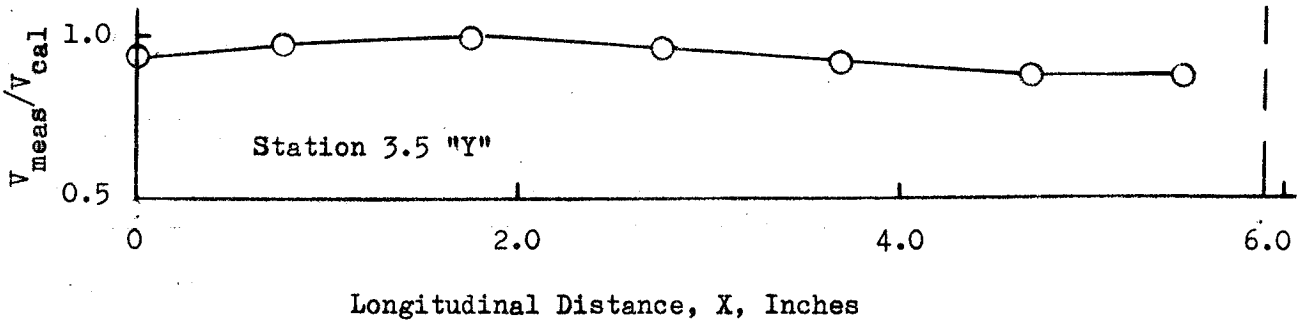

Figure 7 (Cont). Air Stream Velocity Profiles

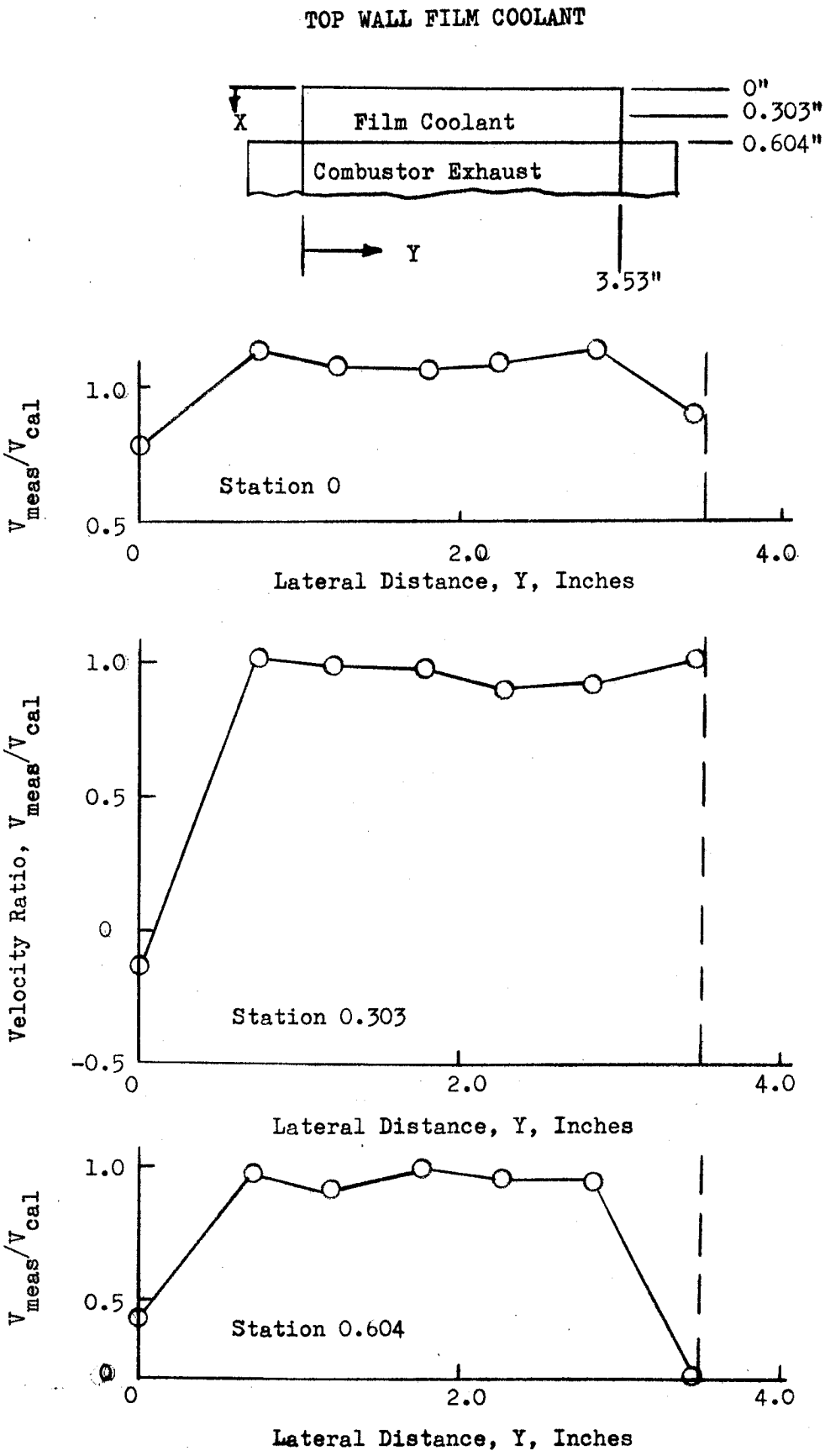

Figure 8. Film Coolant Velocity Profiles

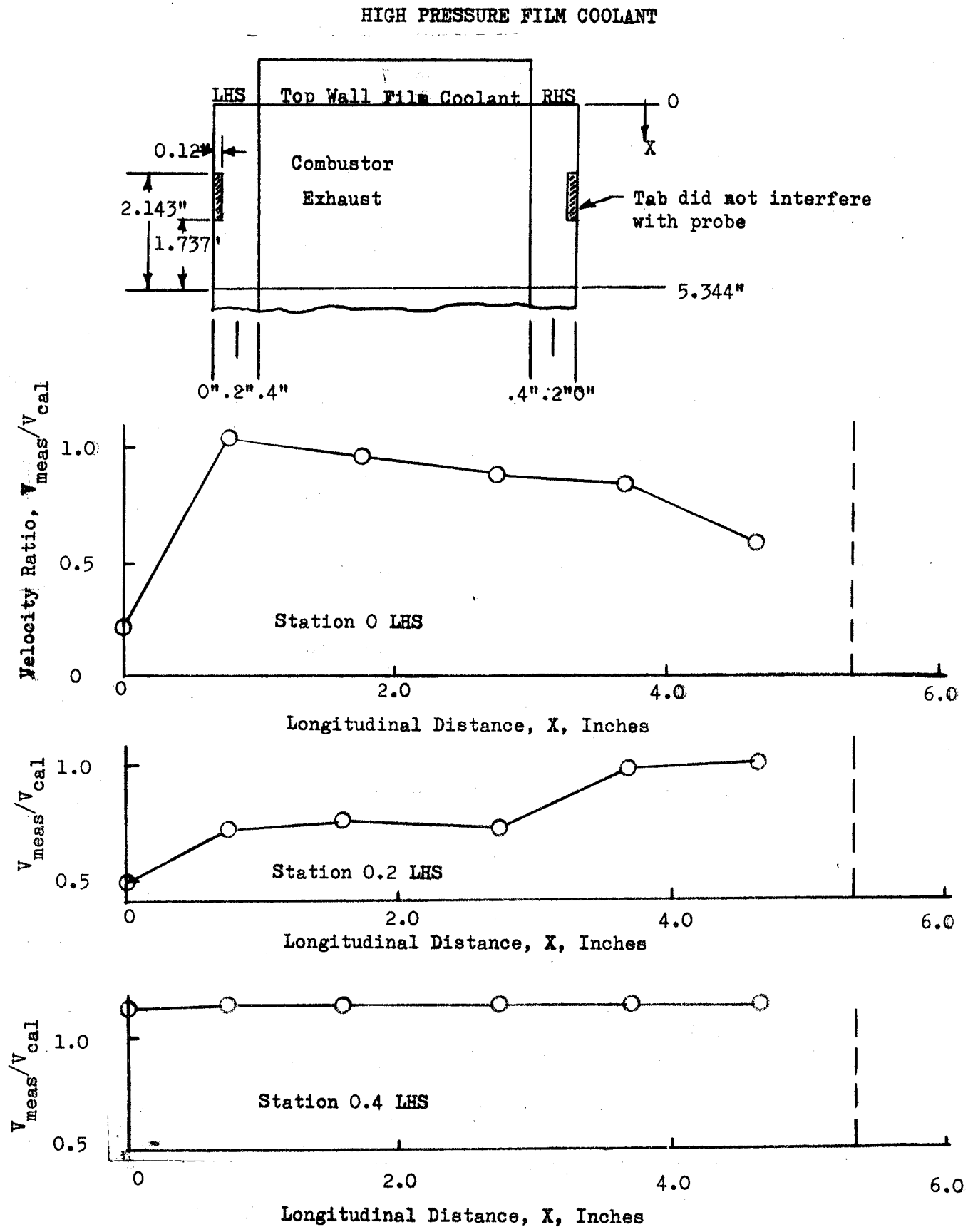

Figure 8 (Cont). Film Coolant Velocity Profiles

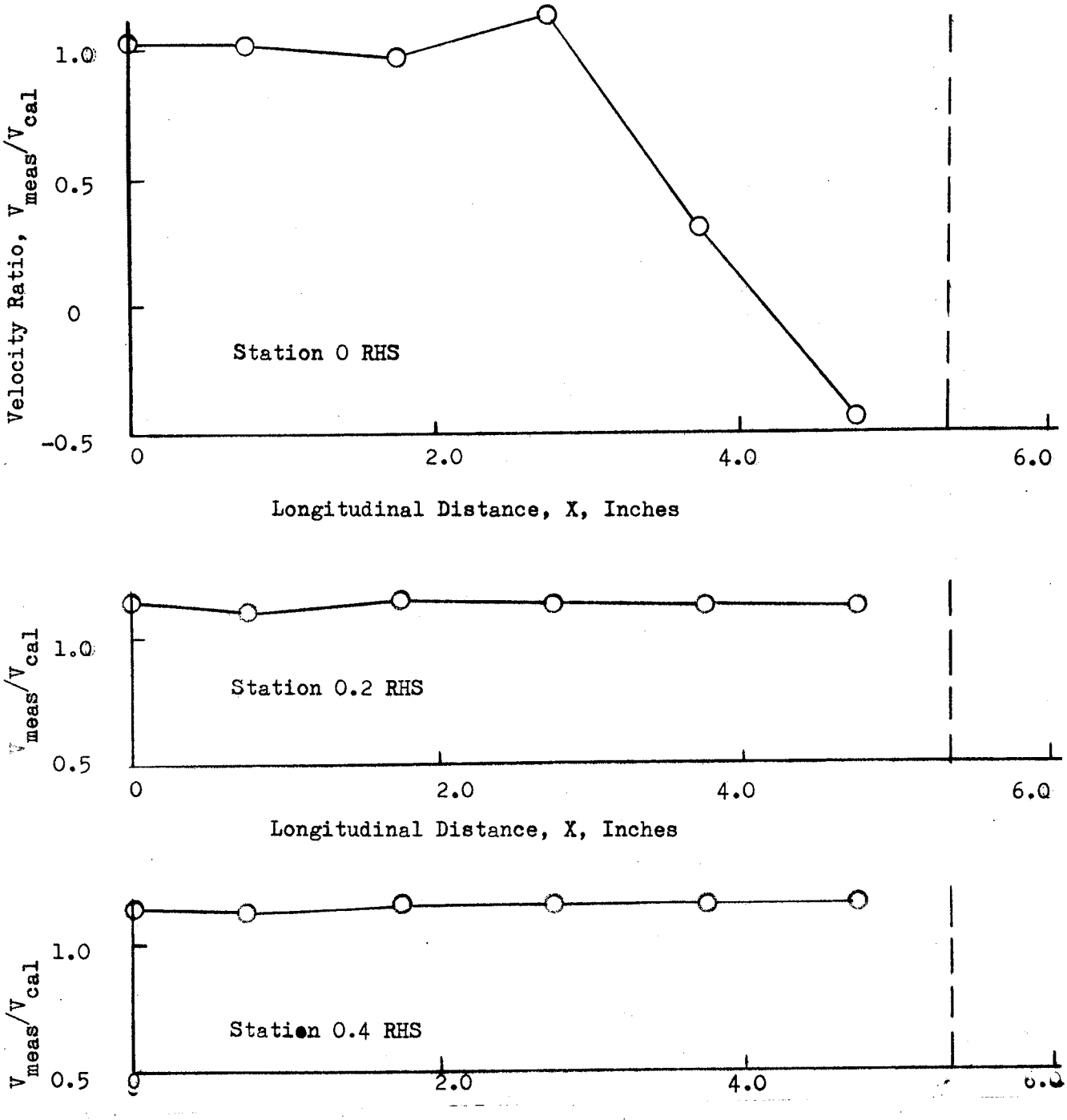

Figure 8 (Cont). Film Coolant Velocity Profiles

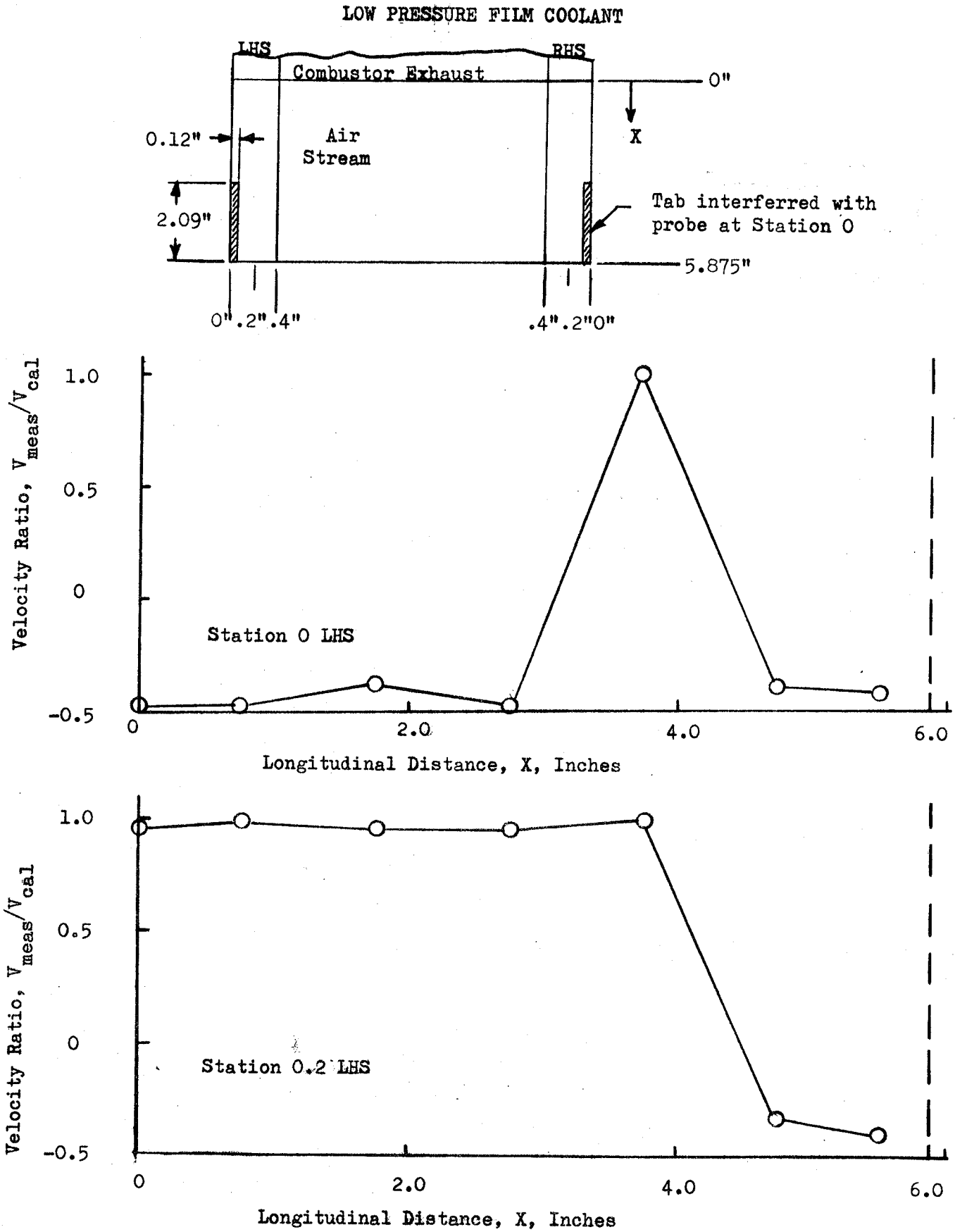

Figure 8 (Cont). Film Coolant Velocity Profiles

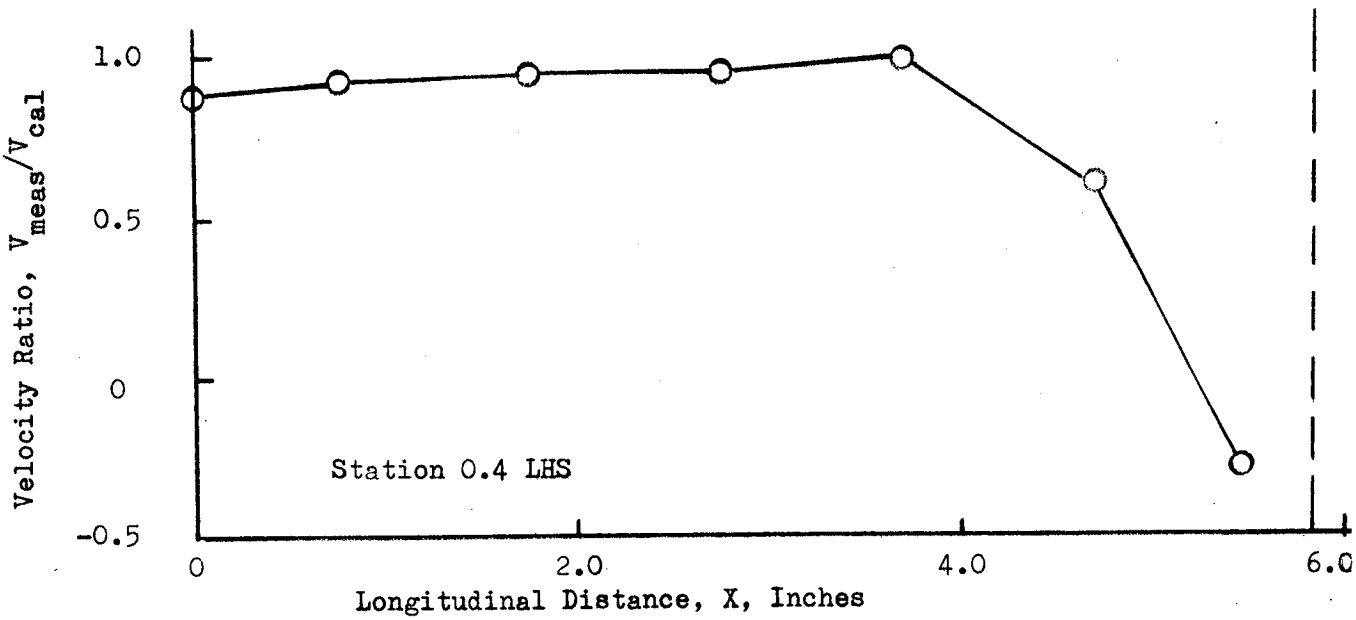

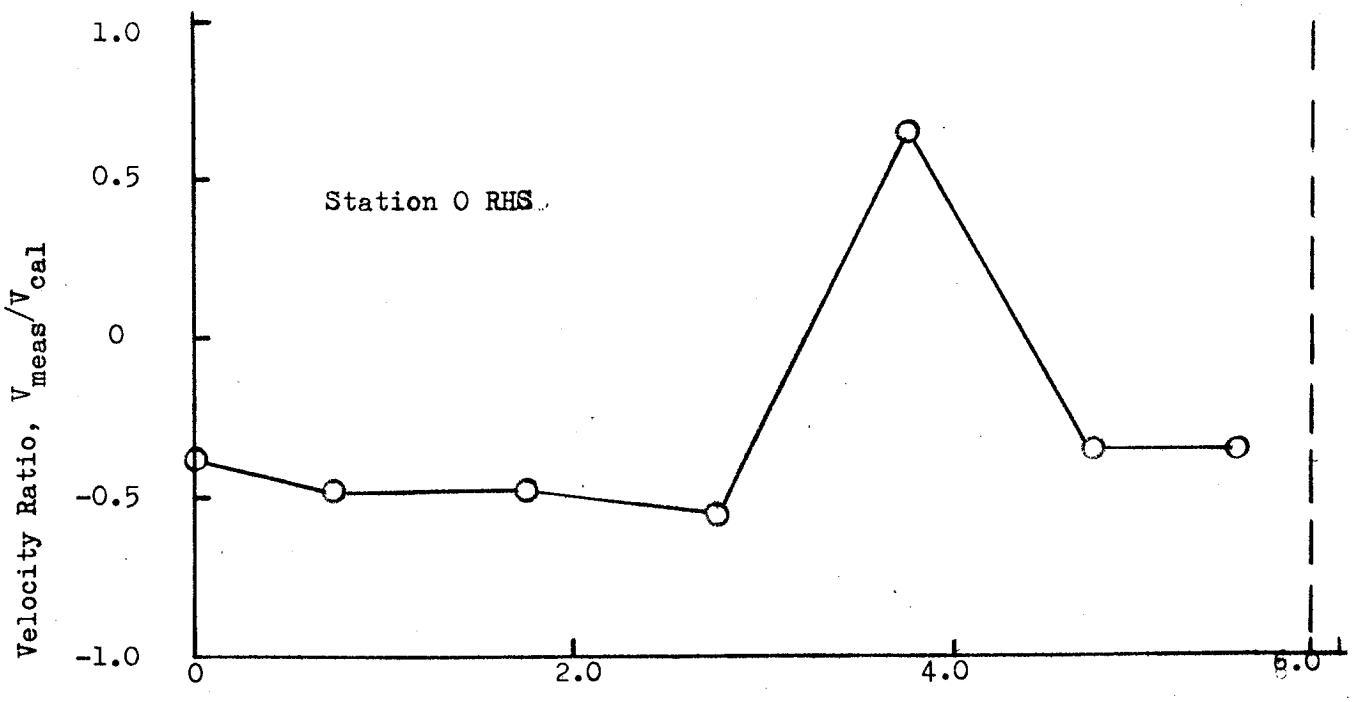

Figure 8 (Cont). Film Coolant Velocity Profiles

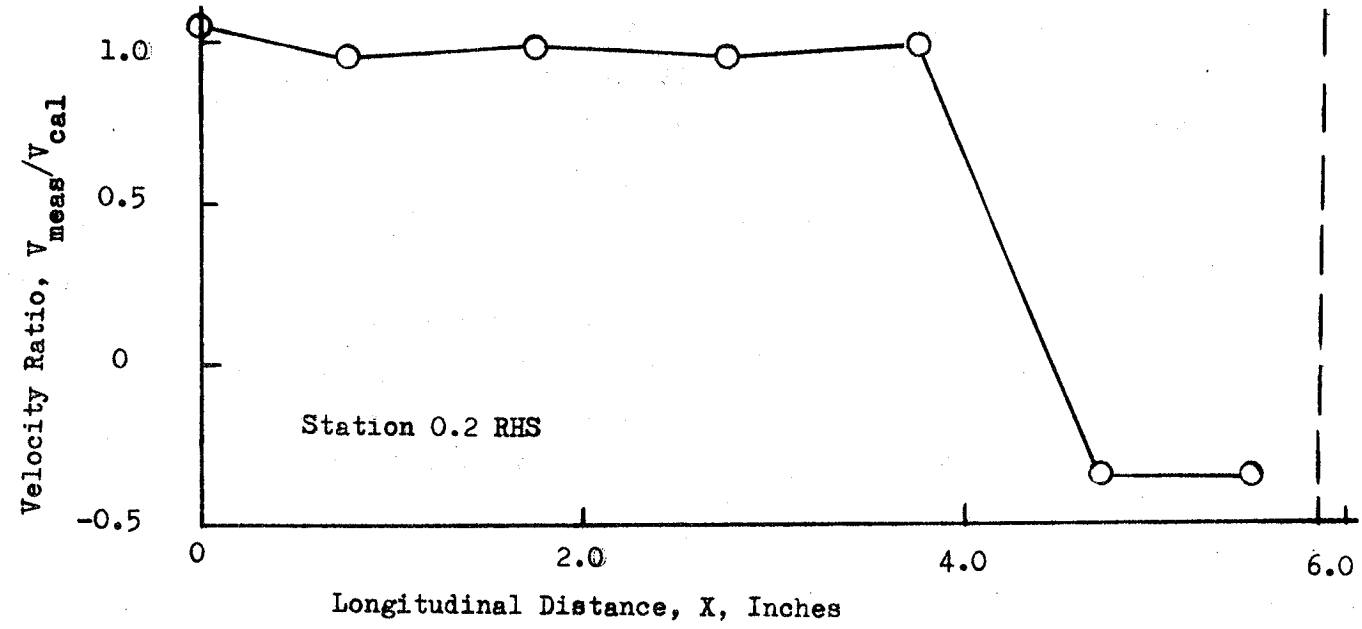

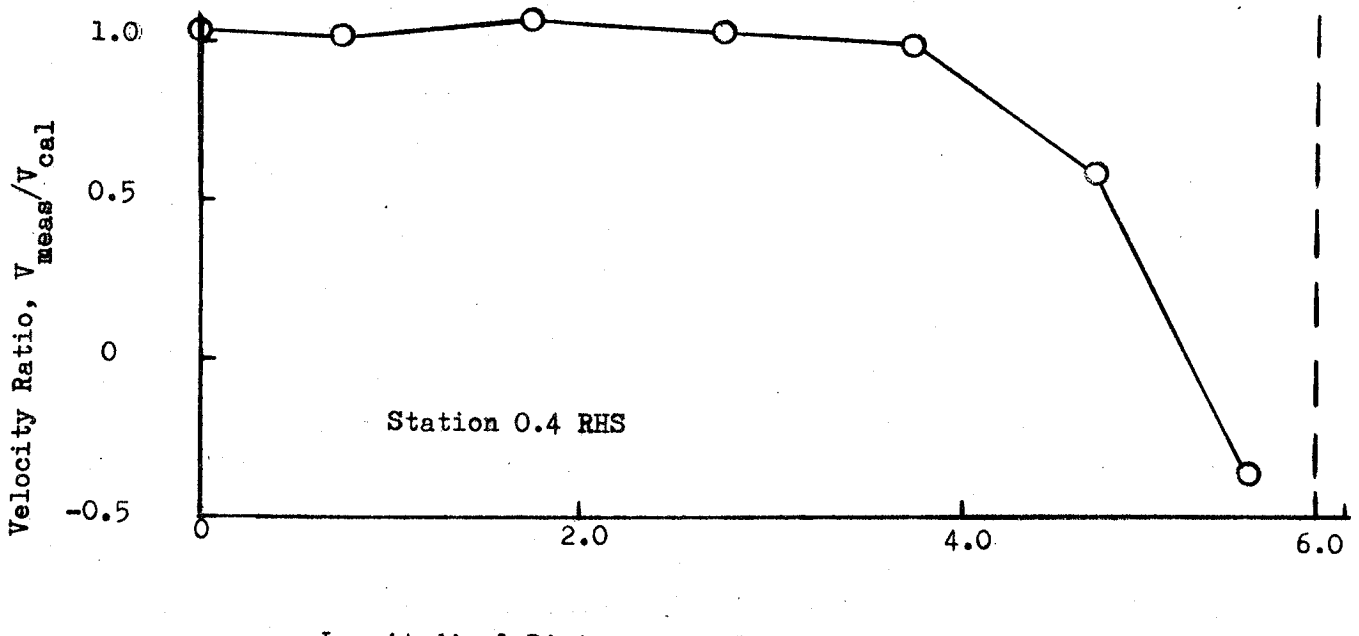

Figure 8 (Cont). Film Coolant Velocity Profiles

configuration. This decrease in length occurs in the combustor length. The new combustor was assembled entirely from existing additional upper combustion chambers found in the storage yard. However, there were not sufficient existing chambers to return the new combustor to its original size. While this caused no problem with c* efficiency (tests revealed it to be greater than 95 percent), it did require all film coolant and certain water flow connections to be shortened three inches.

In addition, analysis of past data obtained during firings of the original combustor and the 2-D nozzle revealed a potential thermal distortion problem at the edge of the thin lip separating the combustor gases from the air stream. This problem was alleviated by changing the water distribution to allow more coolant flow from the high pressure water tank to pass through the nozzle section and by making additional allowances for thermal expansion at the intersection of the nozzle lip with the side wall.

The modifications to the water coolant system required that the water distribution tests be rerun. These tests were conducted and no maldistribution of coolant water was noted. The changes in the plumbing of the water supply permit operation at a safety factor of 3 which is an increase of 0.8 over that obtainable with the previous setup. The water coolant safety factor is defined as the actual water flowrate divided by the theoretical water flowrate required for marginal cooling.

Because of the changes in the water coolant plumbing, long duration firings (greater than 15 seconds) required total coolant water in excess of that available. Installation of a higher capacity water tank was subsequently completed under a Rocketdyne capital job order. The new tank increased the high pressure water supply from 150 to 600 gallons.

Full scale testing commenced on 16 January after a delay of approximately one week because of alignment problems with the zone radiometer and the demonstration of a need for an effective system to eliminate frost on the test section windows. Frost was eliminated by ducting the cold GN_2 exhaust well aft of the test section during the chilldown. The duct was removed just prior to an engine firing. Three successful firings were conducted with durations of 1, 2, and 5 seconds, respectively. Close examination of the hardware revealed a slight amount (.020 x .050 x 3.0) of erosion of the nozzle tip during the 5-second firing. The cause of the erosion was traced to a gross underestimate (by a factor of four) of the heat flux at the tip which was originally calculated based upon the Bartz equation. A revised calculation of the temperature encountered at the tip, utilizing the actual test data, indicated that the minimum distance from the tip to the first coolant passage must be on the order of 0.85 inches. Therefore, the nozzle tip was cut back 0.150 inches. This increased the tip thickness by 0.006 inches. Subsequent firings confirmed this analysis.

An additional difficulty was encountered during the aforementioned tests. The gaseous nitrogen bottle bank which feeds the laboratory bottle bank was reduced in pressure while the laboratory was on the red light. This resulted in a shift in the water tank and hydrogen regulators during the run causing a slightly decreasing water flow rate and a much reduced hydrogen flow rate, i.e., operation at mixture ratio of 10 rather than 5. This condition contributed to the erosion of the nozzle tip. Corrective action, consisting of closing the main gaseous nitrogen bottle bank fill valve prior to testing, was taken to eliminate the possibility of a similar occurrence in the future.

No zone radiometer data were obtained during these instrumentation checkout firings because the mirrors shifted at the beginning of the run. The apparent cause was transmission of engine vibrations through the tunnel which is connected to the engine. Corrective action consisted of placing additional attachment screws on the mirror mounts, placing

cushions under all mirrors, and attaching the tunnel to the engine via a black cloth rather than a direct connection.

The photographic coverage revealed that the UV and IR emission was lower than anticipated. Consequently, these films were all underexposed and only yielded information during ignition. The operating speeds of the cameras were reduced to increase the exposure for subsequent firings. The color photography yielded a good representation of the visible emission occurring in the mixing chamber. The growth of the mixing region into the subsonic stream was clearly depicted, Fig. 9. The specie causing the emission at present is unidentified. Observations with the LASS will enable the determination of its identity.

No testing during the weeks of 1/24 and 1/31 was possible due to adverse weather conditions. Following nine straight days of rain, the temperature dropped to below 32 F at the test site which caused the water supply lines to ice up and also conditioned the various utilities to render a number of control valves inoperable. During this period, a small combustor body water leak was noted dribbling into the air stream. The flowrate at operating conditions was determined to be 3 ml/sec which was considered insignificant.

Full-scale testing resumed 4 February 1969. Again, off-design mixture ratio operation occurred and it was analytically determined to be caused by too large a GN_2 demand during testing. The only change in testing procedure between this test and those where this problem did not occur was a doubling of the H_2O tank pressures. As previously prescribed for other tests, decay in supply pressure was not the cause since normal pressures of 2200 psi and 2800 psi were recorded for the laboratory GN_2 bottle bank and the main supply bottle bank, respectively. In addition, a more serious problem was evident after post-test inspection of the hardware. The 2-D nozzle side wall was warped. This problem is discussed in Appendix 1.

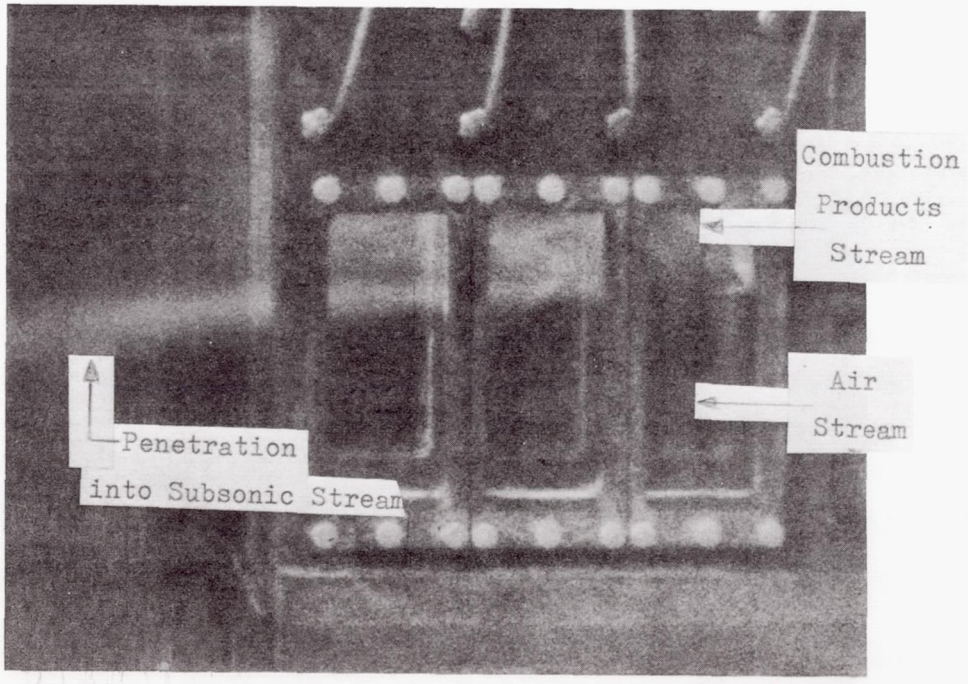

Figure 9. Mixing Region with Cold Air

A summary of hot fire tests and a summary of principal test parameters are given in Tables 1 and 2, respectively. A guide to instrumentation location is shown in Fig. 10.

ANALYSIS

This task was primarily a supporting item for the analytical effort required under Facility Checkout, Instrumentation Installation, Probe Instrumentation, and Testing. Whenever the analytical effort was inextricably linked to the previous items discussed, the results were presented at that time; however, only those items unique to the analysis task will be presented in the following paragraphs.

A hot fire data reduction computer program was written to minimize the time required to reduce the 36 test parameters. Calculations required to reduce the raw data into a workable form were assembled and a computational sequence was formulated. The program performs all the necessary calculations to establish the operating conditions of the various utilities and the initial conditions of the combustion gas, air stream, and film coolant as they enter the mixing chamber. It was utilized in supplying the data for Table 2. A detailed description of the program is given in Appendix 5.

A cursory review of the photographic data from Run 0101 revealed the following information. The UV photograph indicated two distinct boundaries of ultraviolet emission. It was then postulated that these boundaries were an indication of a diffuse reaction region with the outer boundary corresponding to the momentum boundary layer and the inner boundary representing the termination of the diffusion layer and the start of a region of intense chemical reaction. (Normally, a photographic record would be inserted here to illustrate the observation, however, due to the grainy nature of photographs and the low level of contrast, adequate reproduction of these photographs is virtually impossible.) Verification of the preceding interpretation hinges on the correlation

TABLE 1

TESTING SUMMARY

Test No.	Type	Test Duration (Seconds)	Instrumentation & Location	Remarks
0010	Integrated Check-Out	——	Overall, Injector, and Manometer Bank Cameras	Hypergol Function Check
0020	Integrated Check-Out	0.230	Overall, Injector, and Manometer Bank Cameras	Ignition Sequence Check
0030	Integrated Check-Out	0.400	Overall, Injector, and Manometer Bank Cameras	Normal Operation
0040	Integrated Check-Out	2.400	Overall, Injector, and Manometer Bank Cameras	Upper Combustion Chamber Erosion
0050	Combustor Check-Out	1.290	Overall & Injector Cameras	Normal Operation No Film Coolants or Air
0060	Combustor Check-Out	2.355	Overall & Injector Cameras	Normal Operation No Film Coolants or Air
0070	Combustor Check-Out	4.970	Overall & Injector Cameras	Normal Operation No Film Coolants or Air
0080	Instrumentation Check-Out	1.295	Overall, Injector, and Manometer Bank Cameras. Color, False Color, IR & UV Close Up All Three Windows. Zone Radiometer-Window #3 Position 8.	Off Design Mixture Ratio

TABLE 1 (CONT)

TESTING SUMMARY

Test No.	Type	Test Duration (Seconds)	Instrumentation & Location	Remarks
0090	Instrumentation Check-Out	2.095	Overall, Injector, and Manometer Bank Cameras. Color, False Color, IR & UV Close Up All Three Windows. Zone Radiometer-Window #3 Position 8.	Off Design Mixture Ratio
0100	Instrumentation Check-Out	5.265	Overall, Injector, and Manometer Bank Cameras. Color, False Color, IR & UV Close Up All Three Windows. Zone Radiometer-Window #3 Position 8.	Off Design Mixture Ratio - Nozzle Tip Erosion
0101	Instrumentation Check-Out	4.245	Overall, Injector, and Manometer Bank Cameras. Color, False Color, IR & UV Close Up All Three Windows. Zone Radiometer-Window #3 Position 8. Schlieren - Window #1.	Off Design Mixture Ratio-Repeat of Test 0100

TABLE 2

TEST PARAMETERS*

Test No.	Date	P_{atm} psia	T_{atm} F	Relative Humidity %	Air System: Flowrate lb/sec	Air System: T_{mc} F	Air System: P_{mc} psig	Air System: ρ_{mc} lb/ft^3	Air System: V_{mc} ft/sec	Air System: Mach No.
0010	7-18-68	13.8	88	25	2.86	82	0.28	0.0703	284.2	0.249
0020	7-18-68	13.8	88	25	3.15	81	0.31	0.0707	311.7	0.273
0030	7-18-68	13.8	88	25	3.30	81	0.34	0.0709	324.7	0.285
0040	7-18-68	13.8	88	25	4.33	77	0.63	0.0728	415.7	0.366
0050	8-28-68	13.75	94	18	—	—	—	—	—	—
0060	8-28-68	13.75	94	18	—	—	—	—	—	—
0070	8-28-68	13.75	94	18	—	—	—	—	—	—
0080	1-16-69	13.9	70	88	3.45	64	0.50	0.0739	326.6	0.291
0090	1-16-69	13.9	72	88	3.44	66	0.45	0.0736	327.7	0.291
0100	1-16-69	13.9	72	88	3.50	65	0.25	0.0737	331.9	0.296
0101	2-4-69	13.82	74	38	3.42	68	0.36	0.0729	327.7	0.291

*All parameters evaluated at mid duration.

TABLE 2 (CONT)

	Low Pressure Film Coolant								
Test No.	Flowrate lb/sec	T_{mc} F	P_{mc} psig	ρ_{mc}, lb/ft	V_{mc} ft/sec	Mach No.	$\dot{w}_{LOX}$ lb/sec	$\dot{w}_{GH_2}$ ft/sec	P_c psig
0010	0.86	41	-0.26	0.0718	411.1	0.368	3.63	——	——
0020	0.79	46	-0.25	0.0712	379.8	0.338	3.28	1.07	353.8
0030	0.73	54	-0.25	0.7010	359.2	0.318	5.79	1.06	394.0
0040	0.83	52	-0.26	0.0704	404.8	0.359	5.88	1.06	456.0
0050	——	—	——	——	——	——	5.11	1.10	372.0
0060	——	—	——	——	——	——	5.24	1.12	372.0
0070	——	—	——	——	——	——	5.51	1.09	369.0
0080	1.17	-8	-0.18	0.0802	501.8	0.473	6.54	0.65	316.0
0090	1.17	-9	-0.18	0.0804	501.2	0.473	6.63	0.62	324.0
0100	1.22	-3	-0.18	0.0794	528.5	0.496	6.58	0.62	321.0
0101	1.25	-2	-0.31	0.0780	551.0	0.513	6.63	0.66	334.2

TABLE 2 (CONT)

	Low Pressure Film Coolant								
Test No.	Flowrate lb/sec.	T_{mc} F	P_{mc} psig	P_{mc} lb/ft^3	V_{mc} ft/sec	Mach No.	Mixture Ratio	$\dot{w}_{TOT}$	η_{c*}
0010	4.21	-52	0.80	0.0882	1008.3	1.0	——	3.63	——
0020	4.18	-50	0.70	0.0879	1010.4	1.0	3.06	4.35	131.1+
0030	4.08	-43	0.49	0.0864	1018.6	1.0	5.48	6.84	99.7
0040	4.04	-42	0.38	0.0861	1020.6	1.0	5.55	6.94	113.3Δ
0050	——	——	——	——	——	——	4.64	6.21	100.9
0060	——	——	——	——	——	——	4.70	6.36	98.8
0070	——	——	——	——	——	——	5.06	6.60	95.6
0080	4.26	-80	0.40	0.0955	972.7	1.0	10.12	7.19	89.5
0090	4.31	-81	0.50	0.0957	971.6	1.0	10.71	7.25	93.0
0100	4.21	-74	0.20	0.0940	980.1	1.0	10.56	7.21	91.9
0101	4.33	-69	0.85	0.0923	986.5	1.0	10.06	7.29	94.2

+ Duration too short for acurate flowrate measurement

Δ Includes effects of copper and water vaporization

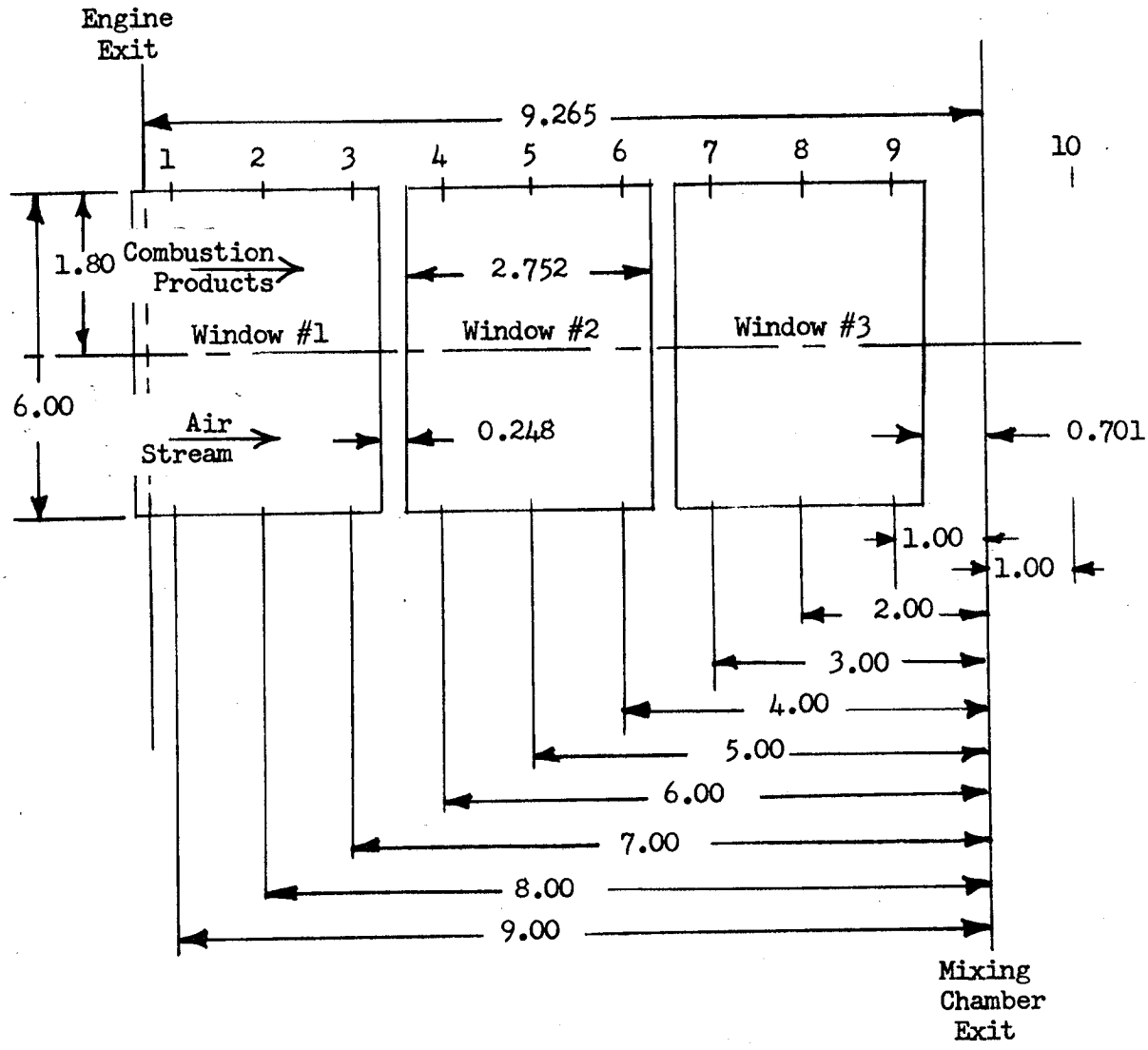

Position	Distance from Start of Mixing Region
1	0.265
2	1.265
3	2.265
4	3.265
5	4.265
6	5.265
7	6.265
8	7.265
9	8.265
10	10.265

All dimensions in inches

Figure 10. Instrumentation Location Positions

of the observations with the color photographs of the mixing region, Fig. 9, and the schlieren data for window No. 1, Fig. 11.

The edge of the mixing region indicated on the schlieren is at an angle of 12.5 degrees which roughly corresponds with the 14 degree angle of the outer boundary on the UV photograph. However, of more significance is the correspondence in both space and angle of the inner boundary and the radiation displayed on the color photograph. The location was identical and the angles were 5.5 and 6.0 degrees, respectively. The above clearly indicates that an appreciable air-exhaust products reaction layer exists even when cold air is utilized. Final proof of these observations must await more accurate spectroscopic data. Figure 12 is a schematic depicting the location of the boundaries, the edge of the mixing region, and the visible emission with respect to a computer prediction (furnished by the contract monitor) of the temperature profiles for mixing between ambient air and a GH_2-LOX combustor exhaust.

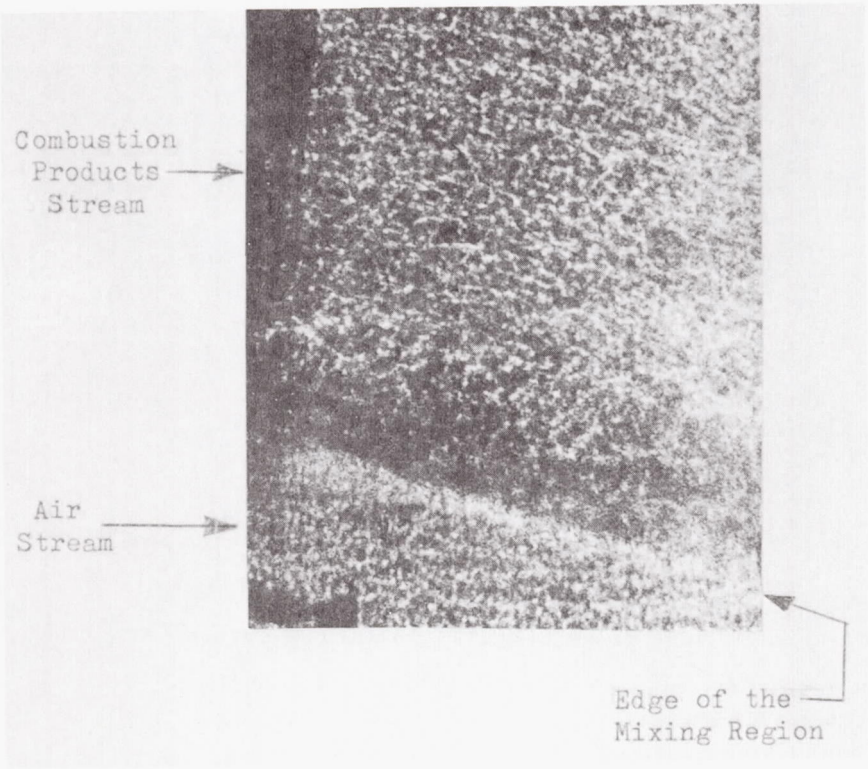

Figure 11. Schlieren through Window No. 1

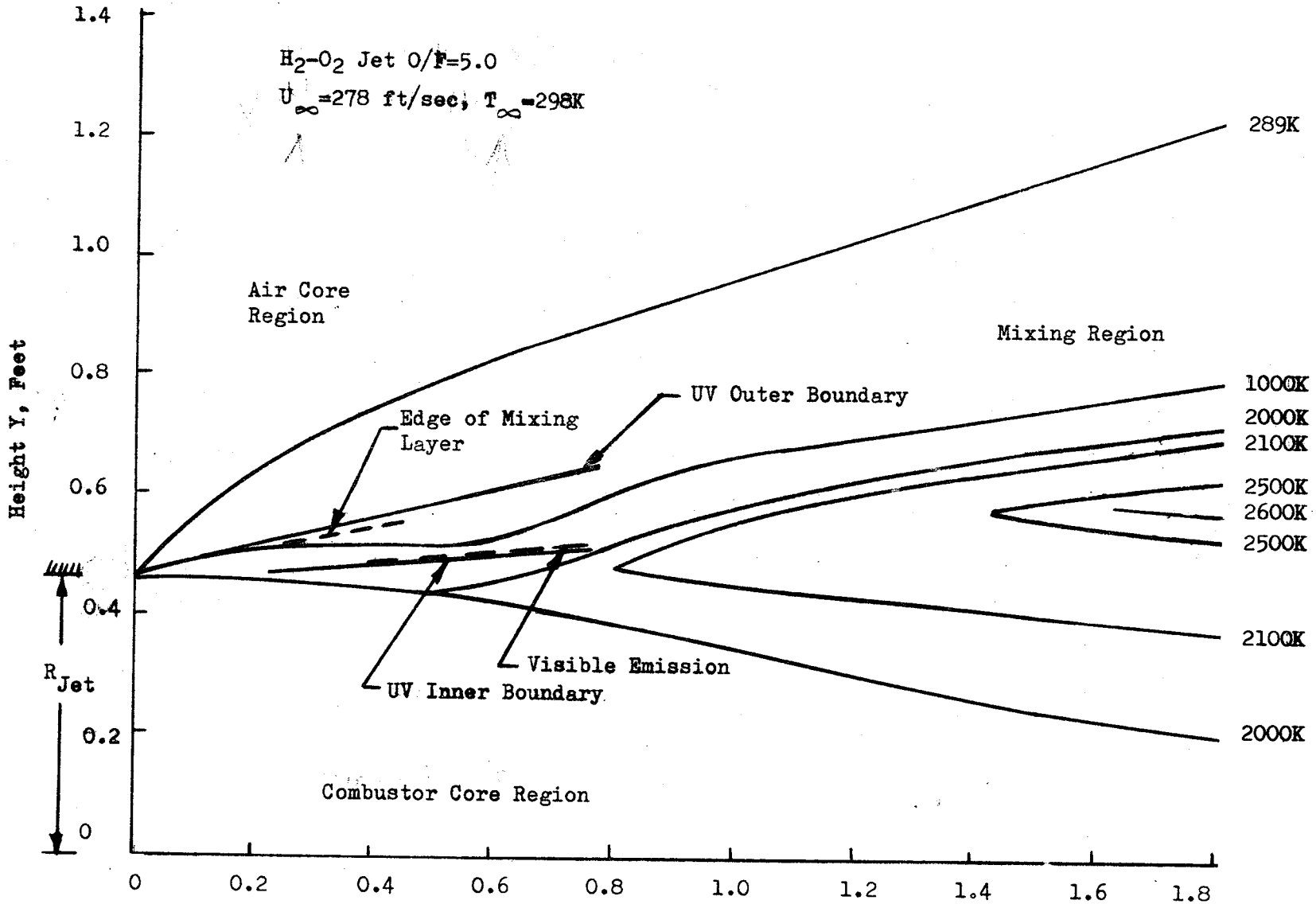

Figure 12. Schematic of Mixing Region

RECOMMENDATIONS

A carefully designed flow facility, appropriate test hardware, and optical instrumentation systems have been assembled for the study of two-dimensional mixing of supersonic hydrogen-oxygen combustion products with a subsonic heated air stream.

It is recommended that the apparatus be utilized in a comprehensive experimental program. This program would provide well controlled precise experimental data for the determination of the effects of temperature ratio, turbulence level, velocity ratio, and changes in ambient conditions upon the mixing. The characterization of the mixing region should include a mapping of temperature, velocity, pressure, concentration, and enthalpy. Recommended experiments that will help to gather the required data are as follows:

1. Diagnostic experiments to determine the two dimensionality of the flow field and the effect of film cooling on the mixing region.
2. A mixing study that includes a precise mapping of the mixing region for the basic case, then a determination of the effects upon the mixing layer produced by changes in the air turbulence level, air temperature, inlet geometry, and velocity ratio.
3. Tests with a CO_2 seeded air stream. The use of this tracer enables further elucidation of the penetration of the air stream into the combustion products stream.
4. Testing, which would require additional hardware, over a more complete range of experimental variables. These would include different mixture ratios, a wide range of combustion product-air stream velocity ratios, and elevated test section pressures.
5. Mixing studies utilizing different propellant combinations at similar conditions tested with the LOX-GH_2 combustor.

REFERENCES

1. Wrubel, J. A.: Performance Analysis of Composite Propulsion Systems, Phase I Final Report, Contract NAS7-521, Rocketdyne, a Division of North American Rockwell Corporation, Canoga Park, California, January 1968.
2. Incropera, F. P., and G. Leppert: "Investigation of Arc Jet Temperature Measurement Techniques," Stanford University, ISA Transactions, Vol. 6, No. 1, January 1967.
3. Vassallo, F. A.: "A Fast Acting Minature Enthalphy Probe," Cornell Aeronautical Lab," AIAA 3rd Aerodynamic Testing Conference, Preprint No. 68-391, April 1968.
4. Kilburg, R. F.: "A High Response Probe for Measurement of Total Temperature and Total Pressure Through a Turbulent Boundary Layer with High Heat Transfer in Supersonic Flow," General Dynamics, AIAA 3rd Aerodynamic Testing Conference, Preprint No. 68-374, April 1968.
5. McCroskey, W. J.: "Density and Velocity Measurements in High Speed Flows," NASA Ames Research Center, AIAA 3rd Aerodynamic Testing Conference, Preprint No. 68-392, April 1968.
6. Anderson, L. A., and R. E. Sheldahl: "Flow-Swallowing Enthalphy Probes in Low Density Plasma Flows," NASA Ames Research Center, AIAA 3rd Aerodynamic Testing Conference, Preprint No. 68-390, April 1968.
7. Buckingham, D. J.: An Optical Method of Measuring Flow Velocity in Arc-Heated Wind Tunnels, Aeronautical Research Council, Great Britain, ARCR & N No. 3439, March 1965.
8. Kenworthy, M. J.: "New Techniques for Supersonic Combustion Measurements," General Electric Company, AIAA Paper 67-223, January 1967.

9. Goodier, B. G.: "Cooled High Temperature Thermocouples for Phoebus Reactors," Los Alamos Scientific Laboratory of the University of California, AIAA 2nd Propulsion Joint Specialists Conference, AIAA Paper 66-556, June 1966.

10. Muntz, E. P., Harris, C. J., and E. M. Kaegi: Techniques for Experimental Investigation of the Properties of Electrically Conducting Hypersonic Flow Fields, General Electric Company, R63SD27, March 1963.

11. Rocketdyne: An Instrumentation System to Study Rocket Exhaust Plume Radiative Processes, R-6288, August 1965.

12. Kenworthy, M. J., Stanforth, C. M., and W. C. Colley: Investigation of Instrumentation and Simulation Techniques for the Supersonic Combustion Process, General Electric Company, AFAPL-TR-66-76, October, 1966.

13. Gordon, S. A.: The Use of Ionization Probes to Determine Rocket Motor Parameters, Aerochem Research Labs, TP-120, September 1965.

14. Nye, J. O. and R. S. Brodkey: "Light Probe for Measurements of Turbulent Concentration Fluctuations," Ohio State University, Review of Scientific Instruments, 38, 26-29, January 1967.

15. Frohm, A.: "Measurement of Concentration Profiles in Jets Using Fizeau Fringes," Cornell University, AIAA Journal, Vol. 5, No. 1, January 1967.

16. Judge, J. F.: "Greyrad Building a Market in Heat Transfer Measurement," Aerospace Technology, January 1968.

17. Ahlborny, A. and A. J. Barnard: "Velocity Measurement by Doppler Effect," University of British Columbia, AIAA Journal, Vol. 4, No. 6, June 1966.

18. Grey, J.: "Cooled Probe Diagnostics of Dense Plasma Mixing and Heat Transfer Processes," Greyrad Corporation, AIChE Journal, Preprint No. 9C, November 1967.

19. Grey, J.: "Thermodynamic Methods of High Temperature Measurements," Princeton University, ISA Transactions, Vol. 4, No. 2, April 1965.

20. Grey, J., Jacobs, P. F., and M. P. Sherman: "Calorimetric Probe for the Measurement of Extremely High Temperature," Princeton University, Review of Scientific Instruments, Vol. 33, No. 7, July 1962.

21. Grey, J. and P. F. Jacobs: "Cooled Electrostatic Probe," Princeton University, AIAA Journal, Vol. 5, No. 1, January 1967.

APPENDIX 1

MAJOR PROGRAM DIFFICULTIES

A wide variety of difficulties were encountered on this program. Presented below is a detailed discussion, in cronological order, of major problems and their solutions.

The initial proof test of the water coolant feed lines for the combustor exhaust nozzle/test section assembly indicated seepage past one of the O-ring seals between the nozzle and the test section side wall. After repeated attempts to effect a positive seal, the problem was traced to a mismatch between one of the O-ring/water manifolds and warpage of the test section side wall.

The mismatch was repaired by placing a spacer in the water manifold to assure a positive O-ring seal, planing the side wall in the area of the water manifolds to reduce the warpage, and custom fitting the hardware during assembly. The side wall warpage occurred when the film coolant ducting was welded in place. After completion of the repairs and assembly of the apparatus, a successful proof test was accomplished at twice the operating pressure of the coolant water. The apparatus was then re-installed on the stand; however, due to the leakage problems a three-week-time delay was incurred.

Prior to the first full-scale integrated checkout of the entire system, anomalous behavior (bed temperature greater than the preset value) of the air heater was noted. The countdown was stopped prior to final propellant loading operations and heater electrical power was turned off. An attempt was made to reduce the bed temperature before continuing with the test preparations by actuating the system and blowing air through the bed. After approximately 5 seconds, sparks were observed in the hot air stream and the blower was immediately shut off. At this time the heater burst into flame and before the fire was brought under control

the heater was destroyed (Fig. A1-1). The cause of the incident was traced to the inadvertent use of zirconium tubing rather than what was believed to be stainless steel tubing in the heater bed. Zirconium is highly reactive with air at approximately 1000F, the operating temperature of the air heater. Replacement of the air heater under a Rocketdyne capital job was completed toward the end of this program.

During full scale system check-outs significant erosion of the upper combustion chamber was experienced (Fig. A1-2 and A1-3) during a 2-second mainstage test. The cause of the erosion was attributed to the formation of ice in the coolant passages during the injector chilldown. Post-test inspection indicated an appreciable quantity of water vapor (from aspiration of the trapped coolant water downstream of the main valves) in the gaseous nitrogen water coolant purge.

Modifications to the coolant water sub-system to prevent freezing in the coolant water passages during injector chill-down were made. An 80 psi water flush was plumbed downstream of the water mains to establish water flow through the coolant passages during the chill-down operation. The signal that opens the water mains also closes the water flush mains, providing a rapid flow transition without permitting stagnation.

The most serious problem was noted after post-test inspection of the hardware for the 4 February test. The 2-D nozzle side wall was warped. This relieved the compression on the O-rings causing an excessive water leak during post-test checkouts. It did not appear that any water leakage occurred during the test. The test apparatus was disassembled to facilitate hardware modifications pending a determination of the cause of the warpage. The thermal and stress analysis indicated that the warpage was caused by pressure loading in the divergent section and thermal stress in the convergent section of the two-dimensional nozzle.

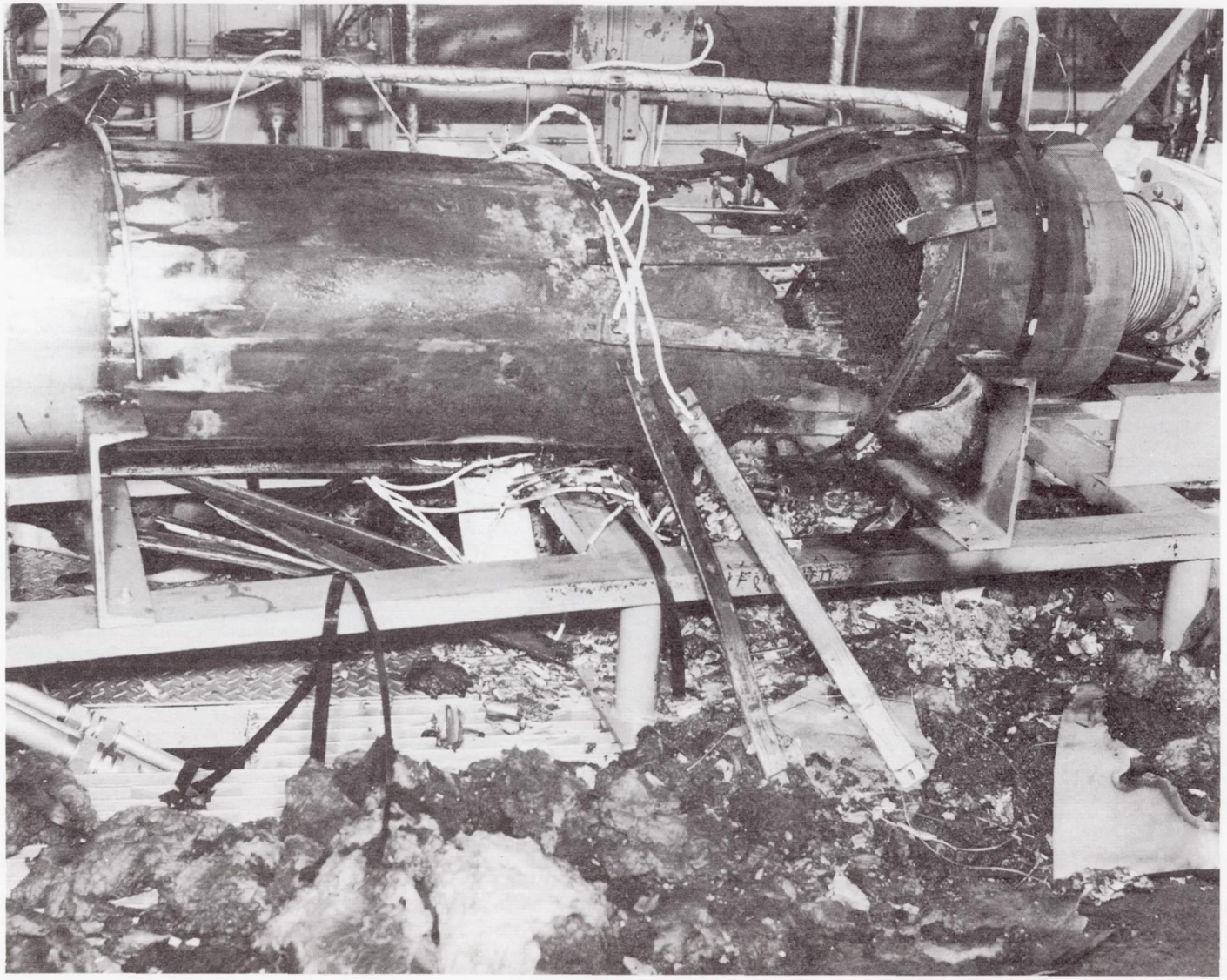

Figure A1-1. Air Heater After Incident

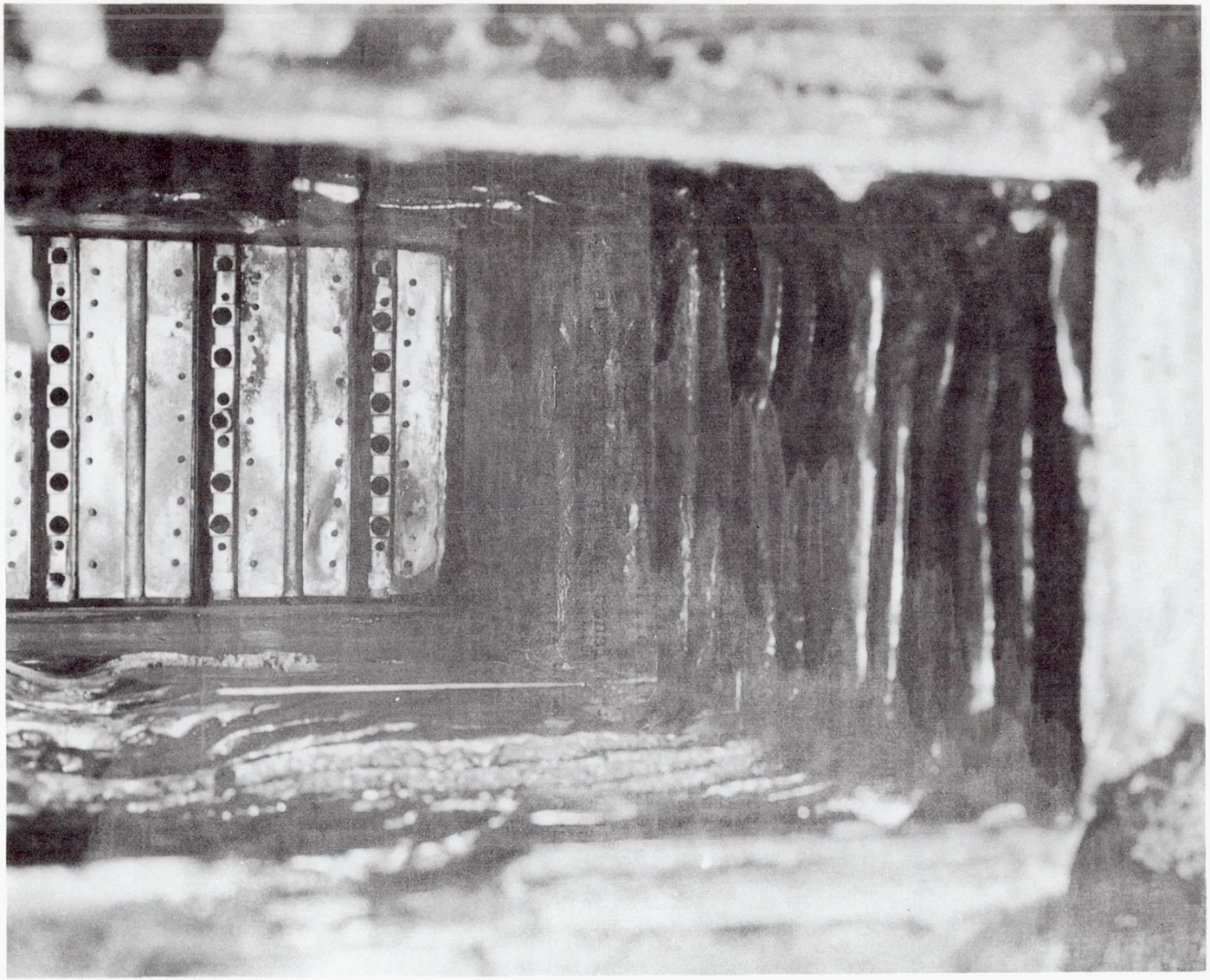

Figure A1-2. Eroded Upper Combustion Chamber - Right Hand Side

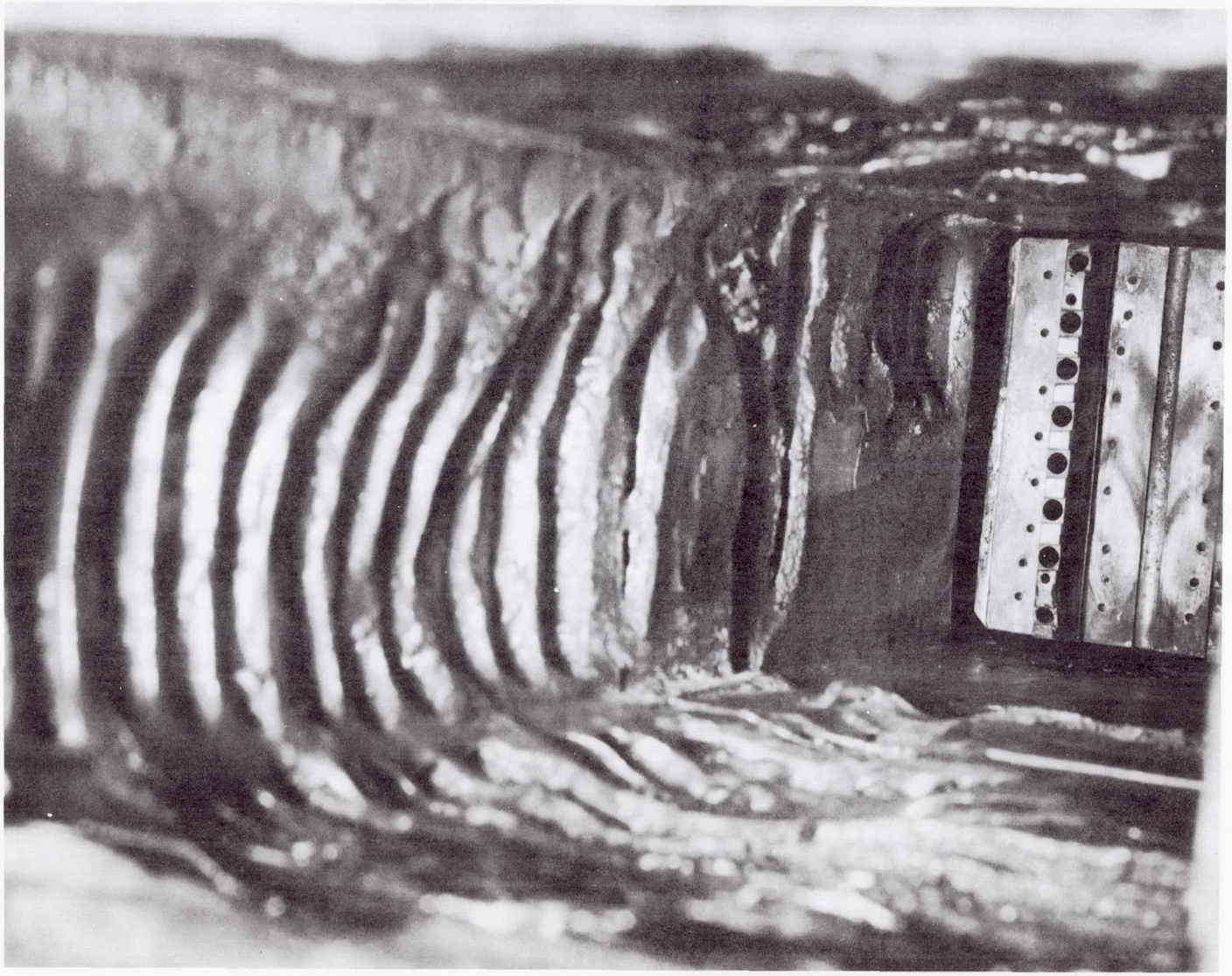

Figure A1-3. Eroded Upper Combustion Chamber - Left Hand Side

Redesign of the hardware has been completed; however, fabrication has been deferred to the anticipated follow-on contract. The modifications consist of reducing the water manifold pressure and welding the water inlet and outlet directly to the nozzle. This eliminates the water leak problem and allows testing to continue even if additional warpage occurs. The present condition of the internal contour of the nozzles is such that it could be fired without significantly altering the 2-D flow field if the water leak did not exist.

APPENDIX 2

ZONE RADIOMETRY

INTRODUCTION

The primary aim of the spectroscopic instrumentation is to experimentally measure temperature and concentration distributions across the mixing region. In particular, the zone radiometer system, developed to study rocket exhaust radiative processes under Contract NAS8-11261 (Ref. A2-1), will be used to determine the temperature and partial pressure profiles for the H_2O molecule from measurements of the spectral emissivity and spectral radiance for various lines of sight. In this Appendix a description is given of the experimental arrangement for zone radiometry measurements, the type of measurements to be carried out, and the data reduction procedures.

EXPERIMENTAL ARRANGEMENT

The zone radiometer spectroscopy system is shown schematically in Fig. 4 of the main text. The greybody source and spectroradiometer were described in complete detail in Ref. A2-1, and will therefore be discussed only briefly here.

The greybody source consists of a 6-inch long, 3/8-inch diamter, electrically heated graphite rod that is mounted in a water-cooled, argon-purged housing. Greybody radiation is optically chopped with a cylindrical "squirrel-cage" chopper to produce an AC signal for absorption measurements. The housing is equipped with a shutter.

Flat mirror M_1 and an 8-inch diameter spherical mirror M_2 form a 1:1 image of the greybody source across a vertical plane perpendicular to the flow axis in the mixing region. The greybody housing is actually mounted above the horizontal optical plane of the system so that it does not obscure a view of the mixing region from other instrumentation. The greybody source optics and flat mirror M_3 may be moved parallel to the flow axis to change the horizontal field of view of the system.

Flat mirrors M_4 and M_5 relay radiation from that part of the mixing region under study to the spectroradiometer.

An optical diagram of the spectroradiometer is shown in Fig. A2-1. Figure A2-2 is a photo of the instrument. The optical path, which is enclosed and purged with dry nitrogen, is of such a length that a 10:1 reduced image of a portion of the mixing region is formed at the monochromator entrance slit by the telescope objective mirror. The field of view of the spectroradiometer at the mixing region is rectangular in cross section (on the order of 3 x 3 millimeters) and perpendicular to the flow axis. The width of this field of view is 10 times the width of the entrance slit. The height of the field of view is determined by an adjustable aperture at the entrance slit. During a test this cam driven aperture will scan different zones (zone radiometry) of the mixing region in the vertical direction. The cross sectional size of the field of view is determined from a trade-off between desired spectral and spatial resolution and available energy.

For emission measurements, the greybody shutter is closed and radiation from the mixing region is optically chopped at the monochromator exit slit. (This chopper is not used during absorption measurements).

The Perkin-Elmer Model 98-G monochromator is equipped with a 240-groves-per-millimeter grating blazed at 3.75 microns and used in first order. Overlapping orders are eliminated by a germanium filter. For the subject program, an uncooled PbS detector is used. The AC output from the detector is amplified, synchronously rectified, and displayed on a strip chart recorder.

An additional flat mirror relay system has been assembled so that the spectroradiometer can view the mixing region outside the combustor from above, rather than horizontally. This system will be used to assist in checking the two-dimensionality of the flow field.

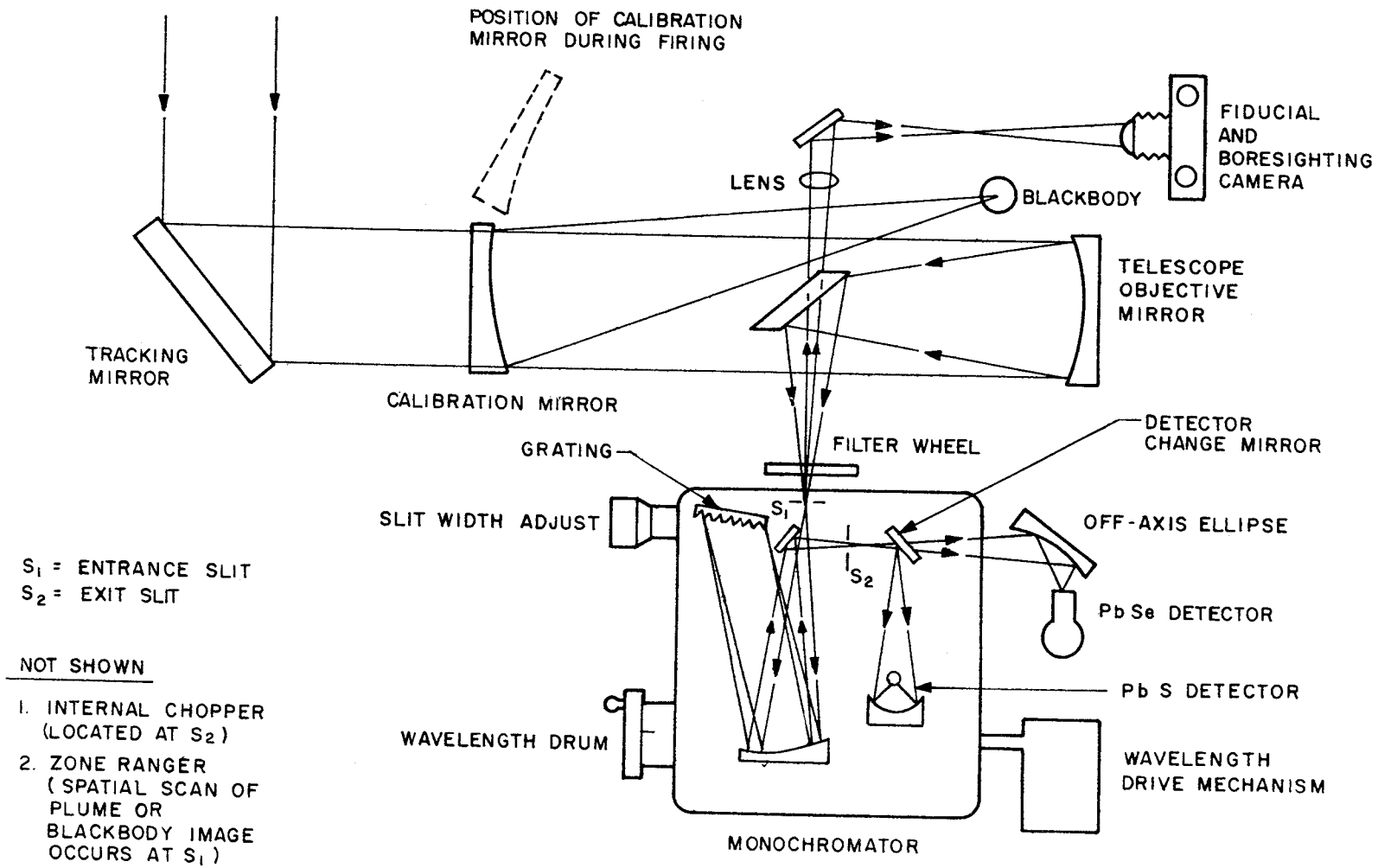

Figure A2-1. Optical Diagram of the Spectroradiometer

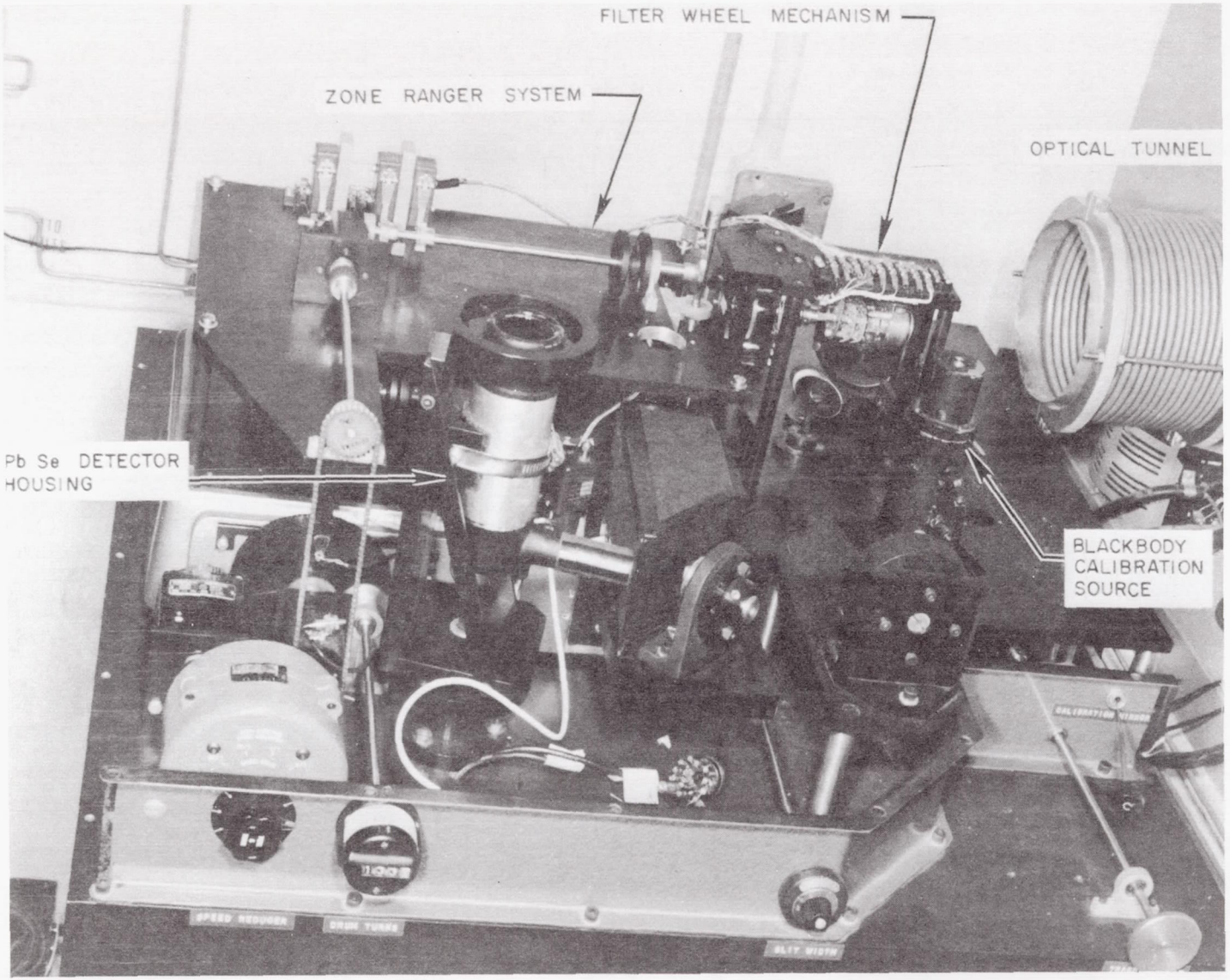

Figure A2-2. Infrared Spectroradiometer

MEASUREMENT TECHNIQUES

Two-Dimensionality Check

The mixing chamber has been designed to produce a two-dimensional flow field, i.e., no gradients in temperature or concentration along horizontal lines-of-sight perpendicular to the flow direction. One method of verifying the two-dimensionality is to view the mixing region along various vertical lines-of-sight lying in a plane perpendicular to the flow direction; there should be no variation in spectral radiance observed from one such line of sight to another. This type of measurement will be carried out early in the test program. These measurements will also indicate the effect of the nitrogen film cooling on the mixing characteristics.

Calibration

Wavelength calibration of the spectroradiometer is carried out by recording atmospheric absorption spectra. Intensity calibration for emission data is made with a blackbody radiation source including the effect of the various mirrors and windows in the optical path. The background spectra for absorption measurements is obtained by scanning the greybody prior to a test. Spatial calibration of the spectrometer field of view is obtained by using the travelling aperature to scan the images of small light sources placed at known positions with respect to the mixing region.

Spectral Scans

The spectroradiometer can be used in a conventional spectral scan mode for either emission or absorption measurements with a fixed line-of-sight through the mixing region. The primary purpose of the spectral scans is to furnish data to allow selection of the optimum wavelength, slit width, and electronic amplification values for the zone radiometry measurements.

Zone Radiometry

On each individual test firing zone radiometry is carried out for emission and absorption measurements at a selected wavelength across a single plane (perpendicular to the flow axis) of the mixing region. Different planes are covered on different tests. On the first half of a test the traveling aperture scans the mixing region image for emission measurements and radiation intensity is recorded as a function of spatial position. For the second half of the test the internal chopper is turned off, and the greybody shutter is opened. Chopped greybody radiation attenuated by combustion products is then recorded as a function of spatial position. Before, or after, a test the blackbody and the greybody are similarly scanned for calibration purposes.

DATA REDUCTION

Because of the two-dimensionality of the flow field, the data reduction procedure is much simpler than described in Ref. A2-1. The data reduction procedure for each line of sight is simply that used for a uniform gas.

Point by point comparison of spatial scans of greybody radiation before a test and greybody radiation attenuated by the flow field during a test allows preparation of graphs of fractional transmission (τ_{LOS}) or emissivity ($\epsilon_{LOS} = 1 - \tau_{LOS}$) as a function of line of sight. In addition, comparison of spatial scans of flow field emission and blackbody emission allows preparation of graphs of spectral radiance (N_{LOS}) as a function of line of sight.

The line of sight temperature is defined by the relation

$$\frac{N_{LOS}}{\epsilon_{LOS}} = N_{BB} \quad (T_{LOS})$$

where N_{BB} (T_{LOS}) is the spectral radiance of a blackbody at temperature T_{LOS} and at the wavelength at which the measurement was carried out.

The H_2O line of sight partial pressure P_{LOS} is determined from the expression

$$\tau_{LOS} = e^{-KL\ P_{LOS}}$$

where L is the path length of the flow field along the line of sight and K is the value of the spectral absorption coefficient of H_2O at T_{LOS} and the wavelength of measurement.

REFERENCES

A2-1 Rocketdyne, An Instrumentation System to Study Rocket Exhaust Plume Radiative Processes, Final Report NAS8-11261, August 1965.

APPENDIX 3

LASS

SPECTROSCOPY WITH THE LASS

A spectroscopic study of the ultraviolet radiation emitted and absorbed by the OH radical in the $^2\Sigma^+ - ^2\Pi$ electronic transition can yield significant information on the kinetic processes causing the radiation, Ref. A3-1 to A3-4 .

The measurements to be taken include:

1. partial pressure of the OH radical
2. effective rotational temperatures of OH in its ground electronic state
3. effective rotational temperatures of OH in its electronically excited state
4. effective electronic excitation temperature of OH.

Measurement 2 is expected to provide the true gas temperature, while the temperatures measured in 3 and 4 may or may not agree with the gas temperature. The agreement is dependent upon whether the region is reacting or in thermal equilibrium. When the temperature measurements disagree, the magnitude of disagreement yields information about the chemical kinetics and is indicative of chemiluminencence. Chemiluminencence is radiation emitted by species formed in an exci state, i.e., radiation originating from a combustion zone. When all temperatures agree, it is normally concluded that the radiation arises from thermal rather than chemical processes. It should be noted that the measured temperatures will also be compared with those determined by measurements in the infrared. A complete delination of the meaning of the various temperatures is beyond the scope of this report and will be included when the experimental data are presented.

Measurements 1 and 2 are obtained from the absorption of a suitable discrete OH spectral line source placed behind the engine, Measurement 3 is determined from relative emission line intensities, and Measurement 4 results from comparison of emission and absorption of a given spectral line. The emission and absorption for these measurements is recorded simultaneously by the technique of electronically separating the chopped absorption signals from the emission signal and recording each one individually. Since the spectral region of interest covers a narrow range, all measurements for a particular axial location can be recorded during a single engine firing of 15 seconds duration.

In addition, the spectroscopy study provides a survey spectra of the ultraviolet and visible radiation from the combustion gases. This will assist in the motion picture photography studies to be described in a later section of this report. These data also allow identification of species, such as the unidentified emitter recorded in the color motion picture.

MEASUREMENT TECHNIQUE

A brief description of the measurements and the relevant data reduction equations are presented below. A more detailed description is available in the references.

Concentration of OH

The concentration of the OH radical is determined from a measurement of absorption of discrete spectral lines. In this technique, the light source, a radio frequency discharge in a tube containing low pressure water vapor, produces an OH emission spectrum of narrow spectral lines. The emission line from this source is absorbed by the broader line in the combustion chamber so that only absorption at the line center is measured.

The concentration of OH is given by the expression (Ref. A3-5)

$$N_{OH} = \frac{Q_R\, Q_V\, b_d P'}{FA_k\, T_{J'J''}} \exp\left(\frac{E_k}{kT}\right) \times 2.40 \times 10^{12} \qquad (1)$$

where E_k is the rotational energy level, k is Boltzmann's constant, Q_R and Q_V are the rotation and vibration partition functions, and b_d is the doppler line half-width. Also, $FA_k = \frac{f}{2J'' + 1}$, where f is the oscillator strength, J'' is the ground state quantum number, $T_{J'J''}$ is a correction factor for vibration-rotation interaction, and T is the rotational temperature.

In addition, $P' = P_{\nu_o} \left\{[\exp(a^2)]\ [\operatorname{erfc}(a)]\right\}^{-1}$

where P_{ν_o} is the absorption coefficient measured at the line center, and

$$a = \frac{b_n + b_c}{b_d} (\ln 2)^{1/2},$$

where b_n and b_c are the natural and collisional half-widths.

In Eq. (1), the values of k, Q_R, Q_V, $T_{J'J''}$, FA_k, b_d, E_k, and a are available in appropriate references. Thus, N_{OH} is determined from a measurement of P_{ν_o} and T.

P_{ν_o} is given by

$$P_{\nu_o} = \frac{I_o}{I}$$

where I and I_o are the transmitted intensities of a line from the discharge lamp through the engine, with and without combustion, respectively. The rotational temperature, T, is measured from P_{ν_o} by the line slope technique.

Measurement of Rotational Temperature of OH Ground State

A. Line Slope Technique

The rotational temperature is determined from the following

equation relating the measured absorption at a line center to the temperature (Ref. A3-2):

$$\log \frac{P_{\nu\,o}}{A_k\, T_{J'J''}} = C - \frac{E_k}{kT} \log e \qquad (2)$$

where C is a constant.

When $P_{\nu\,o}$ is measured, the temperature is determined from the reciprocal of the slope of a graph of

$$\log \frac{P_{\nu\,o}}{A_k\, T_{J'J''}} \quad \text{versus } E_K.$$

B. Iso-Intensity Technique

Another approach for determination of the rotational temperature is given in Ref. A3-1

$$T_R = \frac{(E_x - E_b) \log e}{k\,(\log FA_x\, T_{J'J''} - \log FA_b\, T_{J'J''})} \qquad (3)$$

This technique depends upon the absorption of two lines being equal. The subscripts b and x refer to two lines of equal absorption.

Measurement of Rotational Temperature of OH Excited State

The excited state rotational temperature is measured using equations identical to Eq. (2) and (3), except that the intensity I' of a spectral line emitted by the combustion gas is used in place of P_{ν_o} and E, respectively.

Measurement of Electronic Temperature of OH

The electronic temperature, T_e, is determined from the equation

$$N_g = \frac{I}{I_o} N_{BB}\ (\lambda, T_e)$$

where N_g is the measured radiance of the gas and N_{BB} is the radiance

of a blackbody at the same temperature as the OH electronic temperature, T_e. T_e is determined from tables of the blackbody function.

INSTRUMENT SUB-SYSTEMS

The construction of the spectrum resolving and recording instrument has been completed by the Rocketdyne Research Division. It is a versatile instrument for applications involving the examination and analysis of the ultraviolet and visible radiation emitted by rocket engines and similar sources.

Figure A3-1 is an optical schematic of the LASS. Its principal parts are: (1) a combination spectrograph/spectrometer, (2) the entrance optics, (3) a system for wavelength and intensity calibration, and (4) the electronics (not shown in the figure) for photodetection, data recording, and calibration.

Spectrometer-Spectrograph

A schematic of the combination spectrometer/spectrograph is shown in Figure A3-2. Made by the McPherson Instrument Company, the Model 216 is a 1-meter focal length, stigmatic, Czerny-Turner optical system having an f/no. of 8.7. By using different gratings, the instrument covers a wavelength range from 2000 A to 8 microns. The focusing mirror is twice as large as the collimating mirror and thus intercepts a greater portion of the diffracted light rendering eight inches of the focal plane usable. Utilization of a film cassette in the focal plane permits spectrographic operation. In this mode, the instrument is capable of photographing 1700 A of spectra per exposure with a 1200-line-per-millimeter grating. Since the grating may be rotated between exposures, a series of exposures can cover any desired spectral range. Multiple exposures on each film are made by translating the cassette.

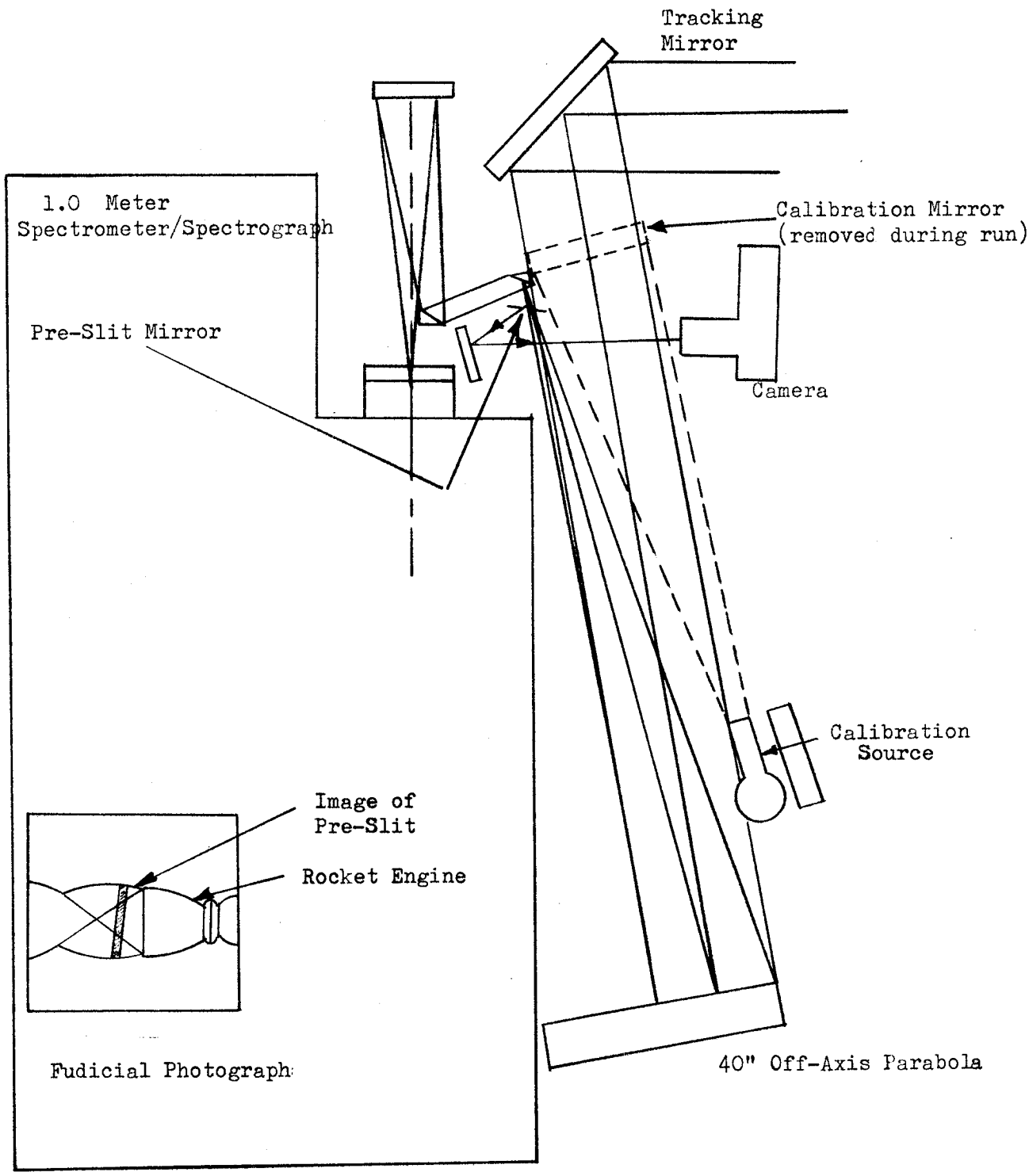

Figure A3-1. Optical Diagram of Large Aperture Spectrometer/Spectrograph

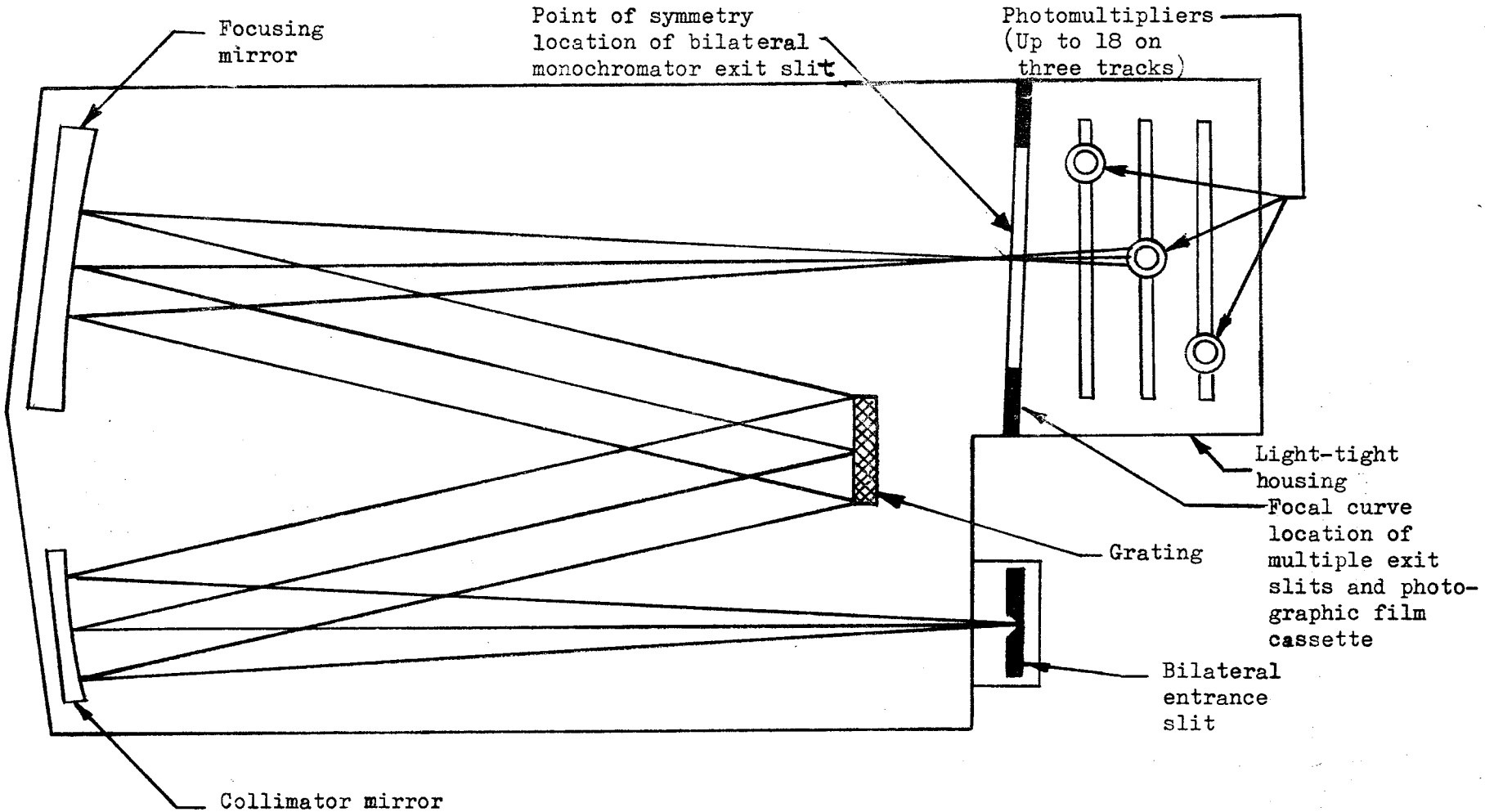

Figure A3-2. Optical Arrangement of the McPherson Model 216 Spectrometer/Spectrograph

For use as a spectrometer, a single adjustable exit slit is mounted at the center of the focal plane. All of the diffracted light corresponding to the wavelength at the observation location passes through the exit slit. The light is detected by a photomultiplier tube mounted on a rack in a light-tight enclosure behind the focal plane. Wavelength scanning is accomplished automatically at a range of speeds from 1 A per minute to 4000 A per minute with a 1200 line per millimeter grating. Utilization of a 600-line-per-millimeter grating doubles the scan rate.

Entrance Optics

The entrance optics consist of two optical subsystems, the collecting optics and the fiducial optics. The collecting optics focus the source radiation onto the entrance slit of the spectrometer/spectrograph, while the fiducial optics show the location of the source on the entrance slit. Since the McPherson Model 216 instrument is stigmatic, the image of the source on the entrance slit has a point-to-point correspondence with the image of the slit on the focal plane of the instrument. In addition, it should be noted that the optical system was designed for minimum optical aberrations.

As shown in Fig.A3-1, the collecting optics gather radiation from the source with a tracking flat mirror and a 6-inch diameter 40-inch focal length off-axis parabolic mirror. These mirrors focus the light on a plane which intersects the plane of the preslit mirror (a mirror with a narrow slice cut through it). Light passing through the pre-slit mirror is reflected off a small plane mirror just behind the pre-slit mirror to a second flat mirror. The light is then reflected by a spherical mirror which focuses the pre-slit onto the entrance slit of the McPherson instrument.

In the fiducial sub-system, the portion of the light striking the pre-slit mirror is reflected onto a flat diagonal mirror and is imaged on the film or view finder in the camera. The image in the

view finder is used to boresight the instrument while the image on the film produces a fiducial photograph as shown schematically in the inset on Fig. A3-1. The shadow of the pre-slit in the fiducial photograph locates the region of the source under investigation.

Calibration System

The calibration system utilizes a calibrated tungsten ribbon filament lamp for intensity calibration and a hollow cathode iron discharge lamp for calibrating wavelength and spectral line intensity. The calibration mirror directs the lamp radiation through the same number of reflections as traversed by the source radiation. Each lamp is operated from separately regulated DC power supplies and the calibration source is selected by a small angular rotation of the calibration spherical mirror. When not in use, this mirror is removed.

Electronics

A highly regulated DC high voltage supply is used for the photomultiplier tubes which can supply power up to the maximum spectrometer capacity of eighteen tubes. The photomultiplier output is normally recorded by an Offner 7-channel strip chart pen recorder system. When the LASS is operated at high scanning speeds, a higher response recording system is required; then the photomultiplier outputs are recorded on magnetic tape.

The absorption source is a water vapor discharge lamp which is excited by a 100 watt, 2450 megahertz RF power generator. The light from this source is mechanically chopped at 400 hertz in order that it can be electronically separated from the combustion radiation.

REFERENCES

A3-1 - Dieke, G. H., and H. M. Crosswhile: Bumblebee Series Report, No. 87, John Hopkins University, 1948.

A3-2 Kostkowski, H. J., and H. P. Broida: National Bureau of Standards Report 4418, Dec. 1954 - Dec. 1955.

A3-3 Lezberg, E. A., Rose, C. M., and R. Friedman: NASA TND-2883, June 1965.

A3-4 Padley, P. J.: Faraday Society, Vol. 56, 1960.

A3-5 Lezberg, E. A., and D. R. Buchels: NASA TND-2441, 1964.

APPENDIX 4

PHOTOGRAPHIC MEASUREMENTS

A number of photographic measurements are utilized to provide supplemental information for comparison with the previously discussed optical methods of data collection. These measurements include schlieren, ultraviolet, infrared, color, false color, and photopyrometry photography. A brief discussion of these techniques follows.

SCHLIEREN PHOTOGRAPHY

Schlieren photography is one approach for the determination of the boundaries of the mixing region in both the horizontal and vertical directions for the check on two-dimensionality of the flow and film coolant effects experiments. This technique provides a cross reference with the data gathered with the zone radiometer and furnishes a visual picture of the phenomena of interest. Utilization was made of Rocketdyne's test site schlieren apparatus. Simple efficient operation is achieved through the use of a specially-designed schlieren lens attachment for a 16-millimeter Fastax camera and a portable parabolic mirror with a rigid mounting base. A high intensity pulsed light source is provided by an EG&G, Inc., Model 501 high-speed stroboscope. The test set-up is shown schematically in Fig. A4-1. For these experiments the knife edge was oriented vertically to accentuate horizontal density gradients. A discussion of the theory of operation of a schlieren system will not be presented here since it is adequately covered in the open literature, e.g., Ref. A4-1 and A4-2.

MOTION PICTURE PHOTOGRAPHY

The initial photographic studies incorporated an array of five cameras to record radiation from the following spectral regions:

1. 3100 A - corresponds to the (0,0) OH band, the region where OH radiates most intensely

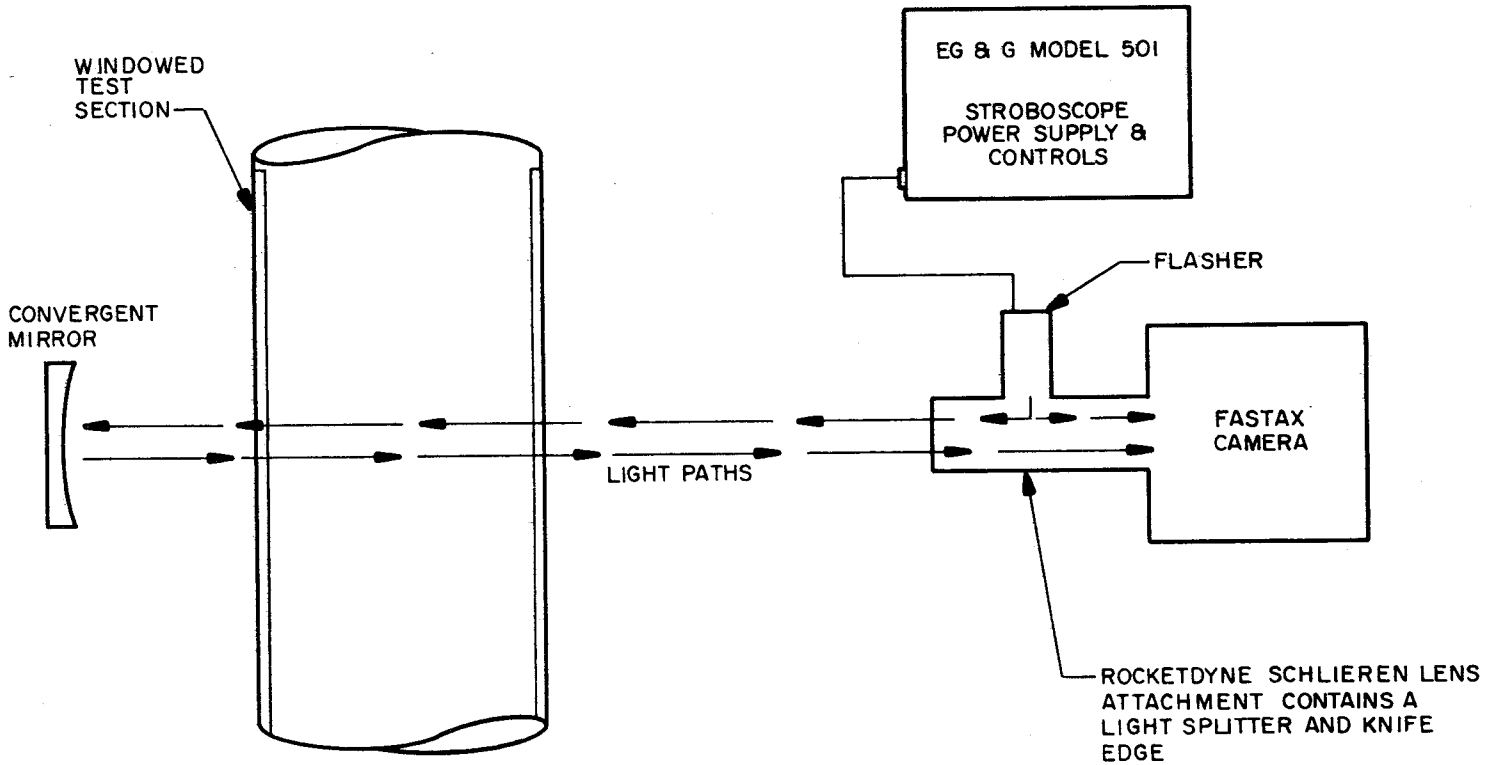

Figure A4-1. Schematic of Schlieren Apparatus

APPENDIX 4

PHOTOGRAPHIC MEASUREMENTS

A number of photographic measurements are utilized to provide supplemental information for comparison with the previously discussed optical methods of data collection. These measurements include schlieren, ultraviolet, infrared, color, false color, and photopyrometry photography. A brief discussion of these techniques follows.

SCHLIEREN PHOTOGRAPHY

Schlieren photography is one approach for the determination of the boundaries of the mixing region in both the horizontal and vertical directions for the check on two-dimensionality of the flow and film coolant effects experiments. This technique provides a cross reference with the data gathered with the zone radiometer and furnishes a visual picture of the phenomena of interest. Utilization was made of Rocketdyne's test site schlieren apparatus. Simple efficient operation is achieved through the use of a specially-designed schlieren lens attachment for a 16-millimeter Fastax camera and a portable parabolic mirror with a rigid mounting base. A high intensity pulsed light source is provided by an EG&G, Inc., Model 501 high-speed stroboscope. The test set-up is shown schematically in Fig. A4-1. For these experiments the knife edge was oriented vertically to accentuate horizontal density gradients. A discussion of the theory of operation of a schlieren system will not be presented here since it is adequately covered in the open literature, e.g., Ref. A4-1 and A4-2.

MOTION PICTURE PHOTOGRAPHY

The initial photographic studies incorporated an array of five cameras to record radiation from the following spectral regions:

1. 3100 A - corresponds to the (0,0) OH band, the region where OH radiates most intensely

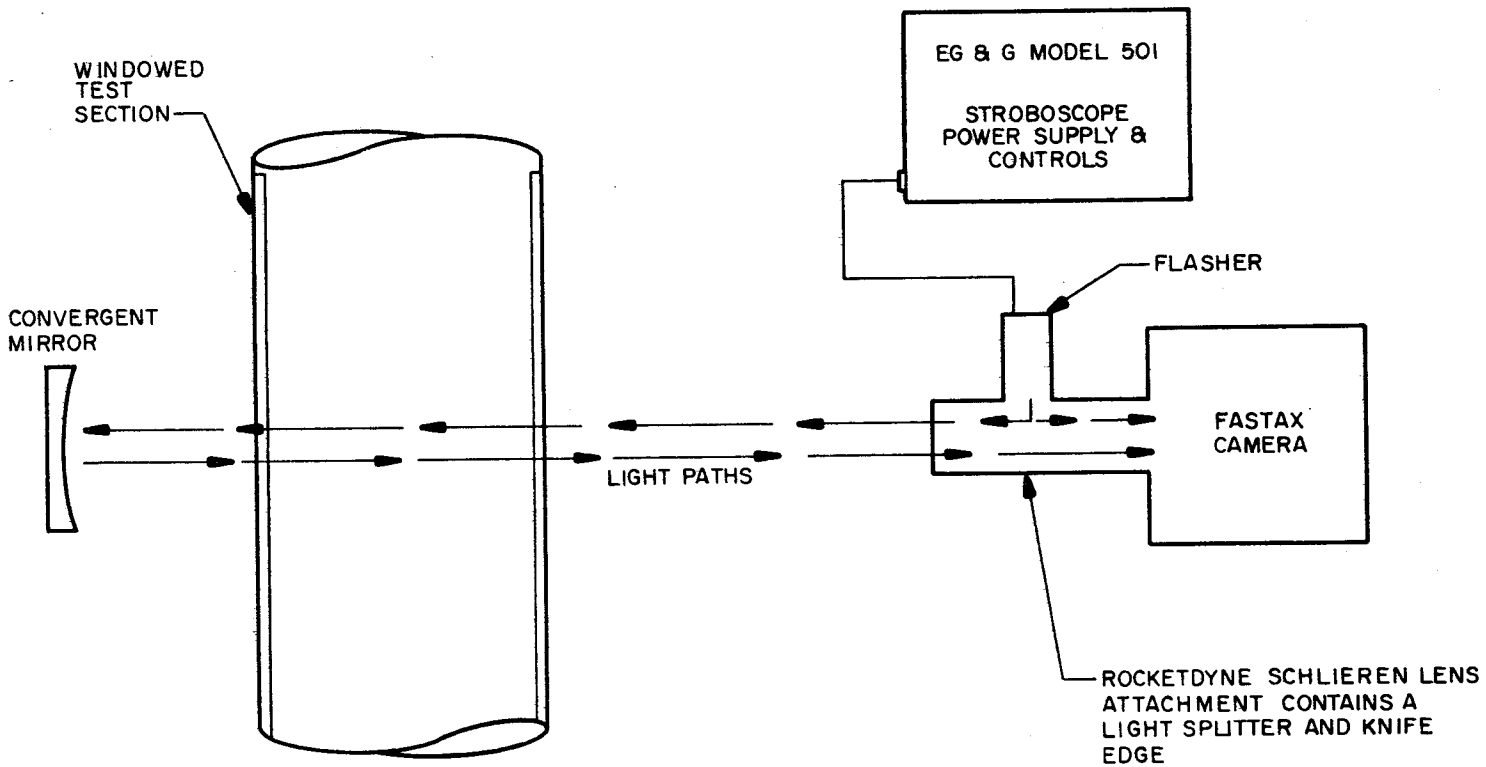

Figure A4-1. Schematic of Schlieren Apparatus

2. 3500-4500 A - the "blue continuum" which may be caused by the recombination reaction

$$H + OH \longrightarrow H_2O + h\nu$$

3. infrared from 7000-8500A - corresponds to weak water emission bands which have been recorded in previous work at Rocketdyne
4. visible from 4000-6300 A - includes some of the blue continuum and impurities which may be present

Table A4-1 presents the spectral regions recorded, the possible emitter species, and types of lens, filters, and films utilized. The film records of the initial test runs were evaluated for their information content and only those spectral regions that yield specifically useful information were used for monitoring subsequent tests.

The cameras were located in a cluster approximately 10 feet from the engine with a direct line of sight perpendicular to the windows. Full photographic coverage was employed on tests 0080 through 0101. Initially, Fastax cameras capable of framing rates up to 8000 frames per second were utilized, however, optical emission was too weak to be recorded at high framing rates. Therefore, on subsequent tests lower framing rate Bell and Howell and Millikan cameras were employed.

The objectives of the motion picture coverage are to 1) determine the spatial distribution of emission from each emitting species, 2) assist in identification of species by intercomparison of the spatial distribution of emission from the different film records, 3) determine the stability of the flow field with respect to time, and 4) provide a visual analog to the spectroscopic data.

For the initial engine tests, photographic coverage was intended to determine the proper film exposures, film and filter combinations, and the spectral region most favorable for flow diagnostics. The partially completed accomplishments to date include:

TABLE A4-1

FASTAX EQUIPMENT SPECIFICATIONS

FOR COMPOSITE PROPULSION SYSTEM

Spectral Region (A)	Chief Emitter	Lens Type	Filter	Film
2850-3150	OH	Quartz, Ultra-violet transmitting	OCLI	2498 RAR
3500-4500	O + OH Recombination	Glass	Corning 0-52 plus Wratten 39	2498 RAR
4000-6300	H_2O, O + OH Recombination, Impurities	Glass	Wratten 2B	Ektachrome EF Daylight
7000-8500	H_2O	Glass	Wratten 89B	False Color IR
3500-6300	H_2O, O + OH Recombination, Impurities	Glass	None	Ektachrome EF Daylight

(1) Emission in the visable spectral region was successfully recorded. Proper exposure is f/2.5 at 64 frames per second.

(2) An unidentified species was recorded in the 7000-8500 A spectral region. Spectroscopic measurements are required for its identification.

(3) Ultraviolet radiation was recorded in the 3100 A spectral region. Proper exposure is f/3.5 at 8 frames per second.

(4) No IR emission was detected, even at the maximum exposure setting of the Bell & Howell camera (f/2.5 and 8 frames per second). However, since the radiation from normal sunlight did not appear on the film for this camera setting, it is possible that a time exposure will reveal IR radiation in the mixing region. This approach will be attempted on future tests.

(5) The 3500-4500 spectral region was not successfully recorded. Further attempts are planned.

PHOTOPYROMETRY

The photopyrometer consists of a Nikon F 35 mm camera equipped with an automatic rewind motor and an ultraviolet transmitting lens, optical interference filters to isolate a narrow band of radiation in the desired spectral region, a tungsten ribbon filament lamp, and an optical calibration system consisting of mirrors and an attenuating step filter, Fig. A4-2.

With the ultraviolet photopyrometer, the radiation from the OH radial can be photographed and a contour map of the OH brightness temperature can be obtained. The map is an aid in defining the spatial extent of combustion. A tungsten lamp ribbon filament of known spectral radiance is also imaged on the film record. The ribbon filament is attenuated by a step filter of known attenuation and thus provides a calibration source for data reduction. The initial step in flow field maping utilizes an automatic-scanning microdensitometer which produces an

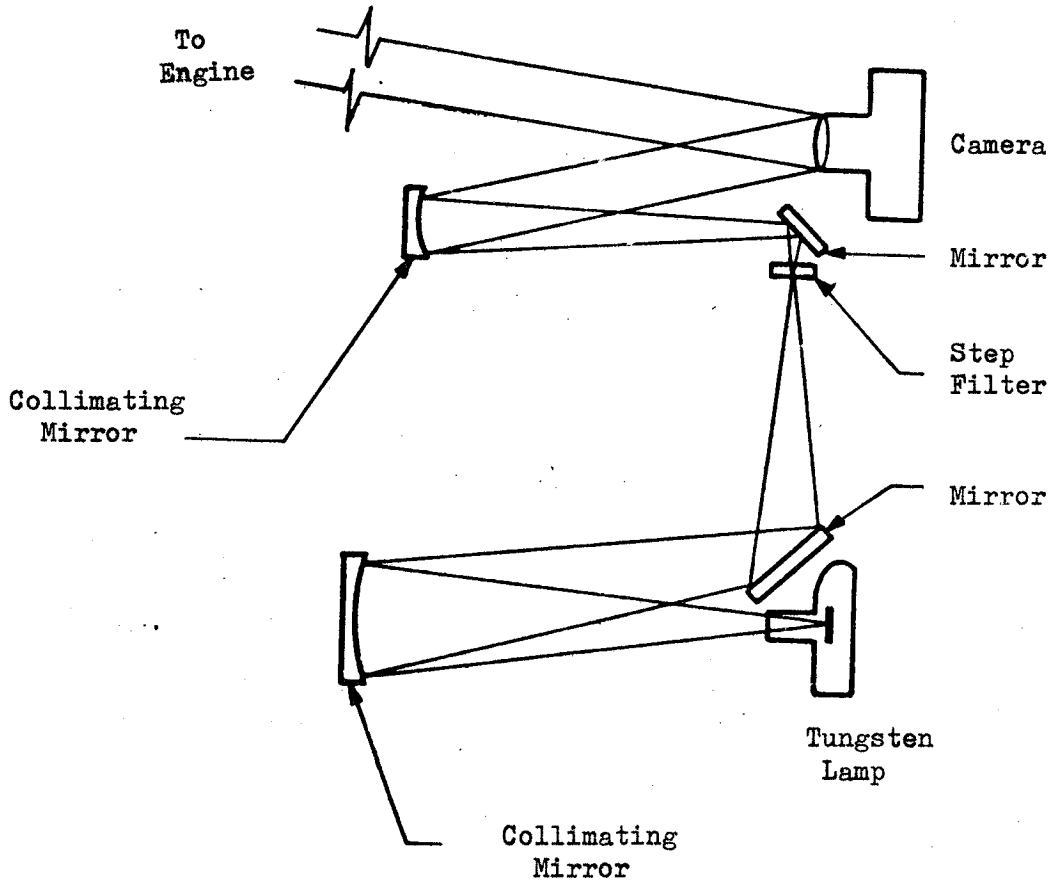

Figure A4-2. Optical Diagram of Photographic Pyrometer

isodensity contour map of the gas flow image. In addition, the microdensitometer produces a density measurement of each zone of the step filtered lamp image. The film response is then determined by graphing the film density of each zone versus the logarithm of radiance. A value of radiance or its equivalent brightness temperature can them be assigned to each isodensity contour in the exhaust plume.

The OH brightness temperature at a given point in the flow field is a function of both OH concentration and the electronic excitation temperature, which may be equal to or greater than the gas translational temperature. Complete interpretation of the photopyrograms is difficult and the various postulations can only be resolved through correlation with the LASS spectroscopic data.

REFERENCES

A4-1. Shapiro, A. H.: The Dynamics and Therodynamics of Compressible Fluid Flow, The Ronald Press Company, New York, 65-67, 1963.

A4-2. Keagy, W. R., Jr., and H. H. Ellis: "The Application of the Schlierin Method to the Quantitative Measurement of Mixing Gases and Jets," Third Symposium on Combustion, Flame, and Explosion Phenomena, Williams & Wilkins Co., Baltimore, Md., 1949.

APPENDIX 5

HOT FIRE DATA REDUCTION COMPUTER PROGRAM

A computer program has been written in FORTRAN language to reduce hot firing data with the General Electric 420 Timesharing Computer.

The program, entitled SSMIX, consists of a main program which handles the majority of the data reduction, two "function" sub-routines which convert millivolt values to temperatures in degrees fahrenheit for chromel-alumel and iron-constantan thermocouples, and a "function" which provides compressible isentropic flow parameters as a function of Mach number.

Attached hereto are the following: program summaries, a definition of program variables (Table A5-1), program listings (Table A5-2), a data input list, and a printout for a typical run (Table A5-6).

PROGRAM SSMIX

This program reduces desired parameters from test firing raw data. Three major sub-systems are involved: (1) LOX-GH_2 rocket motor, (2) GN_2 Film Coolant, and (3) Heated Air. For data reduction purposes these three sub-systems are further divided as follows:

1. LOX-GH_2 Rocket Motor
   a. High Pressure Coolant Water
   b. Low Pressure Coolant Water
   c. LOX Oxidizer
   d. GH_2 Fuel
   e. Engine Performance
2. GN_2 Film Coolant
   a. High Pressure GN_2 Film Coolant
   b. Low Pressure GN_2 Film Coolant
3. Heated Air
   a. Air Stream
   b. Air Heater

Data reduction for each of the above is handled separately in a labeled section of the program.

TABLE A5-1

SSMIX PROGRAM VARIABLES

GENERAL

IRUN	–	Run Number	(Integer)
IDATE	–	Run Date	(Integer)
PA	–	Atmospheric Pressure	(psia)
TATM	–	Atmospheric Temperature	(F)
RH	–	Relative Humidity	(Percent)

HIGH PRESSURE COOLANT WATER

CWH	–	Flowmeter Cycles	(Cycles)
PWHT	–	Tank Pressure	(psig)
PWHI	–	Inlet Pressure	(psig)
VWHT	–	Tank Temperature	(MV)
VWH1	–	1/4-Inch Outlet Temperature	(MV)
VWH2	–	3/4-Inch Outlet Temperature	(MV)
VWH3	–	$1\frac{1}{2}$-Inch Outlet Temperature	(MV)
WWH	–	Flowrate	(lbs/sec)
TWHT	–	Tank Temperature	(F)
TWH1	–	1/4-Inch Outlet Temperature	(F)
TWH2	–	3/4-Inch Outlet Temperature	(F)
TWH3	–	$1\frac{1}{2}$-Inch Outlet Temperature	(F)
DWH1	–	1/4-Inch Outlet Delta Temp	(F)
DWH2	–	3/4-Inch Outlet Delta Temp	(F)
DWH3	–	1-1/2-Inch Outlet Delta Temp	(F)

LOW PRESSURE COOLANT WATER

CWL	–	Flowmeter Cycles	(Cycles)
PWLT	–	Tank Pressure	(psig)
PWLI	–	Inlet Pressure	(psig)
VWLT	–	Tank Temperature	(MV)
VWL1	–	1-Inch Outlet Temperature	(MV)

TABLE A5-1 (CONT)

WWL	-	Flowrate	(lbs/sec)
TWLT	-	Tank Temperature	(F)
TWL1	-	1-Inch Outlet Temperature	(F)
DWL1	-	1-Inch Outlet Delta Temperature	(F)

AIR STREAM

PSD	-	Stream Pressure in Duct	(psig)
VSD	-	Stream Temperature in Duct	(MV)
TSD	-	Stream Temperature in Duct	(F)
RSD	-	Stream Density in Duct	(lbs/ft^3)
PRA	-	Pressure Ratio. PA/PSD	
YA	-	Expansion Factor	
WA	-	Flowrate	(lbs/sec)
TA	-	Mixing Chamber Inlet Air Temperature	(R)
TAC	-	Mixing Chamber Inlet Air Temperature	(F)
RA	-	Mixing Chamber Inlet Air Density	(lbs/ft^3)
VA	-	Mixing Chamber Inlet Air Velocity	(ft/sec)
AA	-	Mixing Chamber Inlet Air Acoustic Velocity	(ft/sec)
XMA	-	Mixing Chamber Inlet Air Mach Number	
PPA	-	Isentropic Flow Pressure Ratio P/Po	
AAA	-	Isentropic Flow Area Ratio A/A*	
PAMC	-	Mixing Chamber Inlet Air Pressure	(psig)

LOW PRESSURE GN_2 FILM COOLANT

PNL	-	Manifold Pressure	(psig)
VNL	-	Manifold Temperature	(MV)
TNL	-	Manifold Temperature	(F)
PRNL	-	Pressure Ratio PA/PNL	
YNL	-	Expansion Factor	
WNL	-	Flowrate	(lbs/sec)
TNLMC	-	Mixing Chamber Inlet Temperature	(R)
TNLMCC	-	Mixing Chamber Inlet Temperature	(F)
RNL	-	Mixing Chamber Inlet N_2 Density	(lbs/ft^3)

TABLE A5-1 (CONT)

VENL	-	Mixing Chamber Inlet N_2 Velocity	(ft/sec)
ANL	-	Mixing Chamber Inlet N_2 Acoustic Velocity	(ft/sec)
XMNL	-	Mixing Chamber Inlet N_2 Mach Number	
PPNL	-	Isentropic Flow Pressure Ratio P/Po	
AANL	-	Isentropic Flow Area Ratio A/A*	
PNLMC	-	Mixing Chamber Inlet N_2 Pressure	(psig)

HIGH PRESSURE GN_2 FILM COOLANT

PNH	-	Manifold Pressure	(psig)
VNH	-	Manifold Temperature	(MV)
TNH	-	Manifold Temperature	(F)
PRNH	-	Pressure Ratio PA/PNH	
YNH	-	Expansion Factor	
WNH	-	Flowrate	(lbs/sec)
TNHMC	-	Mixing Chamber Inlet N_2 Temperature	(R)
TNHMCC	-	Mixing Chamber Inlet N_2 Temperature	(F)
RNHMC	-	Mixing Chamber Inlet N_2 Density	(lbs/ft^3)
VENH	-	Mixing Chamber Inlet N_2 Velocity	(ft/sec)
ANH	-	Mixing Chamber Inlet N_2 Acoustic Velocity	(ft/sec)
PNHMC	-	Mixing Chamber Inlet N_2 Pressure	(psig)

LOX OXIDIZER

PC	-	Chamber Pressure	(psig)
COX	-	Flowmeter Cycles	(Cycles)
POXT	-	Tank Pressure	(psig)
POXI	-	Inlet Pressure	(psig)
VOXI	-	Inlet Temperature	(MV)
VOXC	-	Injector Cooldown Temperature	(MV)
TOXI	-	Inlet Temperature	(F)
TOXC	-	Injector Cooldown Temperature	(F)
TK	-	Inlet Temperature	(K)
RS	-	Saturation Density	(lbs/ft^3)
PV	-	Vapor Pressure	(psia)
B	-	Adiabatic Compressibility	

TABLE A5-1 (CONT)

ROX	-	LOX Density	(lbs/ft^3)
WOX	-	LOX Flowrate	(lbs/sec)
DPOXI	-	Injector Delta Pressure	(psi)

HYDROGEN FUEL

PHVI	-	Venturi Inlet Pressure	(psig)
PHI	-	Inlet Pressure	(psig)
VHI	-	Inlet Temperature	(MV)
THI	-	Inlet Temperature	(F)
XKH	-	Isentropic Flow Coefficient	
PHIC	-	Inlet Pressure	(psia)
ZH	-	Compressibility Factor	
WH	-	Flowrate	(lbs/sec)
DPHI	-	Injection Delta Pressure	(psi)

PERFORMANCE PARAMETERS

PRPC	-	Pressure Ratio PC/PA	
XMR	-	Mixture Ratio	
WT	-	Total Flow	(lbs/sec)
CSTAR	-	C*	(ft/sec)
TC4	-	Theoretical C* @ MR = 4.0	(ft/sec)
TC5	-	Theoretical C* @ MR = 5.0	(ft/sec)
TC6	-	Theoretical C* @ MR = 6.0	(ft/sec)
TCSTAR	-	Theoretical C* @ MR of Test	(ft/sec)
CN	-	C* Efficiency	(Percent)

AIR HEATER

VAH1	-	Heater Bed Temperature 1	(MV)
VAH2	-	Heater Bed Temperature 2	(MV)
VAH3	-	Heater Bed Temperature 3	(MV)
VAH4	-	Heater Bed Temperature 4	(MV)
TAH1	-	Heater Bed Temperature 1	(F)
TAH2	-	Heater Bed Temperature 2	(F)
TAH3	-	Heater Bed Temperature 3	(F)
TAH4	-	Heater Bed Temperature 4	(F)

TABLE A5-2

SSMIX - LOGIC

```
5C * * * * PRØGRAM SSMIX      1/9/69      J T. SABØL * * * *
10C
15 CALL ØPENF (1,"XDATA",2)
20 READ(1,)IRUN,IDATE,PA,TATM,RH
25C      *****HIGH PRESSURE WATER SYSTEM*****
30 READ(1,)CWH,PWHT,PWHI,VWHT,VWH1,VWH2,VWH3
35 WWH=.1129*CWH
40 TWHT=ICØN(VWHT)
45 TWH1=ICØN(VWH1)
50 TWH2=ICØN(VWH2)
55 TWH3=ICØN(VWH3)
60 DWH1=TWH1-TWHT
65 DWH2=TWH2-TWHT
70 DWH3=TWH3-TWHT
75C      *****LØW PRESSURE WATER SYSTEM*****
80 READ(1,)CWL,PWLT,PWLI,VWLT,VWL1
85 WWL=.1102*CWL
90 TWLT=ICØN(VWLT)
95 TWL1=ICØN(VWL1)
100 DWL1=TWL1-TWLT
105C                *****AIR SYSTEM*****
110 READ(1,)PSD,VSD
115 TSD=CRAL(VSD)
120 RSD=2.7*(PSD+PA)/(TSD+460.)
125 PRA=PA/(PSD+PA)
130 YA=SQRT(((1.-.732**4.)/((1.-.732**4.)*PRA**1.42857))*(((3.5*
135&PRA**1.42857)*(1.-PRA**.285714))/(1.-PRA)))
140 WA=16.27*YA*SQRT(PSD*RSD)
145 TA=(PRA**.286)*(TSD+460.)
150 TAC=TA-460.
155 RA=2.7*(PSD+PA)/(TSD+460.)
160 VA=6.99*WA/RA
165 AA=49.*TA**.5
170 XMA=VA/AA
175 CALL CFLØW(XMA,PPA,AAA)
180 PAMC=((WA*SQRT((TSD+460.)/.997)*AAA*PPA)/10.959)-PA
185C      *****LØW PRESSURE NITRØGEN SYSTEM*****
190 READ(1,)PNL,VNL
195 TNL=ICØN(VNL)
200 PRNL=PA/(PNL+PA)
205 YNL=SQRT(((1.-.577**4.)/((1.-.577**4.)*PRNL**1.42857))*(((3.5*
210&PRNL**1.42857)*(1.-PRNL**.285714))/(1.-PRNL)))
215 WNL=4.79*YNL*SQRT(((PNL+PA)/(TNL+460.))*PNL)
```

TABLE A5-2 (CONT)

```
 220 TNLMC=((.989*PA/(PNL+PA))**.286)*(TNL+460.)
 225 TNLMCC=TNLMC-460.
 230 RNL=2.61*PA/TNLMC
 235 VENL=34.4*WNL/RNL
 240 ANL=49.9*(TNLMC**.5)
 245 XMNL=VENL/ANL
 250 CALL CFL0W(XMNL,PPNL,AANL)
 255 PNLMC=((WNL*SQRT((TNL+460.)/.997)*AANL*PPNL)/2.2333)-PA
260C      *****HIGH PRESSURE GN2 FILM C00LANT*****
265 READ(1,)PNH,VNH
270 TNH=IC0N(VNH)
275 IF((PNH+PA).GE.(1.7*PA)) G0 T0 10
280 PRNH=PA/(PNH+PA)
285 YNH=SQRT(((1.-.475**4.)/((1.-.475**4.)*PRNH**1.42857))*(((3.5*
290&PRNH**1.42857)*(1.-PRNH**.285714))/(1.-PRNH)))
295 WNH=6.88*YNH*SQRT((PNH+PA)/(TNH+460.))*PNH)
300 TNHMC=((PA*.988/(PNH+PA))**.286)*(TNH+460.)
305 TNHMCC=TNHMC-460.
310 RNHMC=2.61*PA/TNHMC
315 VENH=22.7*WNH/RNHMC
320 ANH=49.9*(TNHMC**.5)
325 G0 T0 20
330 10 WNH=3.38*(PNH+PA)/SQRT(TNH+460.)
335 TNHMC=.8333*(TNH+460)
340 TNHMCC=TNHMC-460.
345 RNHMC=2.61*PA/TNHMC
350 VENH=49.9*TNHMC**.5
355 20 PNHMC=(.1563*WNH*SQRT((TNH+460.)/.997))-PA
360C      *****L0X 0XIDIZER CALCULATI0NS*****
365 READ(1,)PC,C0X,P0XT,P0XI,V0XI,V0XC
370 T0XI=IC0N(V0XI)
375 T0XC=IC0N(V0XC)
380 TK=(T0XI+459.668)/1.8
385 RS=62.428227*(1.414202-.001033016*TK-2.23E-5*TK**2.)
390 PV=PA*EXP(5.238279-7.2953481/TK-41958.931/TK**2.)
395 B=8.05790431E-5-1.8993851E-6*TK+1.2860036E-8*TK**2.
400 R0X=RS*(10.**B*(P0XI+PA-PV)+1.)**.1
405 W0X=.297E-3*C0X*R0X
410 DP0XI=P0XI-PC
415C      *****HYDR0GEN FUEL CALCULATI0NS*****
420 READ(1,)PHVI,PHI,VHI
425 THI=IC0N(VHI)
430 XKH=(((THI+60.)/200.)*.00013)+.01362
435 PHIC=PHI+PA
440 ZH=4.62585E-5*PHIC+.99
445 WH=((PHVI+PA)/SQRT(THI+460.))*SQRT(1./ZH)*XKH
```

TABLE A5-2 (CONT)

```
450 DPHI=PHI-PC
455C      *****PERFØRMANCE PARAMETERS*****
460 PRPC=(PC+PA)/PA
465 XMR=WØX/WH
470 WT=WØX+WH
475 CSTAR=130.*(PC+PA)/WT
480 TC4=((((PC+PA)-300.)/200.)*15.)+8146.
485 TC5=((((PC+PA)-300.)/200.)*30.)+7893.
490 TC6=((((PC+PA)-300.)/200.)*40.)+7600.
495 IF(XMR-5.)30,40,50
500 30 TCSTAR=((5.-XMR)*(TC4-TC5))+TC5
505 GØ TØ 55
510 40 TCSTAR=TC5
515 GØ TØ 55
520 50 TCSTAR=TC5-((XMR-5.)*(TC5-TC6))
525 55 CN=(CSTAR/TCSTAR)*100.
530C      *****AIR HEATER TEMPERATURES*****
535 READ(1,)VAH1,VAH2,VAH3,VAH4
540 TAH1=CRAL(VAH1)
545 TAH2=CRAL(VAH2)
550 TAH3=CRAL(VAH3)
555 TAH4=CRAL(VAH4)
560C             *****PRINTØUTS*****
565 PRINT,"          * * * * * * M I X I N G   P R Ø G R A M * *
570&* * * "
575 PRINT,!2,"     NØTE:  DIMENSIØNS FØR PARAMETERS ARE AS FØLLØWS:"
580 PRINT,!,"            TEMPERATURES - F          DENSITIES - #/FT3"
585 PRINT,"            PRESSURES - PSIG          FLØWS - #/SEC"
590 PRINT,"            VELØCITIES - FT/SEC"
595 PRINT,!2,"          * * * * * * * * * * * * * * * * * * * * *
600&* * * *"
605 PRINT,!2,"RUN - ",IRUN,"              ","DATE - ",IDATE
610 PRINT 70,PA,TATM,RH
615 PRINT,!2,!,"          ***** HIGH PRESSURE WATER SYSTEM *****"
620 PRINT 75,WWH,PWHT,PWHI,TWHT,DWH1,DWH2,DWH3
625 PRINT,!2,!,"          ***** LØW PRESSURE WATER SYSTEM *****"
630 PRINT 80,WWL,PWLT,PWLI,TWLT,DWL1
635 PRINT,!2,!,"                    ***** AIR SYSTEM *****"
640 PRINT 85,WA,PSD,PAMC,TSD,TAC,RA,VA,AA,XMA
645 PRINT,!2,!,"          ***** LØW PRESSURE NITRØGEN SYSTEM *****"
650 PRINT 90,WNL,PNL,PNLMC,TNL,TNLMCC,RNL,VENL,ANL,XMNL
655 PRINT,!2,!,"          ***** HIGH PRESSURE NITRØGEN SYSTEM *****"
660 IF((PNH+PA).GE.(1.7*PA)) GØ TØ 60
665 PRINT 95,WNH,PNH,PNHMC,TNH,TNHMCC,RNHMC,VENH,ANH
670 GØ TØ 65
675 60 PRINT 100,WNH,PNH,PNHMC,TNH,TNHMCC,RNHMC,VENH
```

TABLE A5-2 (CONT)

```
680 65 PRINT,↑2,↑,"          ***** LØX ØXIDIZER CALCULATIØNS *****"
685 PRINT 105,WØX,PØXT,PØXI,TØXI,TØXC,DPØXI
690 PRINT,↑2,↑,"          ***** HYDRØGEN FUEL CALCULATIØNS *****"
695 PRINT 110,WH,PHVI,PHI,THI,DPHI
700 PRINT,↑2,↑,"          ***** PERFØRMANCE PARAMETERS *****"
705 PRINT 115,PC,PRPC,XMR,WT,CSTAR,TCSTAR,CN
710 PRINT,↑2,↑,"       ***** AIR HEATER BED TEMPERATURES *****"
715 PRINT 120,TAH1,TAH2,TAH3,TAH4
720 70 FØRMAT(/,"P ATM - "F5.2,5X,"T ATM - "F4.0,5X,"RH - "F4.1,
725&5X,"PC/PA IDEAL - 29.35")
730 75 FØRMAT(/,"FLØW - "F5.2,5X,"P TANK - "F6.1,5X,"P IN - "F6.1,
735&5X,"T TANK - "F4.0,//,"DT1 - "F4.0,5X,"DT2 - "F4.0,5X,
740&"DT3 - "F4.0)
745 80 FØRMAT(/,"FLØW - "F5.2,5X,"P TANK - "F6.1,5X,"P INLET - "
750&F6.1,//,"T TANK - "F4.0,7X,"DELTA T - "F4.0)
755 85 FØRMAT(/,"FLØW - "F4.2,5X,"P SD - "F4.3,5X,"P MC - "F4.2,
760&//,"T SD - "F5.0,5X,"T MC - "F5.0,5X,"RHØ MC - "F5.4,//,
765&"V MC - "F6.1,5X,"A - "F6.1,5X,"M - "F4.3)
770 90 FØRMAT(/,"FLØW - "F4.2,5X,"P N2 - "F4.2,5X,"P MC - "F6.2,//,
775&"T N2 - "F3.0,5X,"T MC - "F3.0,5X,"RHØ MC - "F5.4,//,
780&"V MC - "F6.1,5X,"A - "F6.1,5X,"M - "F4.3)
785 95 FØRMAT(/,"FLØW - "F4.2,5X,"P N2 - "F4.1,5X,"P MC - "F6.2,
790&5X,"T N2 - "F3.0,//,"T MC - "F4.0,5X,"RHØ MC - "F5.4,5X,
795&"VEL N2 - "F6.1,5X,"A - "F6.1)
800 100 FØRMAT(/,"FLØW - "F4.2,5X,"P N2 - "F4.1,5X,"P MC - "F6.2,
805&5X,"T N2 - "F3.0,//,"T MC - "F4.0,5X,"RHØ MC - "F5.4,5X,
810&"VEL N2 - "F6.1)
815 105 FØRMAT(/,"FLØW - "F4.2,5X,"P TANK - "F5.1,5X,"P IN - "F5.1,
820&//,"T IN - "F5.0,5X,"T CØØL - "F5.0,5X,"DP INJ - "F5.1)
825 110 FØRMAT(/,"FLØW - "F4.2,5X,"P VEN IN - "F6.1,5X,"P IN - "F6.1,
830&//,"T H2 - "F4.0,5X,"DP INJ - "F5.1)
835 115 FØRMAT(/,"PC - "F5.1,5X,"PC/PA - "F5.2,5X,"MR - "F5.2,5X,
840&"TØTAL FLØW - "F4.2,//,"C* - "F5.0,5X,"THEØR C* - "F5.0,5X,
845&"ETA C* - "F5.1)
850 120 FØRMAT(/,"T BED 1 - "F5.0,3X,"T BED 2 - "F5.0,3X,
855&"T BED 3 - "F5.0,3X,"T BED 4 - "F5.0)
860 PRINT,↑2,↑,"          * * * * * * * * * * * * * * * * * * * *
865&* * * * *"
870 PRINT,↑2,↑2
999 END
```

SSMIX DATA INPUT

Data are entered in permanent file XDATA. Nine lines of data are inputted as shown below.

1 IRUN, IDATE, PA, TATM, RH
2 CWH, PWHT, PWHI, VWHT, VWH1, VWH2, VWH3
3 CWL, PWLT, PWLI, VWLT, VWL1
4 PSD, VSD
5 PNL, VNL
6 PNH, VNH
7 PC, COX, POXT, POXI, VOXI, VOXC
8 PHVI, PHI, VHI
9 VAH1, VAH2, VAH3, VAH4

It should be noted that a line number is required and a comma is needed to separate each data variable.

SUBROUTINES

Function Icon

This function performs temperature scaling of millivolt values from iron-constantan thermocouples with a 150F reference junction in the range of -11.2 to +53.2 millivolts (-320 to 1800F). Scaling is accomplished by separating the 64.4 millivolt range into smaller ranges, each having been fitted with a third-order polynomial equation. The breakdown is as follows:

.2 MV Range	-11.2 to -11.0 MV
1.0 MV Range	-11.0 to -10.0 MV
2.0 MV Ranges	-10.0 to 0 MV
4.0 MV Ranges	0 to +52.0 MV
1.0 MV Range	+52.0 to +53.0 MV
.2 MV Range	+53.0 to +53.2 MV

The program (Table A5-3) selects the correct equation from the millivolt value and solves for the temperature. Accuracy is ± 1.0 F of NBS standards.

Function Cral

This function performs temperature scaling of millivolt values of chromel-alumel thermocouples with a 32 F reference junction in the range 0 to 55 millivolts (32 to 2504 F). Scaling is accomplished by treating the 55-millivolt range as eleven 5-millivolt ranges, each having been fitted with a third order polynomial equation. The program (Table A5-4) selects the correct equation from the millivolt value and solves for the temperature. Accuracy is ± 1.0 F of NBS standards.

Function CFlow

This function provides the compressible isentropic flow parameters P/P_o (pressure ratio) and A/A* (area ratio) in the Mach number range from .20 to .60 for a perfect gas, k = 1.4.

The program (Table A5-5) contains arrays of P/Po and A/A* for .01 Mach number increments. The tables were abstracted from The Dynamics and Thermodynamics of Compressible Fluid Flow, Vol. I, by Ascher H. Shapiro, Ronald Press Co., New York, 1953.

Operation of this function is based upon the Mach number calculated in the main program. It first checks the Mach number to insure it is within the range of .20 to .60. If not, values of zero are returned to the main program. If the Mach number is in the proper range, the program enters a loop comparing the input Mach number to those stored in the array. When the array Mach number equals or exceeds the input Mach number the two bracketing values of P/Po and A/A* are chosen and a linear interpolation performed. The interpolated values are then returned to the main program.

TABLE A5-3

FUNCTION ICON - LOGIC

```
7000 FUNCTIØN  IC0N(XMV)
7005C
7010C  IRØN CØNSTANTAN THERMØC0UPLE MILLIVØLT TØ DEGREES F CØNVERSIØN
7015C  150 DEGREE REFERENCE JUNCTIØN TEMPERATURE
7020C       J T. SABØL    12/18/68
7025C
7030       IF(XMV.GE.-11.2.AND.XMV.LE.53.2) GØ TØ 5
7035       T=9999.
7040       GØ TØ 140
7045   5   IF(XMV) 10,50,50
7050  10   IF(XMV.LT.-10..AND.XMV.GT.-11.) GØ TØ 40
7055       IF(XMV.LE.-11.) GØ TØ 45
7060       N=IABS(INT(XMV/2))
7065       I=N+1
7070       V=XMV+2.*N
7075       GØ TØ (15,20,25,30,35,35),I
7080  15   T=-.15*V*V+33.85*V+150.
7085       GØ TØ 130
7090  20   T=-.5*V*V+34.5*V+81.7
7095       GØ TØ 130
7100  25   T=-.8*V*V+35.9*V+10.7
7105       GØ TØ 130
7110  30   T=-1.3*V*V+38.4*V-64.3
7115       GØ TØ 130
7120  35   T=-2.65*V*V+43.05*V-146.3
7125       GØ TØ 130
7130  40   V=XMV+10.
7135       T=-8.*V*V+54.*V-243.
7140       GØ TØ 130
7145  45   V=XMV+11.
7150       T=-50.*V*V+65.*V-305.
7155       GØ TØ 130
7160  50   IF(XMV.GT.52..AND.XMV.LT.53.) GØ TØ 120
7165       IF(XMV.GE.53.) GØ TØ 125
7170       N=INT(XMV/4.)
7175       I=N+1
7180       V=XMV-4.*N
7185       GØ TØ (55,60,65,70,75,80,85,90,95,100,105,110,115,115),I
7190  55   T=-.0875*V*V+33.525*V+150.
7195       GØ TØ 130
7200  60   T=-.05*V*V+32.6*V+282.7
7205       GØ TØ 130
```

TABLE A5-3 (CONT)

```
7210  65 T=.075*V*V+32.2*V+412.3
7215     GØ TØ 130
7220  70 T=0.*V*V+32.5*V+542.3
7225     GØ TØ 130
7230  75 T=-.0125*V*V+32.725*V+672.3
7235     GØ TØ 130
7240  80 T=-.0375*V*V+32.575*V+803.
7245     GØ TØ 130
7250  85 T=-.0875*V*V+31.975*V+932.7
7255     GØ TØ 130
7260  90 T=-.1*V*V+31.1*V+1059.2
7265     GØ TØ 130
7270  95 T=-.1625*V*V+29.975*V+1182.
7275     GØ TØ 130
7280 100 T=-.1*V*V+28.7*V+1299.3
7285     GØ TØ 130
7290 105 T=-.025*V*V+28.15*V+1412.5
7295     GØ TØ 130
7300 110 T=.375*V*V+27.65*V+1524.7
7305     GØ TØ 130
7310 115 T=-.0375*V*V+30.575*V+1641.3
7315     GØ TØ 130
7320 120 V=XMV-52.
7325     T=.4*V*V+29.8*V+1763.
7330     GØ TØ 130
7335 125 V=XMV-53.
7340     T=20.*V*V+26.*V+1793.2
7345 130 IF(T) 135,140,140
7350 135 ICØN=INT(T-.5)
7355     GØ TØ 999
7360 140 ICØN=INT(T+.5)
7365 999 RETURN
7370     END
800
```

TABLE A5-4

FUNCTION CRAL - LOGIC

```
8000 FUNCTION CRAL(XMV)
8005C
8010C CHROMEL-ALUMEL THERMOCOUPLE MILLIVOLT TO DEGREES CONVERSION
8015C 32 DEGREE REFERENCE JUNCTION TEMPERATURE
8020C     J. T. SABOL      12/27/68
8025C
8030      IF(XMV.GE.0.0.AND.XMV.LE.55.) GO TO 5
8035      T=9999.
8040      GO TO 65
8045    5 N=INT(XMV/5.)
8050      I=N+1
8055      V=XMV-5.*N
8060      GO TO (10,15,20,25,30,35,40,45,50,55,60,60),I
8065   10 T=-.216*V*V+44.94*V+32.
8070      GO TO 65
8075   15 T=-.048*V*V+45.*V+251.3
8080      GO TO 65
8085   20 T=-.125*V*V+44.08*V+475.1
8090      GO TO 65
8095   25 T=-.048*V*V+42.72*V+692.3
8100      GO TO 65
8105   30 T=-.016*V*V+42.28*V+904.7
8110      GO TO 65
8115   35 T=.064*V*V+42.36*V+1115.7
8120      GO TO 65
8125   40 T=.168*V*V+42.74*V+1329.1
8130      GO TO 65
8135   45 T=.208*V*V+43.88*V+1547.
8140      GO TO 65
8145   50 T=.176*V*V+45.68*V+1771.6
8150      GO TO 65
8155   55 T=.240*V*V+47.32*V+2004.4
8160      GO TO 65
8165   60 T=.240*V*V+50.2*V+2247.
8170   65 CRAL=INT(T+.5)
8175   99 RETURN
8180      END
```

TABLE A5-5

FUNCTION CFLOW - LOGIC

```
9000 SUBR0UTINE CFL0W(XMK,PP0,AAS)
9005C
9010C PR0GRAM CALCULATES THE C0MPRESSIBLE ISENTR0PIC FL0W FUNCTI0NS
9015C P/P0 AND A/A* IN THE MACH NUMBER RANGE 0F .20 T0 .60
9020C          J. T. SAB0L          1/29/69
9025C
9030     DIMENSI0N XM(41),PP(41),AA(41)
9035     DATA XM,PP,AA/.20,.21,.22,.23,.24,.25,.26,.27,.28,.29,
9040&    .30,.31,.32,.33,.34,.35,.36,.37,.38,.39,.40,.41,.42,.43,
9045&    .44,.45,.46,.47,.48,.49,.50,.51,.52,.53,.54,.55,.56,.57,
9050&    .58,.59,.60,.9725,.9697,.9668,.9638,.9607,.9574,.9540,
9055&    .9506,.9470,.9432,.9394,.9355,.9315,.9273,.9231,.9187,
9060&    .9143,.9097,.9051,.9004,.8956,.8907,.8857,.8806,.8755,.8702,
9065&    .8649,.8595,.8541,.8486,.8430,.8373,.8316,.8258,.8200,.8141,
9070&    .8082,.8022,.7962,.7901,.7840,2.96,2.82,2.70,2.59,2.49,
9075&    2.40,2.31,2.23,2.16,2.09,2.035,1.976,1.921,1.870,1.822,1.778,
9080&    1.735,1.696,1.658,1.623,1.590,1.558,1.528,1.500,1.474,1.448,
9085&    1.424,1.401,1.380,1.359,1.339,1.321,1.303,1.286,1.270,1.255,
9090&    1.240,1.226,1.213,1.200,1.188/
9095     IF(XMK.LT..20.0R.XMK.GT..60) G0 T0 40
9100     D0 10 I=1,41
9105     IF(XM(I)-XMK) 10,20,30
9110 10  C0NTINUE
9115 20  PP0=PP(I)
9120     AAS=AA(I)
9125     G0 T0 50
9130 30  J=I-1
9135     A1=(XMK-XM(J))*100.
9140     PP0=PP(J)-((PP(J)-PP(I))*A1)
9145     AAS=AA(J)-((AA(J)-AA(I))*A1)
9150     G0 T0 50
9155 40  PP0=0.
9160     AAS=0.
9165 50  C0NTINUE
9170     RETURN
9175     END
```

TABLE A5-6

PROGRAM SSMIX TYPICAL OUTPUT

```
      * * * * * * M I X I N G   P R Ø G R A M * * * * * *

   NØTE:  DIMENSIØNS FØR PARAMETERS ARE AS FØLLØWS:

          TEMPERATURES - F          DENSITIES - #/FT3
          PRESSURES - PSIG          FLØWS - #/SEC
          VELØCITIES - FT/SEC

      * * * * * * * * * * * * * * * * * * * * * * * * * *

RUN -       101              DATE -     20469

P ATM - 13.82     T ATM -  50.     RH - 38.0     PC/PA IDEAL - 29.35

       ***** HIGH PRESSURE WATER SYSTEM *****

FLØW - 28.90     P TANK - 1060.0     P IN -  910.0     T TANK -  50.

DT1 -  99.     DT2 -  27.     DT3 -  20.

       ***** LØW PRESSURE WATER SYSTEM *****

FLØW - 29.20     P TANK - 1050.0     P INLET -  856.0

T TANK -  52.       DELTA T -  26.

                ***** AIR SYSTEM *****

FLØW - 3.42     P SD - .596     P MC - 0.36

T SD -   74.     T MC -   68.     RHØ MC - .0729

V MC -  327.7     A - 1125.5     M - .291
```

TABLE A5-6 (Cont)

***** LØW PRESSURE NITRØGEN SYSTEM *****

FLØW - 1.25 P N2 - 1.98 P MC - -.31

T N2 - 22. T MC - 2. RHØ MC - .0780

V MC - 551.0 A - 1073.1 M - .513

***** HIGH PRESSURE NITRØGEN SYSTEM *****

FLØW - 4.33 P N2 - 13.9 P MC - 0.85 T N2 - 9.

T MC - -69. RHØ MC - .0923 VEL N2 - 986.5

***** LØX ØXIDIZER CALCULATIØNS *****

FLØW - 6.63 P TANK - 736.0 P IN - 698.0

T IN - -296. T CØØL - -146. DP INJ - 363.8

***** HYDRØGEN FUEL CALCULATIØNS *****

FLØW - 0.66 P VEN IN - 1102.0 P IN - 540.0

T H2 - 69. DP INJ - 205.8

***** PERFØRMANCE PARAMETERS *****

PC - 334.2 PC/PA - 25.18 MR - 10.06 TØTAL FLØW - 7.29

C* - 6204. THEØR C* - 6650. ETA C* - 94.2

***** AIR HEATER BED TEMPERATURES *****

T BED 1 - 50. T BED 2 - 50. T BED 3 - 50. T BED 4 - 50.

* *

REPORT DISTRIBUTION LIST FOR CONTRACT NAS7-521

		Copies
NASA Marshall Space Flight Center		
Marshall Space Flight Center, Alabama 35812		
Attn:	Technical Manager, David Seymour, S&E-AERO-AT	5
	Office of Technical Information, MS-IP	2
	Keith Chandler, S&E-ASTN-PA	1
	Technical Library	1
	Hans G. Paul, R-P&VED	2
	Purchasing Office, PR-EC	1
	Don Thompson, S&E-ASTN-PAA	1
	Patent Office, M-PAT	1
	Technology Utilization Office, MS-T	1
NASA Headquarters, Washington, D.C. 20546		
Attn:	Chief, Liquid Propulsion Technology, OART, RPL	3
	Jack Suddreth, OART, RPL	2
	Alfred Gessow, OART, RR-2	1
	Director, Launch Vehicles and Propulsion, OSSA, SV	1
	Director, Advanced Manned Missions, OMSF, MT	1
	Chief, Air Breathing Propulsion, RAP	1
	Chief, Fluid Dynamics, RRF	1
	Director, Technology Utilization Division, OTU	1
NASA Ames Research Center		
Moffett Field, California 94035		
Attn:	Mission Analysis Division	1
	Hans M. Mark	2

	Copies
NASA Scientific and Technical Information Facility P.O. Box 33 College Park, Maryland 20740	10
NASA Goddard Space Flight Center Greenbelt, Maryland 20771 Attn: Merland L. Moseson, Code 620	2
NASA Pasadena Office 4800 Oak Grove Drive Pasadena, California 91103 Attn: Henry Burlage, Jr., Propulsion Div., 38	2
JPL Support Contracts Branch, Fred Abbott, Bldg. 150, Rm. 502	1
Patents and Contracts Management	1
Dr. Duane Dippery MS354-357	1
NASA Langley Research Center Langley Station Hampton, Virginia 23365 Attn: Edward Cortwright, Director	2
Kenneth Pierpont, MS353	2
NASA Lewis Research Center 21000 Brookpark Road Cleveland, Ohio 44135 Attn: Dr. Abe Silverstein, Director	2
Irving Johnson, MS500-205	2

	Copies
Paul Herr, MS500-209	1
Office of Technical Information	1
James Dugan, MS501-2	1
NASA Manned Spacecraft Center	
Houston, Texas 77001	
Attn: Joseph G. Thibodaux, Jr., Chief, Propulsion and	
Power Division	2
Office of Technical Information	1
NASA John F. Kennedy Space Center	
Cocoa Beach, Florida 32931	
Attn: Dr. Kurt H. Debus	2
Aeronautical Systems Division	
Air Force Systems Command	
Wright-Patterson Air Force Base	
Dayton, Ohio 45433	
Attn: D. L. Schmidt, Code ASRCNC-2	1
Air Force Missile Development Center	
Holloman Air Force Base, New Mexico	
Attn: Maj. R. E. Bracken, Code MDGRT	1
Air Force Missile Test Center	
Patrick Air Force Base, Florida	
Attn: L. J. Ullian	1

	Copies
Space and Missile Systems Organization Los Angeles, California Attn: Col. Clark, Technical Data Center	1
Arnold Engineering Development Center Arnold Air Force Station Tullahoma, Tennessee Attn: Dr. H. K. Doetsch	1
Bureau of Naval Weapons Department of the Navy Washington, D.C. Attn: J. Kay, RTMS-41	1
Defense Documentation Center Headquarters Cameron Station, Building 5 5010 Duke Street Alexandria, Virginia 22314 Attn: TISIA	1
Headquarters, U.S. Air Force Washington 25, D.C. Attn: Col. C. K. Stambaugh, AFRST	1
Picatinny Arsenal Dover, New Jersey 07801 Attn: I. Forsten, Chief Liquid Propulsion Laboratory, SMUPA-DL	1

	Copies
Air Force Rocket Propulsion Laboratory Research and Technology Division Air Force Systems Command Edwards, California 93523 Attn: Mr. H. Main, RPRR	1
U.S. Army Missile Command Redstone Arsenal Alabama 35809 Attn: Dr. Walter Wharton	1
U.S. Naval Weapons Station China Lake, California 93557 Attn: Chief, Missile Propulsion Division, Code 4562	1
Chemical Propulsion Information Agency Applied Physics Laboratory 8621 Georgia Avenue Silver Spring, Maryland 20910 Attn: Tom Reedy	1
Aerojet-General Corporation P.O. Box 296 Azusa, California 91703 Attn: W. L. Rodgers	1

	Copies
Aerojet-General Corporation P.O. Box 1947 Technical Library, Bldg. 2015, Dept. 2410 Sacramento, California 95809 Attn: R. Stiff	1
Aeronutronic Division Philco Corporation Ford Road Newport Beach, California 92663 Attn: D. A. Garrison	1
Aerospace Corporation 2400 East El Segundo Boulevard P.O. Box 95085 Los Angeles, California 90045 Attn: John G. Wilder, MS-2293	1
Arthur D. Little, Inc. 20 Acorn Park Cambridge, Massachusetts 02140 Attn: Library	1
Astrosystems International, Inc. 1275 Bloomfield Avenue Fairfield, New Jersey 07007 Attn: A. Mendenhall	1

	Copies
Atlantic Research Corporation Edsall Road and Shirley Highway Alexandria, Virginia 22314 Attn: Dr. Ray Friedman	1
Avco Systems Division Wilmington, Massachusetts Attn: Howard B. Winkler	1
Beech Aircraft Corporation Boulder Division Box 631 Boulder, Colorado Attn: J. H. Rodgers	1
Bell Aerosystems Company P.O. Box 1 Buffalo, New York 14240 Attn: W. M. Smith	1
Bellcomm 955 L'Enfant Plaza, S.W. Washington, D.C. Attn: H. S. London	1

	Copies
Bendix Systems Division Bendix Corporation 3300 Plymouth Road Ann Arbor, Michigan Attn: John M. Brueger	1
Boeing Company P.O. Box 3707 Seattle, Washington 98124 Attn: J. D. Alexander	1
Boeing Company 1625 K Street, N.W. Washington, D.C. 20006 Attn: Library	1
Boeing Company P.O. Box 1680 Huntsville, Alabama 35801 Attn: Ted Snow	1
Missile Division Chrysler Corporation P.O. Box 2628 Detroit, Michigan 48231 Attn: John Gates	1

	Copies
Wright Aeronautical Division Curtiss-Wright Corporation Wood-Ridge, New Jersey 07075 Attn: G. Kelley	1
Astropower Laboratory McDonnell-Douglas Aircraft Company 2121 Paularino Newport Beach, California 92663 Attn: Dr. George Moe Director, Research	1
Missile and Space Systems Division McDonnell-Douglas Aircraft Company 3000 Ocean Park Boulevard Santa Monica, California 90406 Attn: R. W. Hallet, Chief Engineer Advanced Space Technology	1
Research Center Fairchild Hiller Corporation Germantown, Maryland Attn: Ralph Hall	1

	Copies
Republic Aviation Corporation Fairchild Hiller Corporation Farmingdale, Long Island, New York Attn: Library	1
General Dynamics/Convair Division Library & Information Services (128-00) P.O. Box 1128 San Diego, California 92112 Attn: Frank Dore	1
Missile and Space Systems Center General Electric Company Valley Forge Space Technology Center P.O. Box 8555 Philadelphia, Penna. Attn: F. Mezger	1
F. E. Schultz	1
Grumman Aircraft Engineering Corporation Bethpage, Long Island New York Attn: Joseph Gavin	1
Honeywell, Inc. Aerospace Division 2600 Ridgway Road	

Minneapolis, Minnesota

Attn: Gordon Harms 1

Hughes Aircraft Co.

Aerospace Group

Centinela and Teale Streets

Culver City, California

Attn: E. H. Meier, V. P. and Div. Mgr.

Research and Dev. Div. 1

Walter Kidde and Company, Inc.

Aerospace Operations

567 Main Street

Belleville, New Jersey

Attn: R. J. Manville

Dir. of Research Engr. 1

Ling-Temco-Vought Corporation

P.O. Box 5907

Dallas, Texas 75222

Attn: Warren C. Trent 1

Lockheed Missiles and Space Company

P.O. Box 504

Sunnyvale, California 94088

Attn: J. Guill, Technical Information Center 1

	Copies
Lockheed Missiles and Space Company Huntsville Research and Engineering Center 4800 Bradford Blvd., N.W. Huntsville, Alabama 35805 Attn: Mrs. Beverly Audah	1
Lockheed Propulsion Company P.O. Box 111 Redlands, California 92374 Attn: H. L. Thackwell	1
The Marquardt Corporation 16555 Saticoy Street Van Nuys, California 91409 Attn: Howard McFarland	1
Baltimore Division Martin Marietta Corporation Baltimore, Maryland 21203 Attn: John Calathes (3214)	1
Denver Division Martin Marietta Corporation P.O. Box 179 Denver, Colorado 80201 Attn: Dr. Morganthaler	1

	Copies
Orlando Division Martin Marietta Corporation P.O. Box 5837 Orlando, Florida Attn: J. Ferm	1
McDonnell-Douglas Aircraft Corporation P.O. Box 516 Municipal Airport St.Louis, Missouri 63166 Attn: R. A. Herzmark	1
Space & Information Systems Division North American Rockwell Corporation 12214 Lakewood Boulevard Downey, California 90241 Attn: Library	1
Rocketdyne (Library 586-306) North American Rockwell Corporation 6633 Canoga Avenue Canoga Park, California 91304 Attn: Dr. R. J. Thompson, Jr.	1
S. F. Iacobellis	1

	Copies
Northrop Space Laboratories 3401 West Broadway Hawthorne, California Attn: Dr. William Howard	1
Astro-Electronics Division Radio Corporation of America Princeton, New Jersey 08540 Attn: Y. Brill	1
Reaction Motors Division Thiokol Chemical Corporation Denville, New Jersey 07832 Attn: Dwight S. Smith	1
Thiokol Chemical Corporation Huntsville Division Huntsville, Alabama Attn: John Goodloe	1
Space Division Aerojet-General Corporation 9200 East Flair Avenue El Monte, California 91734 Attn: S. Machlawski	1

	Copies
Stanford Research Institute 333 Ravenswood Avenue Menlo Park, California 94025 Attn: Dr. Gerald Marksman	1
TRW Systems Group TRW Incorporated One Space Park Redondo Beach, California 90278 Attn: G. W. Elverum	1
TAPCO Division TRW, Incorporated 23555 Euclid Avenue Cleveland, Ohio 44117 Attn: P. T. Angell	1
Research Laboratories United Aircraft Corporation 400 Main Street East Hartford, Connecticut 06108 Attn: Erle Martin	1
Hamilton Standard Division United Aircraft Corporation Windsor Locks, Connecticut 06096 Attn: R. Hatch	1

	Copies
United Technology Center 587 Methilda Avenue P.O. Box 358 Sunnyvale, California 94088 Attn: Dr. D. Altman	1
Florida Research and Development Pratt and Whitney Aircraft United Aircraft Corporation P.O. Box 2691 West Palm Beach, Florida 33402 Attn: R. J. Coar	1
Rocket Research Corporation 520 South Portland Street Seattle, Washington 98108 Attn: Foy McCullough, Jr.	1
Vickers, Inc. P.O. Box 302 Troy, Michigan Attn: Library	1
Louisiana State University Department of Chemical Engineering Baton Rouge, Louisiana Attn: Dr. Richard J. Farmer	1

	Copies
Sunstrand Aviation 2421 Eleventh Street Rockford, Illinois 61101 Attn: R. W. Reynolds	1
General Applied Science Laboratory, Inc. Merrick and Stewart Avenues Westbury, Long Island New York 11590 Attn: Dr. Ray Edleman	1

UNCLASSIFIED

Security Classification

DOCUMENT CONTROL DATA - R & D

(Security classification of title, body of abstract and indexing annotation must be entered when the overall report is classified)

1. ORIGINATING ACTIVITY (Corporate author)	2a. REPORT SECURITY CLASSIFICATION
Rocketdyne, a Division of North American Rockwell Corporation, 6633 Canoga Avenue, Canoga Park, California 91304	2b. GROUP

3. REPORT TITLE

PERFORMANCE ANALYSIS OF COMPOSITE PROPULSION SYSTEMS

4. DESCRIPTIVE NOTES (Type of report and inclusive dates)

Phase II Final Report (25 March 1968 through 24 March 1969)

5. AUTHOR(S) (First name, middle initial, last name)

Wrubel, J. A.

6. REPORT DATE	7a. TOTAL NO. OF PAGES	7b. NO. OF REFS
29 April 1969	116	21

8a. CONTRACT OR GRANT NO.	9a. ORIGINATOR'S REPORT NUMBER(S)
b. PROJECT NO.	R-7825
c.	9b. OTHER REPORT NO(S) (Any other numbers that may be assigned this report)
d.	

10. DISTRIBUTION STATEMENT

11. SUPPLEMENTARY NOTES	12. SPONSORING MILITARY ACTIVITY
	National Aeronautics and Space Administration Marshall Space Flight Center

13. ABSTRACT

The improved understanding of gas-stream turbulent mixing is contingent upon obtaining a more comprehensive description of the resultant flow field and a more precise evaluation of the turbulent transport properties. The second phase of a continuing program to accomplish these goals is described herein. The flow field being experimentally studied is the two-demensional mixing of fuel-rich supersonic hydrogen-oxygen combustion products and a subsonic heated airstream. The mixing is accomplished in a chamber accessible to both optical- and probe-type instrumentation systems. The second phase of the program included flow facility check-out, instrumentation installation, probe instrumentation survey, and preliminary testing.

DD FORM 1 NOV 65 1473

UNCLASSIFIED

Security Classification

14. KEY WORDS	LINK A		LINK B		LINK C	
	ROLE	WT	ROLE	WT	ROLE	WT
Gas Stream Turbulent Mixing						
Turbulent Transport Properties						
Supersonic Hydrogen-Oxygen Combustion Products						
Subsonic Heated Airstream						